

THE UNIVERSITY OF CALGARY

THE PRODUCTION OF SASKATCHEWAN HEAVY OILS
USING STEAM-ASSISTED GRAVITY DRAINAGE

by

S. Sugianto

A THESIS

SUBMITTED TO THE FACULTY OF GRADUATE STUDIES
IN PARTIAL FULFILLMENT OF THE REQUIREMENTS FOR THE
DEGREE OF
MASTER OF SCIENCE

DEPARTMENT OF CHEMICAL AND PETROLEUM ENGINEERING

CALGARY, ALBERTA

JANUARY, 1988

© S. Sugianto 1988

Permission has been granted to the National Library of Canada to microfilm this thesis and to lend or sell copies of the film.

The author (copyright owner) has reserved other publication rights, and neither the thesis nor extensive extracts from it may be printed or otherwise reproduced without his/her written permission.

L'autorisation a été accordée à la Bibliothèque nationale du Canada de microfilmer cette thèse et de prêter ou de vendre des exemplaires du film.

L'auteur (titulaire du droit d'auteur) se réserve les autres droits de publication; ni la thèse ni de longs extraits de celle-ci ne doivent être imprimés ou autrement reproduits sans son autorisation écrite.

ISBN 0-315-42429-X

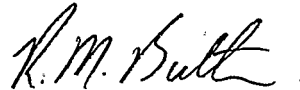
THE UNIVERSITY OF CALGARY

FACULTY OF GRADUATE STUDIES

The undersigned certify that they have read, and recommend to the Faculty of Graduate Studies for acceptance, a thesis entitled,

"THE PRODUCTION OF SASKATCHEWAN HEAVY OILS USING
STEAM-ASSISTED GRAVITY DRAINAGE"

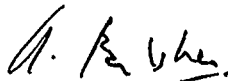
submitted by Setiahardjon Sugianto in partial fulfillment of the requirements for the degree of Master of Science.



Dr. R.M. Butler, Committee Chairman
Department of Chemical & Petroleum Engineering



Dr. R.G. Moore
Department of Chemical & Petroleum Engineering



Dr. A. Badakhshan
Department of Chemical & Petroleum Engineering



Dr. N.C. Wardlaw
Department of Geology & Geophysics

March 24, 1988.

Date

ABSTRACT

In Saskatchewan, there are many heavy oil reservoirs containing bottom water. Attempts to produce by primary production are often uneconomical because of excessive water cuts. The problem is well understood; it results from the much lower viscosity of water compared to that of oil. This causes the water to "cone" upward into the production well.

An experimental program, using the steam-assisted gravity drainage process involving the use of horizontal wells, was conducted to study the potential of producing Saskatchewan heavy oils from reservoirs where recovery is limited by water coning.

Twelve experiments were performed using a two-dimensional scaled reservoir model containing an active aquifer system. The experiments used a simulated Winter Cummings heavy oil (14° API gravity) with injected steam pressures between 119 and 170 kPa and with bottom water zone thicknesses from 0 to 41% of the total thickness.

The cumulative oil recovery varied from 48% to 87% of original oil in place. The rate of recovery was more favourable under the following conditions:

1. Thinner bottom water zone.
2. Smaller interwell spacing.
3. Higher permeability of the reservoir.

4. Higher steam injection pressure for runs without bottom water.

It was found that, when bottom water was present, the cumulative oil recovery was less when the steam injection pressures which were used were higher. The thickness of the bottom water zone and the well configurations employed had a significant effect on the ultimate cumulative oil recovery. The experimental trials revealed that a high recovery of heavy oils where the horizontal production well is placed below the water/oil contact is also possible by utilizing a specific operating strategy for the production well.

ACKNOWLEDGEMENTS

I would like to thank my supervisor, Dr. R.M. Butler, for his guidance, support and encouragement throughout the course of my work. His invaluable suggestions have increased my vision into many natural phenomena.

I would like to thank my colleagues in Dr. Butler's research group, particularly to Mr. W. Wong for his assistance during the laboratory work, Mr. K. Chung and Mr. T. Ong and Dr. G. Petela for their friendship, encouragement and inspiration.

I am also grateful to Mrs. Patricia Stuart-Bakes for typing the manuscript.

Appreciation is extended to the Canada-Saskatchewan Heavy oil/Fossil Fuel Research Programme for providing the research funds and financial support.

I am indebted to Miss Lisa Wong for her patience, understanding and encouragement throughout this work.

I dedicate this thesis to my parents whose years of support, guidance and encouragement have made this thesis possible.

TABLE OF CONTENTS

Chapter No.	Description	Page No.
	ABSTRACT	iii
	ACKNOWLEDGEMENTS	v
	TABLE OF CONTENTS	vi
	LIST OF TABLES	ix
	LIST OF FIGURES	x
	LIST OF SYMBOLS	xiv
1.	INTRODUCTION	1
2.	LITERATURE REVIEW	10
3.	EXPERIMENTS	15
3.1	Design of Experiment	15
3.2	Apparatus	19
3.3	Preparation and Experimental Procedures	21
3.4	Sample Analysis	26
3.5	Scaled Reservoir Model Characterization	28
3.6	Operating Conditions	31
3.6.1	Repeatability of Experimental Results	31
3.6.2	Effect of Reservoir Permeability	31
3.6.3	Effect of Steam Injection Pressure	37
3.6.3.1	Case Without a Bottom Water Zone	37
3.6.3.2	Case With a Bottom Water Zone	37
i)	Before Steam Breakthrough at the Production Well	
ii)	After Steam Breakthrough at the Production Well	
3.6.4	Effect of Interwell Spacing	38
3.6.4.1	Case Without a Bottom Water Zone	
3.6.4.2	Case With a Bottom Water Zone	
3.6.5	Effect of Effective Thickness of the Bottom Water Zone	39
3.6.6	Effect of the Location of the Production Well	39

Chapter No.	Description	Page No.
4	THEORY	40
4.1	Drainage Rate Prediction	40
4.1.1	Dimensionless Time	40
4.1.2	Extended Definition of "m"	41
4.1.3	Viscosity-Temperature Relation	42
4.1.4	Dimensionless Drainage Rate	42
4.1.5	Total Drainage Rate	43
4.2	Percent Oil Recovery During Depletion of the Reservoir	43
4.3	Scaling Criteria for the Field Condition	44
5	RESULTS	45
5.1	Mechanism	45
5.1.1	Oil Displacement by Steam During the Initial Communication Period	45
5.1.2	Steam-Assisted Gravity Drainage After the Initial Communication Period	47
5.2	Temperature Distribution in the Reservoir Model	51
5.2.1	Experimental Runs Without a Bottom Water Zone	51
5.2.2	Experimental Runs With a Bottom Water Zone	52
5.3	Initial Communication Period Prediction	53
5.4	Repeatability of Results	59
5.5	Effect of Steam Injection Pressure	62
5.5.1	Experimental Runs Without a Bottom Water Zone	62
5.5.2	Experimental Runs With a Bottom Water Zone	65
	i) Before Breakthrough	
	ii) After Breakthrough	
5.6	Effect of Bottom Water Zone Thickness	68
5.7	Effect of Location of Production Well	71
5.8	Effect of Interwell Spacing	77
5.8.1	Experimental Run Without a Bottom Water Zone	78
5.8.2	Experimental Run With a Bottom Water Zone	78

Chapter No.	Description	Page No.
5.9	Effect of Effective Permeability to the Flow of the Oil	83
6	DISCUSSION	86
6.1	Effect of Steam Injection Pressure on the Steam Breakthrough	86
6.2	Effect of Steam Injection Pressure on the Production Performance	87
6.3	Effect of Bottom Water Zone Thickness on the Production Performance	89
6.4	Effect of Location of Production Well on the Production Performance	90
6.5	Effect of Interwell Spacing on the Production Performance	92
6.6	Comparison of the Production Performance of Experimental Runs and Theoretical Predictions	92
6.7	Applications in Canada's Oil Fields	103
7	SUMMARY AND CONCLUSIONS	116
8	RECOMMENDATIONS	120
	APPENDIX A Computer Program for Calculating the Material Balance	122
	APPENDIX B Computer Program for Predicting the Production Performance Using the Steam-Assisted Gravity Drainage Theory. Developed by Butler et al (1981)	128
	BIBLIOGRAPHY	131

LIST OF TABLES

Table No.	Description	Page No.
1	Physical Properties of 2 and 3 mm Glass Beads	32
2	Summary of Operating Conditions for all Experimental Runs	33
3	Summary of the Results for all Experimental Runs	46
4	Comparison of Initial Communication Period Between Experimental Results and Theoretical Predictions	54
5	Comparison of Initial Communication Period Predicted by Analytical Method for Various Heavy Oils and Bitumens Found In Alberta and Saskatchewan for Typical Heavy Oil and Bitumen in Alberta and Saskatchewan	57
6	Scaling Parameters for Experimental Run No. 10 and the Field	95
7	Scaling Parameters for Experimental Run No. 11 and the Field	96
8	Reservoir and Economic Parameters for Calculating the Effect of Well Spacing Variations to Winter Reservoir Production Performances and Economics	110

LIST OF FIGURES

Figure No.	Description	Page No.
1	Beginning of Steam Injection Period in Conventional Heavy Oil Reservoirs Containing a Bottom Water Zone	3
2	Early Period of Steam Chamber Development in Conventional Heavy Oil Reservoirs Containing a Bottom Water Zone	4
3	Middle Period of Steam Chamber Development in Conventional Heavy Oil Reservoirs Containing a Bottom Water Zone	5
4	Steam Breakthrough Period in Conventional Heavy Oil Reservoirs Containing a Bottom Water Zone	6
5	Late Period of Steam Chamber Development in Conventional Heavy Oil Reservoirs Containing a Bottom Water Zone	7
6	Schematic Diagram for the Experiment Without a Bottom Water Zone	17
7	Schematic Diagram for the Experiment With a Bottom Water Zone	18
8	Photograph of the Complete Experimental Set-Up Consisting of a Two-Dimensional Visual Reservoir Model and the Aquifer System	20
9	Chart for Simulating Winter Cummings Heavy Oil	23
10	Experiment Preparations for Saturating The Reservoir Model with Heavy Oil and Water	25
11	Photograph of Centrifuging Test Apparatus (IEC Model K)	29
12	Photograph of the Permeability Test Apparatus	29
13	Schematic Diagram of Permeameter	30

Figure No.	Description	Page No.
14	Operating Pressure Profile for Experimental Laboratory Programs	34
15	Well Configurations for Experimental Runs No. 1-9	35
16	Well Configurations for Experimental Runs No. 10-12	36
17	Temperature Distribution in the Reservoir Model at Various Times (Before Steam Breakthrough)	48
18	Temperature of Produced Fluid as a Function of Time	49
19	Temperature Distribution in the Reservoir Model at Various Times (After Steam Breakthrough)	50
20	Comparison of Initial Communication Period Between Experimental Results and Theoretical Predictions	55
21	Oil Production Rate as a Function of Time (Runs No. 1 and 2)	60
22	Percent Oil Recovery as a Function of Time (Runs No. 1 and 2)	61
23	Oil Production Rate as a Function of Time (Runs No. 2 and 3)	63
24	Percent Oil Recovery as a Function of Time (Runs No. 2 and 3)	64
25	Oil Production Rate as a Function of Time (Runs No. 5 and 6)	66
26	Percent Oil Recovery as a Function of Time (Runs No. 5 and 6)	67
27	Oil Production Rate as a Function of Time (Runs No. 7 and 8)	69
28	Percent Oil Recovery as a Function of Time (Runs No. 7 and 8)	70

Figure No.	Description	Page No.
29	Percent Oil Recovery as a Function of Time (Runs No. 10, 11 and 12)	72
30	Oil Production Rate as a Function of Time (Runs No. 10, 11 and 12)	73
31	Percent Oil Recovery as a Function of Time (Runs No. 5, 7 and 9)	75
32	Oil Production Rate as a Function of Time (Runs No. 5, 7 and 9)	76
33	Oil Production Rate as a Function of Time (Runs No. 4 and 10)	79
34	Percent Oil Recovery as a Function of Time (Runs No. 4 and 10)	80
35	Oil Production Rate as a Function of Time (Runs No. 5 and 11)	81
36	Percent Oil Recovery as a Function of Time (Runs No. 5 and 11)	82
37	Oil Production Rate as a Function of Time (Runs No. 2 and 4)	84
38	Percent Oil Recovery as a Function of Time (Runs No. 2 and 4)	85
39	Oil Production Rate as a Function of Time (Run No. 10)	97
40	Percent Oil Recovery as a Function of Time (Run No. 10)	98
41	Oil Production Rate as a Function of Percent Oil Recovery (Run No. 10)	99
42	Oil Production Rate as a Function of Time (Run No. 11)	100
43	Percent Oil Recovery as a Function of Time (Run No. 11)	101
44	Oil Production Rate as a Function of Percent Oil Recovery (Run No. 11)	102

Figure No.	Description	Page No.
45	Illustration for Experiment No. 10 Extrapolated to Field Conditions	105
46	Illustration for Experiment No. 11 Extrapolated to Field Conditions	106
47	Oil Steam Ratio as a Function of Spacing between Horizontal Wells	112
48	Average Oil Production Rate as a Function of Spacing Between Horizontal Wells	113
49	Project Life as a Function of Spacing Between Horizontal Wells	114
50	Supply Cost as a Function of Spacing Between Horizontal Wells	115

LIST OF SYMBOLS

All of the equations in the text are dimensionally consistent and any set of consistent physical units can be employed.

- B_3 dimensionless scaling constant defined by equation (4.7)
- g acceleration due to gravity, m/day^2 or $m/sec.^2$
- H reservoir height, m
- K effective permeability to flow of oil, m^2
- m dimensionless parameter defined by equation (4.2)
- OOIP original oil in place, m^3
- t time, day or sec.
- t_d dimensionless time defined by equation (4.1)
- T temperature at distance ϵ from the interface, $^{\circ}C$
- T_r initial reservoir temperature, $^{\circ}C$
- T_s steam temperature, $^{\circ}C$
- W half interwell spacing, m
- WOC water oil contact
- Q total drainage rate, m^3/day m of horizontal well length
- Q_d dimensionless drainage rate defined by equation (4.4)
- α thermal diffusivity, m^2/day or $m^2/sec.$
- ν kinematic viscosity of oil at any temperature, m^2/day or $m^2/sec.$
- ν_s kinematic viscosity of oil at steam temperature, m^2/day or $m^2/sec.$
- ϕ porosity, dimensionless fraction
- ρ_o density of oil, kg/m^3

CHAPTER 1

INTRODUCTION

Many heavy oil reservoirs in Saskatchewan and Alberta have a bottom water zone underlying the oil zone. The heavy oil deposits lying in such reservoirs with pay thickness greater than 10 m are significant ($147 \times 10^6 \text{ m}^3$ or 925×10^6 barrels oil in place) and represent a potentially valuable energy source. Although the reservoirs are relatively thick and permeable, they cannot be produced efficiently by conventional methods. One reason is the tendency for the water to "cone" into the production well. Typical field trials lead to excessive water cuts. For example, the Winter reservoir in Saskatchewan yields less than 1% of the OOIP using primary production. The wells in the Winter reservoir have had to be abandoned after a few months production because of excessive water production.

The objective of this work was to study the potential application of the steam-assisted gravity drainage process to heavy oil reservoirs where recovery is limited by water coning. A reservoir model was constructed and was scaled to simulate conditions in the Winter field.

Kasrie and Farouq Ali (1984) illustrated a mechanism of conventional steam flooding for a heavy oil reservoir containing a bottom water zone. They indicated that the injected steam will tend to penetrate into the bottom water zone because of higher conductivity. This would result in an uneconomical steam/oil

ratio due to inefficiency in heating the oil zone, and excessive water would be produced. Therefore, a new modified version of steamflooding that could avoid prohibitive heat loss into the bottom water zone is desirable for heavy oil reservoirs containing bottom water.

In the steam-assisted gravity drainage process studied here, steam is injected continuously through horizontal wells located near to the top of the reservoir; these injection wells are located vertically above horizontal production wells which are placed at the bottom of the reservoir. In the initial operation, the injected steam moves downward and sideways and forms a steam chamber. The steam displaces oil into the production wells. Because of the mobility of Winter heavy oils, displacement can be achieved with oil at the initial reservoir temperature. The steam condenses and the condensate fingers through the oil and is produced as water at the production well. The pressure in the production well is controlled so as to be slightly above the aquifer pressure. The rate of advance of the steam/water interface will increase as it moves closer to the production wells. This process is illustrated in Figures 1 to 5.

After the initial operation, when the steam chamber extends nearly to the production well, the steam injection rate is decreased to prevent excessive steam bypass (Figure 4). The steam chamber continues to grow downward and sideways. The steam condenses at the interface and heats the oil beyond. The

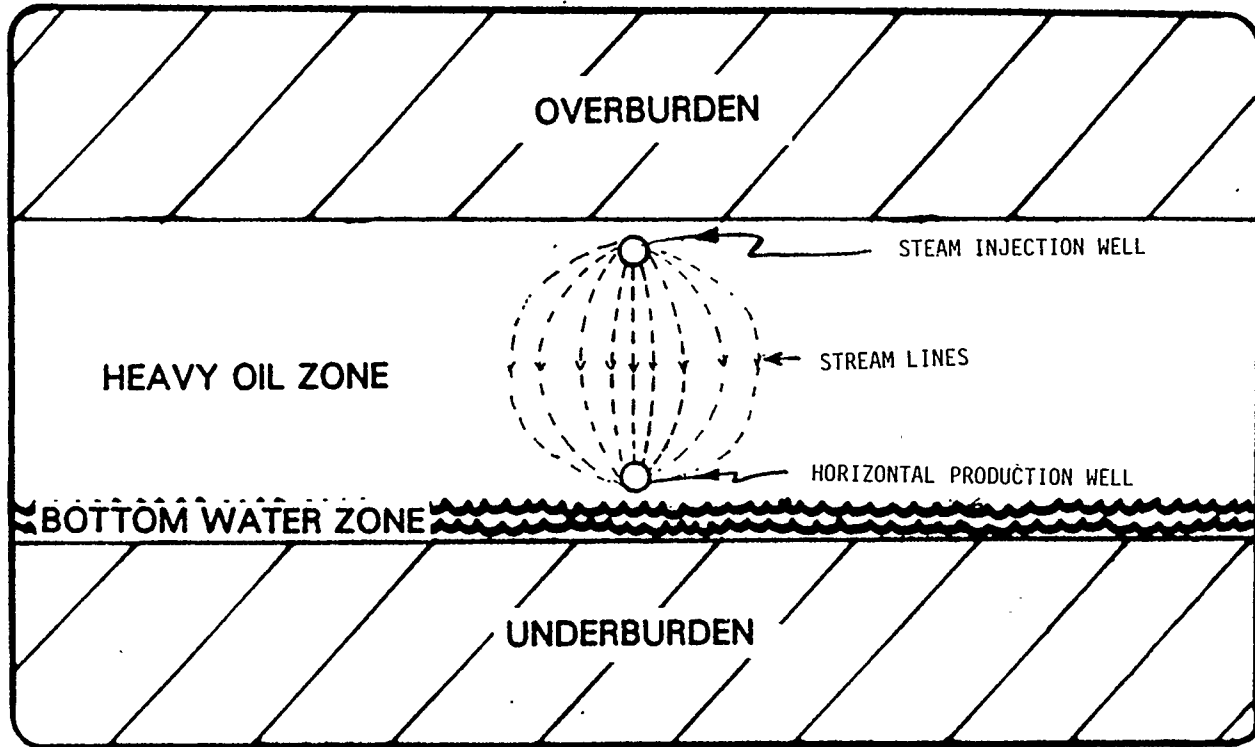


Figure 1: Beginning of Steam Injection Period in Conventional Heavy Oil Reservoirs Containing a Bottom Water Zone

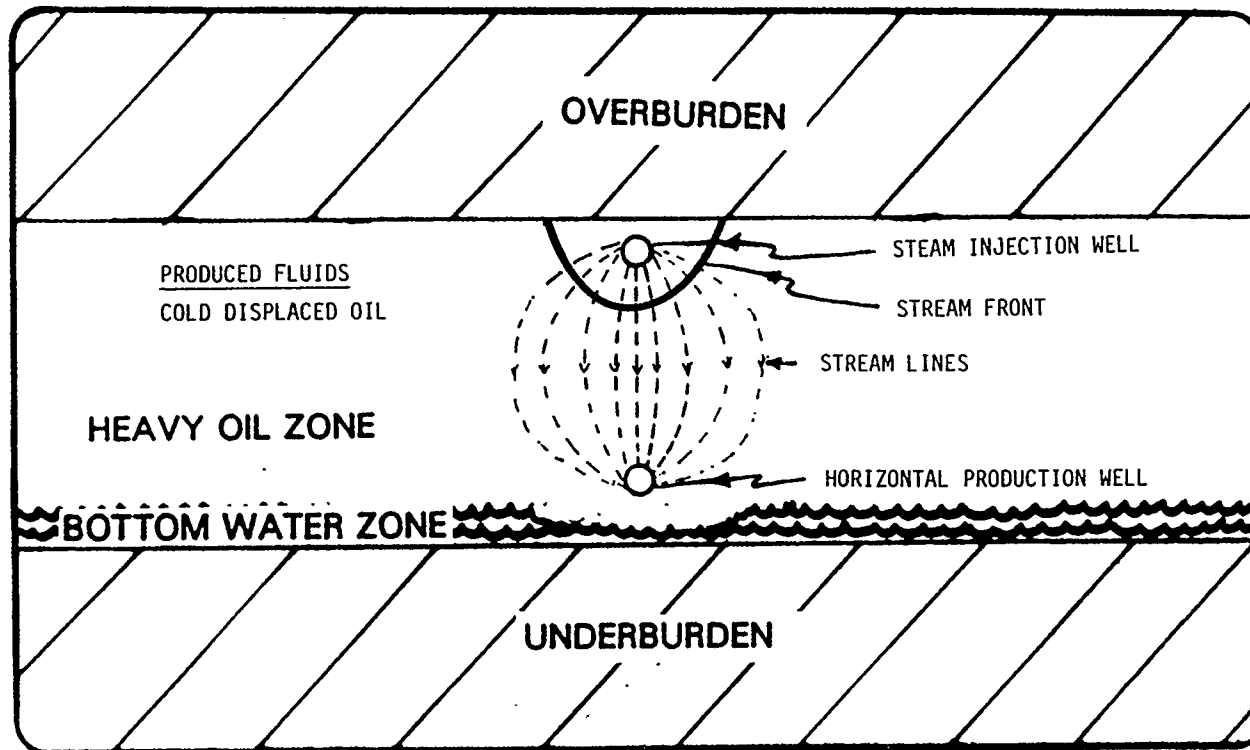


Figure 2: Early Period of Steam Chamber Development in Conventional Heavy Oil Reservoirs Containing a Bottom Water Zone

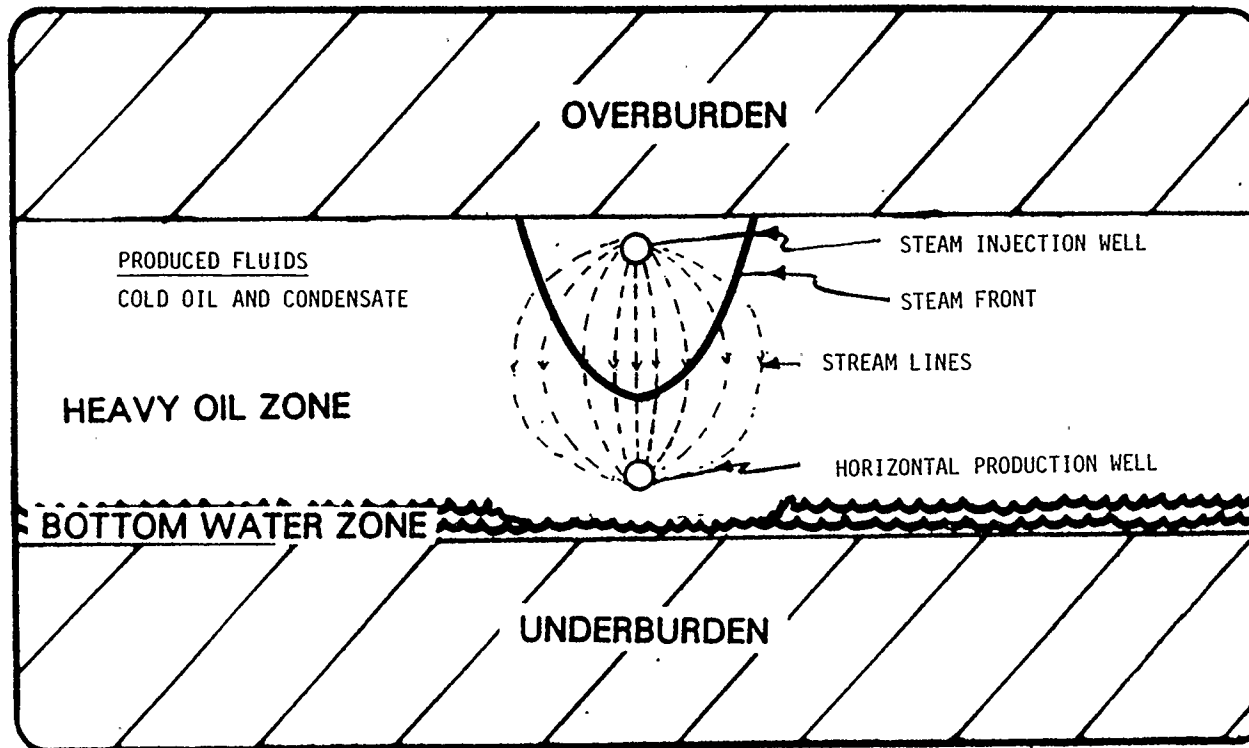


Figure 3: Middle Period of Steam Chamber Development in Conventional Heavy Oil Reservoirs Containing a Bottom Water Zone

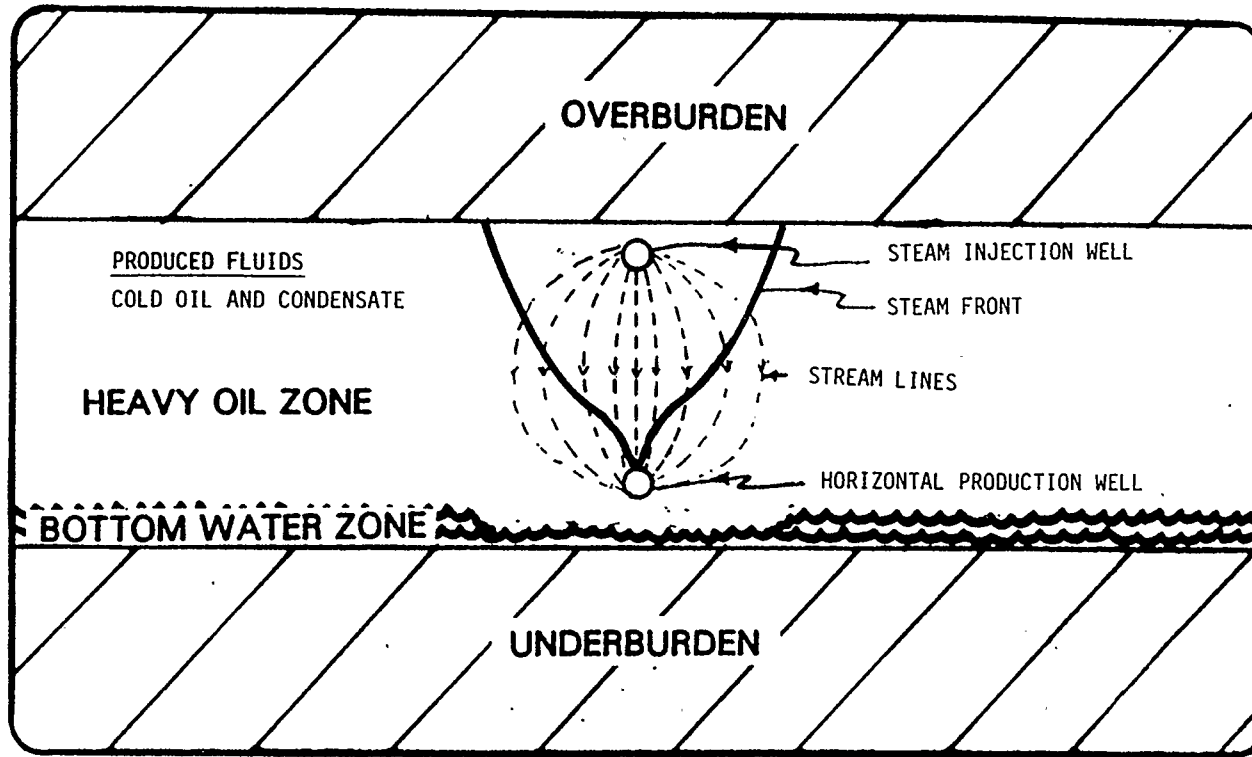


Figure 4: Steam Breakthrough Period in Conventional Heavy Oil Reservoirs Containing a Bottom Water Zone

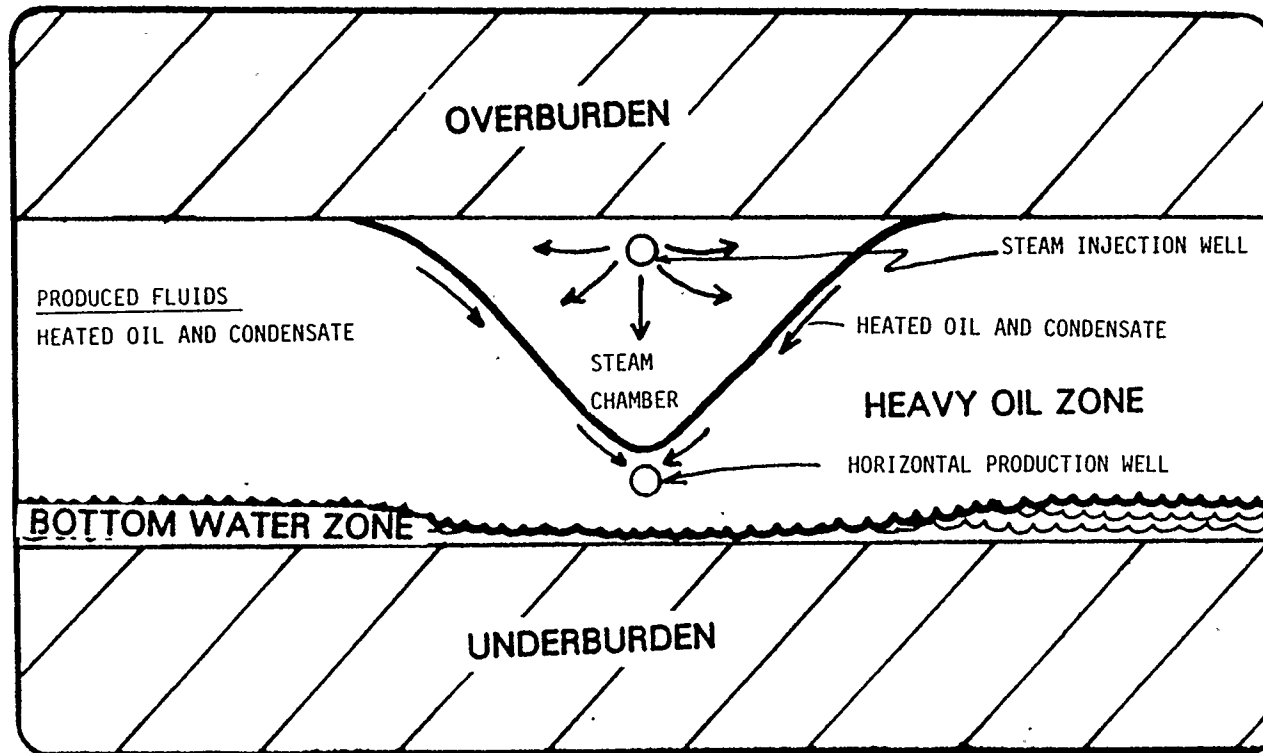


Figure 5: Late Period of Steam Chamber Development in Conventional Heavy Oil Reservoirs Containing a Bottom Water Zone. (Slight Modification to the "Steam-Assisted Gravity Drainage Concept")

condensate from the steam and the heated oil drain, driven by gravity, toward the production wells. Theoretical and experimental studies explaining this phase of the process have been described by Butler et al (1980, 1981, 1985, 1987); this is shown in Figure 5. Their theoretical predictions show a good agreement with the experiments.

The advantage of the technique used in this study is that the steam injection pressure and the production well pressure involved in the steam-assisted gravity drainage phase can be adjusted to be slightly higher than the bottom water zone pressure so that there is little tendency for the underlying water layer to move upward into the production well. The production well pressure is controlled (by adjusting the steam injection) to be somewhat higher than the bottom water zone to avoid water coning upwards to the well and also the well is throttled to avoid the steam bypassed into the well. In this manner, prohibitive heat loss to the bottom water zone can be avoided together with excessive bypass of steam. During operation, the production well will thus be slightly above the aquifer pressure and the steam chamber pressure will be slightly higher still.

Laboratory experiments were conducted using a scaled, low pressure, two dimensional reservoir model with an active aquifer system. In the model, the aquifer was connected by two tubes to an external, constant-pressure water reservoir. The effects of

the following variables were investigated:

1. Steam injection pressure.
2. Thickness of the aquifer.
3. Well spacing.
4. Permeability of the reservoir.
5. Location of the production well.

Successful operation was also obtained with the horizontal production well below the water/oil contact (WOC).

In these experiments, the water in the immediate vicinity of the production well became displaced during the early phases of the operation by the intrusion of oil.

The experimental results and mathematical modelling were used to study the above effects. From these results and calculations, it is possible to predict the time for establishing the initial communication path, and the field scaled drainage rate and the oil/steam ratio as functions of properties such as the reservoir parameters and the inter well spacing.

CHAPTER 2

LITERATURE REVIEW

Field experience and laboratory experiments show that the presence of bottom water in a heavy oil reservoir can have a detrimental effect on the ultimate oil recovery and the steam/oil ratio. Ehrlich, R. (1977) was one of the earlier researchers to indicate this effect in laboratory experiments. He conducted a conventional steam flood using a very viscous oil (5×10^6 cp Wabasca bitumen). He reported that once the injected steam penetrated the bottom water zone, the steam penetration could not be stopped and the bottom water zone was saturated with heated oil migrated downwards due to the gravity force. Some of the oil was left in the bottom water zone and the resulting steam/oil ratio was high.

Prats (1977) conducted a comprehensive study of the effect of a bottom water zone in conventional steam flooding a high viscosity oil (2×10^5 cp Peace River bitumen). He used five models of the reservoir which consisted of variations in the thickness, permeability and saturation of the oil and underlying water zones, composed of several configurations in 7-spot well patterns. He reported that an in-situ, variable pressure steam recovery operation in Peace River should yield a steam/oil ratio of 4 for reservoir sands of 27 m thickness with a thin bottom water layer to provide sufficient initial injection. However, if the thickness of the reservoir sands was reduced to 12 m, the

potential steam/oil ratio will increase to 4.5. The ultimate oil recovery exceeded 60% of the OOIP under any reservoir conditions for all five reservoir models tested.

Later, Huygen and Lowry (1979) investigated the steam flooding of Wabasca bitumen (5×10^6 cp oil) with the presence of a bottom water zone in a three dimensional scaled model. They found that the bottom water zone acted as a pressure sink where the injected steam would tend to migrate into the bottom water zone which had a higher conductivity. As the oil became hot (90-120°C) and mobile, it was pushed by the hot condensate into the bottom water zone. Little oil was produced at the beginning and more oil was left in the bottom water zone. The results of steam flooding a Wabasca bitumen with high initial oil saturation (88%) showed high oil recovery (67% of OOIP) and a high steam/oil ratio (5.0), whereas, lower initial saturation (60%) gave lower oil recovery (37% of OOIP), and a higher steam/oil ratio (12.5).

Doscher and Huang (1979) conducted laboratory experiments to study the effect of a bottom water zone equal to 15% of the total pay thickness in steam flooding a very viscous oil (139540 cst at 4°C). They indicated that as the steam injection rate was increased, the oil production was delayed and the resulting steam-oil ratio increased. Also the steam/oil ratio is higher for the case of reservoirs with a bottom water zone.

Farouq Ali (1983) reviewed all field tests, laboratory models and mathematical simulation results for thermal recovery processes of heavy oil reservoirs containing bottom water or a gas cap. He indicated the possibility of conducting a successful steam flood in reservoirs with the presence of bottom water or a gas cap. For the in-situ combustion process, the bottom water zone would lead to severe air channeling. Using mathematical simulators, he observed the effect of various thicknesses of the bottom water zone on a steam flood. He found a delay in oil production, higher steam/oil ratios and more volumes of water production as the bottom water zones increased. He indicated that a higher steam injection rate led to steam channeling into the bottom water zone and also to more oil being driven out by steam into the bottom water zone. He found that increasing the bottom water thickness had an adverse effect on the oil recovery and steam/oil ratio.

Kasrie and Farouq Ali (1984) reviewed the applications of thermal recovery processes for heavy oil recovery in the presence of bottom water from the mechanistic standpoint. They illustrated steam flooding in the presence of a bottom water zone. For viscous oil, the injected steam would tend to migrate into the bottom water zone due to higher conductivity. The steam would heat the oil and the oil would be mobilized and migrate into the bottom water zone; oil would be left in the bottom water zone. They observed that thick water zones would delay the steam flood response and more volumes of water would be produced.

These problems would reduce the profitability of the potential commercial steam flood project.

Butler, R.M. et al (1979,1981,1985 a & b, 1987) developed a new concept of steam flooding with the use of horizontal wells to systematically deplete heavy oil reservoirs and to improve the reservoir contact and production rates. The process is called "Steam-Assisted Gravity Drainage".

The concept of the steam-assisted gravity drainage process is that the steam is injected continuously through injection well(s) located above a horizontal production well where heated oil and condensate are removed continuously. As the process proceeds, the steam chamber grows in size and heat conducted from the perimeter of the chamber decreases the oil viscosity. The oil, together with the condensate from the steam, drain downwards, driven by the gravity forces, to the horizontal production well. The production well is operated so that the liquids are withdrawn from the reservoir but the pressure is not allowed to fall to the point where steam can flow out of the production well.

Griffin and Trofimenkoff (1984) conducted laboratory experiments for both low pressure and high pressure models using the steam-assisted gravity drainage process. They found that the theoretical predictions developed by Butler et al showed a good agreement with their experimental results for low pressure models.

Jain and Khosla (1985) investigated the potential of utilizing gravity drainage and horizontal wells on the steamflooding of Athabasca bitumen (435,000 cp at 25°C). They used a computer model to study the development of operating strategies and production performance predictions for horizontal wells. They found that the oil production rates had the same trend with the theoretical predictions developed by Butler et al (1981) although the rate of recovery predicted by their simulation study was slower than that predicted by Butler et al. Using a configuration of a 400 m long horizontal production well and two vertical injectors, their simulation study showed that from a 3 hectare pattern, approximately 59% of the OOIP can be produced from a typical Fort McMurray formation over a period of 7.8 years with an average production of 50 m³ per day and a cumulative steam/oil ratio of 8.3.

Chung and Butler (1987) conducted laboratory experiments to observe the effect of the geometry of a steam injection well. They indicated that steam injected near the top of the reservoir was more desirable because the rate of oil recovery would be higher than if the steam was injected at the bottom of the reservoir.

CHAPTER 3

EXPERIMENTS

3.1 Design of the Experiment

Two arrangements of the experimental set-up were utilized to investigate the steam-assisted gravity drainage process for recovering heavy oil from reservoirs containing a bottom water zone.

1) Experimental runs without the bottom water zone.

A schematic diagram is shown in Figure 6. Steam is injected near the top of the reservoir model. The steam chamber grows sideways and downwards to displace the cold oil into the production well located at the bottom of the reservoir model. Steam condenses at the interface and releases heat into the oil zone. Condensate from the steam fingers through the oil and reaches the production well in a relatively short time. Later, the steam front will reach the production well, then the production well is throttled to avoid the steam bypass. The oil and condensate are withdrawn continuously until only a small amount of oil can be produced.

2) Experimental runs with bottom water zone.

A schematic diagram of the apparatus is illustrated in Figure 7. The model is connected to a water reservoir tank such that the bottom water in the reservoir model

can flow freely in and out of the reservoir model. This system will act as an active aquifer in a real reservoir condition.

Steam is injected near to the top of the reservoir. A steam chamber grows sideways and downwards to displace the cold oil into the production well and the bottom water out of the reservoir model.

An inert gas such as nitrogen is used to balance the pressure in the reservoir model and the water tank. The injected steam pressure is set 7-10 kPa higher than the water tank pressure. The main reason for this is to avoid the intrusion of the bottom water layer into the steam chamber and the production well. If the bottom water moves and floods into the steam chamber, the production of oil will be disrupted and delayed or may even result in experimental failure. The production well must also be controlled to avoid excessive bottom water withdrawal and also, later, steam bypass.

The steam condenses at the interface and liberates heat into the surrounding reservoir. Some heated oil will migrate into the bottom water zone. This oil will be left in the bottom zone and cannot be recovered because the gravity force cannot push the oil upwards into the production well. The oil and condensate are removed continuously until only a small amount of oil can be

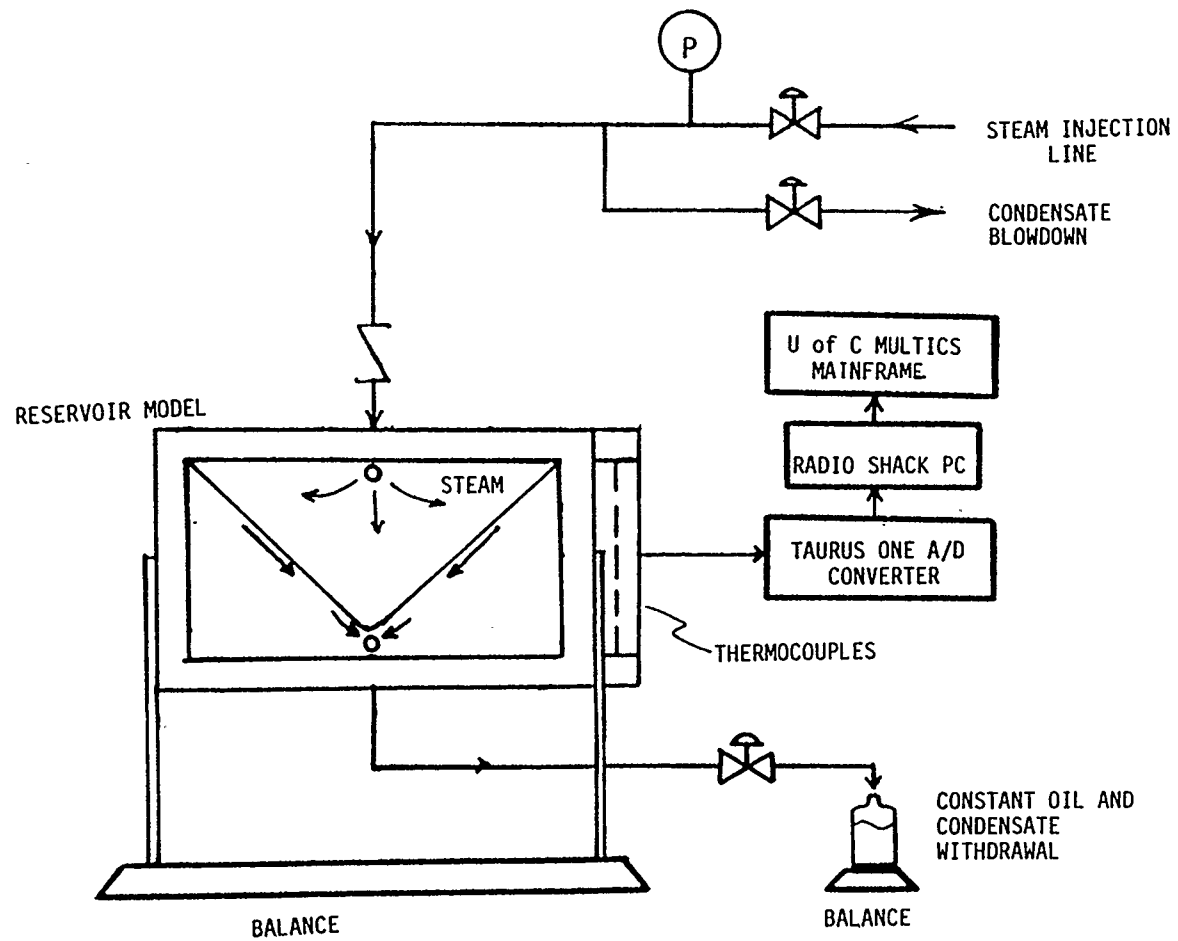


Figure 6: Schematic Diagram for the Experiment without a Bottom Water Zone

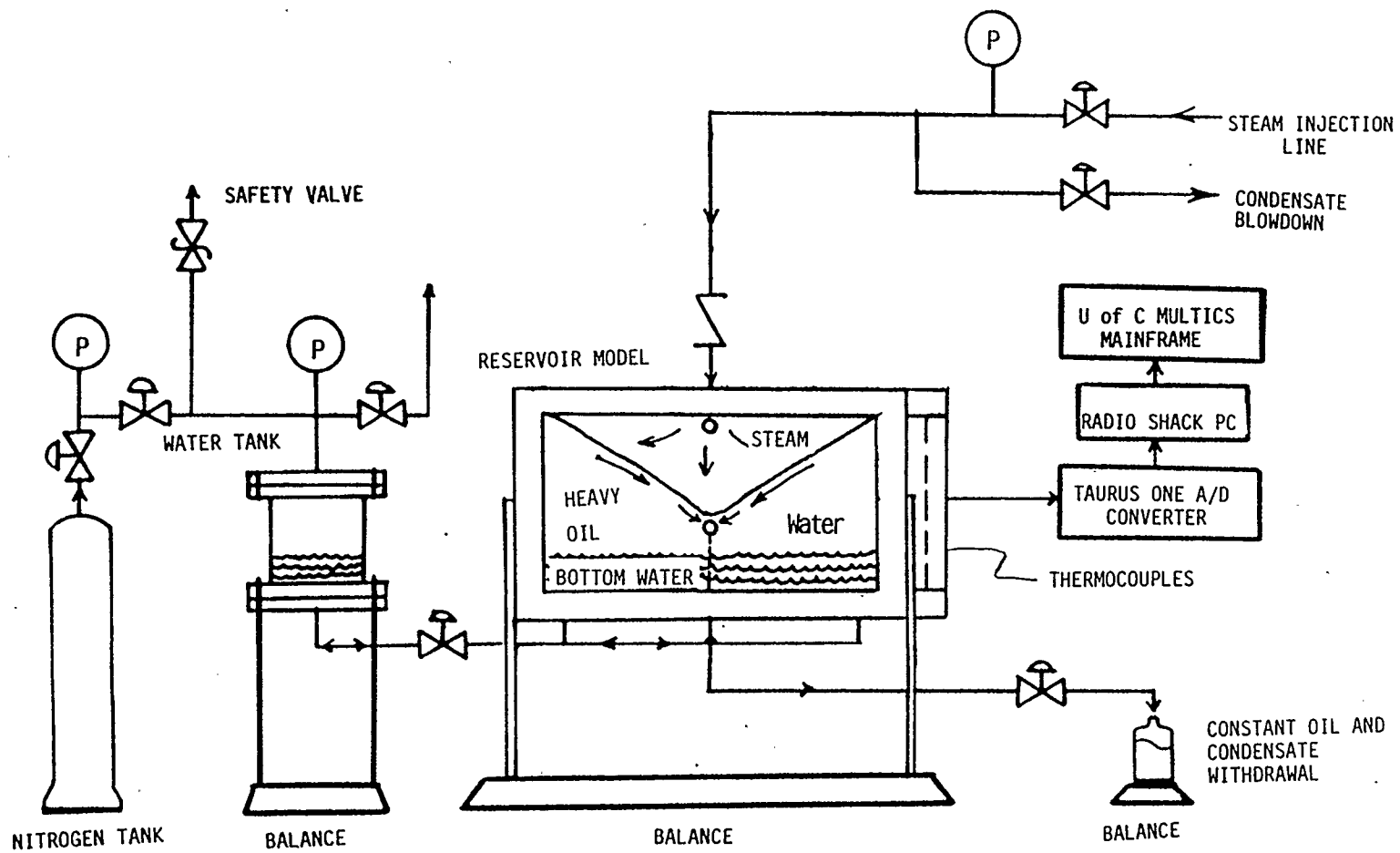


Figure 7: Schematic Diagram for the Experiment with a Bottom Water Zone.

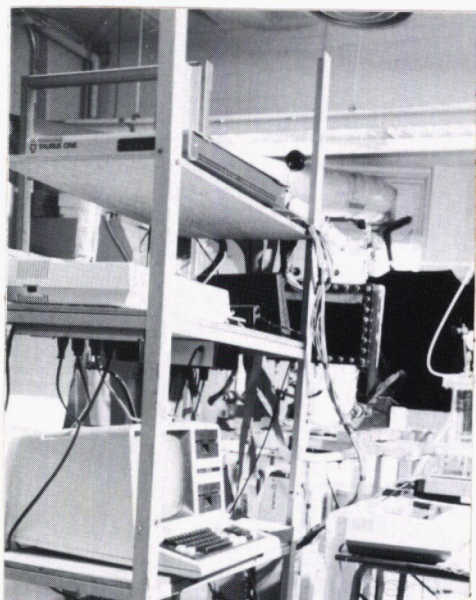
recovered.

3.2 Apparatus

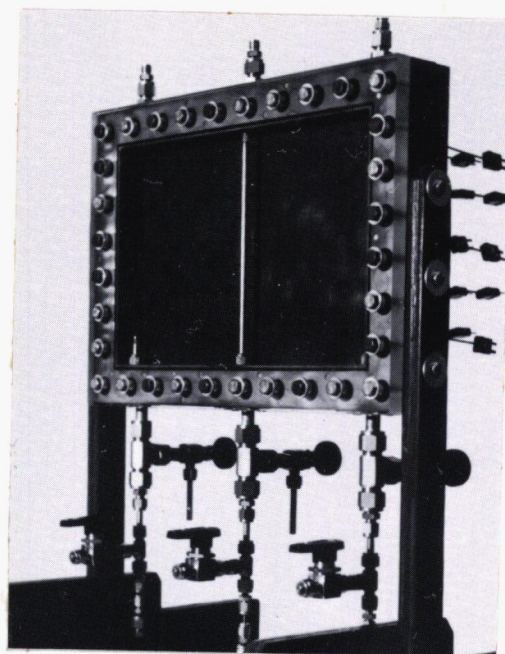
A photograph of the complete experimental set up consisting of a two-dimensional visual reservoir model and its aquifer system is shown in Figure 8.

The reservoir model was 35 cm. wide, 22 cm. high and 3 cm. thick with five sides made of reinforced phenolic resin; one of the large sides was made of transparent plexiglass. The model can be envisaged as a vertical portion of the real reservoir. Styrofoam sheets, 2.5 cm. thick, were used to insulate the entire model, except for the one side made of transparent plexiglass. This allowed visualization and photography of the displacement mechanism of heavy oil by the steam chamber. There were three 0.95 cm. (3/8") fittings on the bottom and the top of the model. All fittings could be easily modified to serve either as an injection well or a production well. There were 42 copper-constantan, T-type thermocouples located throughout the model to monitor the temperature distribution during the experimental runs.

The water reservoir tank had an inside diameter of 7.1 cm. and a height of 23 cm. and was constructed of transparent plexiglass. Two 0.635 cm. (1/4") fittings were located on the top and the bottom of the water tank. Flexible plastic tubing was used to connect the reservoir model and the water tank. A needle valve was placed in the middle of the plastic tubing connecting



Photograph of Computerized
Data Acquisition System



Photograph of a Two-Dimensional
Reservoir Model

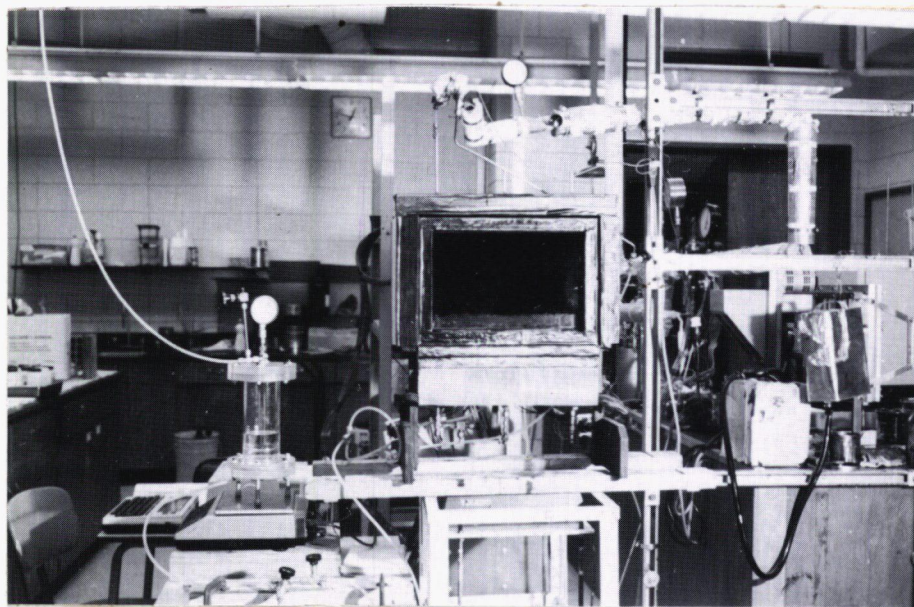


Figure 8: Photograph of the Complete Experimental Set-up Consisting
of a Two-Dimensional Visual Reservoir Model and the
Aquifer System.

the reservoir model and the water tank to control the flow of bottom water in and out of the model. This valve was normally open. A regulator valve on the top of a nitrogen tank was used to control the nitrogen supply at 143 kPa (6 psig). A pressure gauge and a needle valve were also located on the top of the water tank to control the balancing pressure supplied by the nitrogen tank. A pressure relief valve was located in the middle of the tubing connecting the water tank and the nitrogen tank. This safety precaution was taken to avoid over pressurizing the water tank in case the regulator valve on the top of the nitrogen tank failed.

All the apparatus described above was pressure tested up to 239 kPa (20 psig). For safety reasons, a maximum operating pressure of 170 kPa was used in the experiments.

3.3 Preparation and Experimental Procedures

In preparing for an experimental run, glass beads had to be packed into the reservoir model through the three fittings along the upper edge of the model. This work was performed with the model secured to a vibrating table. The main reason for this was to ensure a consistent, uniformly random packing of the porous pack.

The oil used in each experimental run was prepared by mixing Tangleflags North heavy oil of 13.5 API^o gravity (supplied by Sceptre Resources Limited), with a small amount of kerosene. The

objective of this dilution was to simulate the viscosity of Winter Cummings heavy oil (3000 cp at 27.8°C). A mixing chart between the Tangleflags North heavy oils and kerosene was developed to predict the dilution required. (see Figure 9). The chart was developed by measuring viscosities of various composition mixtures of the Tangleflags North heavy oil and kerosene at various temperatures. The viscosity measurements were done using a concentric cylinder viscometer (viscometer UK Model UKRV-8) with a constantly controlled temperature bath. Before the viscosity measurements were taken, calibration tests were performed with ASTM Standard viscosity oils with a viscosity range of 1486 to 8131 cp.

Before filling the reservoir model with the simulated oil, the oil was always tested to ensure viscosity readings of approximately 3000 cp at 27.8°C. For experimental runs without a bottom water zone, the filling procedure was simple. The reservoir model was completely saturated with the oil by upward flooding at room temperature. For experimental runs with a bottom water zone, the filling procedure was divided into three stages. First, the reservoir model was turned upside down so that the oil could flood the reservoir model from the bottom up to a predetermined weight. The reservoir model was mounted on an electronic balance so that the oil filling could be stopped when the desired weight was attained.

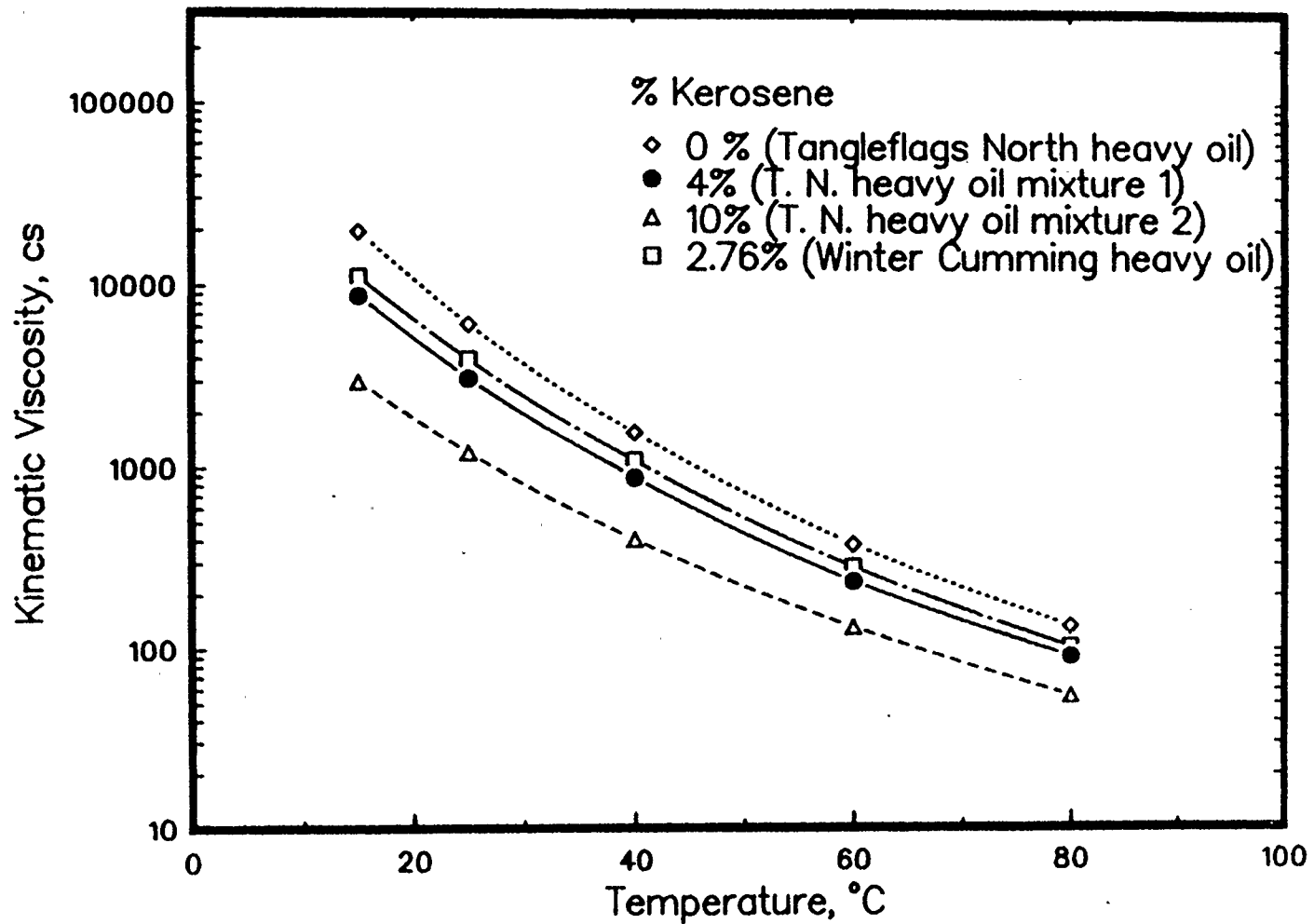


Figure 9: Chart for Simulating Winter Cummings Heavy Oil (Simulating by Mixing Tangleflags North (T.N.) Heavy Oil and Kerosene)

In the second stage the reservoir model was filled with water. This part of the work was delayed until just before the experimental runs. The main reason for this was to avoid water fingering into the oil zone. The empty space on the top of the heavy oil in the reservoir model was flooded with water through two fittings located near the top of the reservoir model. The air displaced by water was withdrawn through the other fitting. After the water filling process was done, the reservoir model was turned upside down. In the third stage, water was recycled continuously using a very low flow rate for three minutes to assure that no air bubbles were trapped in the reservoir model during the water filling process. These filling procedures for both experimental schemes with (right side) and without (left side) bottom water are shown in Figure 10. The water used in the experiments was fresh tap water.

The steam supply for the experimental runs was taken from the University steam plant. A regulator was used to control the steam supply to a pressure in the range between 115 to 205 kPa (2-15 psig). Heating tapes were used to maintain the steam supply line at up to 5°C above the saturated steam temperature so as to obtain dry steam (100% steam) at the injection well. The steam supply line was insulated with fibreglass insulation to avoid excessive heat loss.

During the experimental run, a Bolex model H16 SB/SBM movie camera was used to shoot time lapse movies of the development of

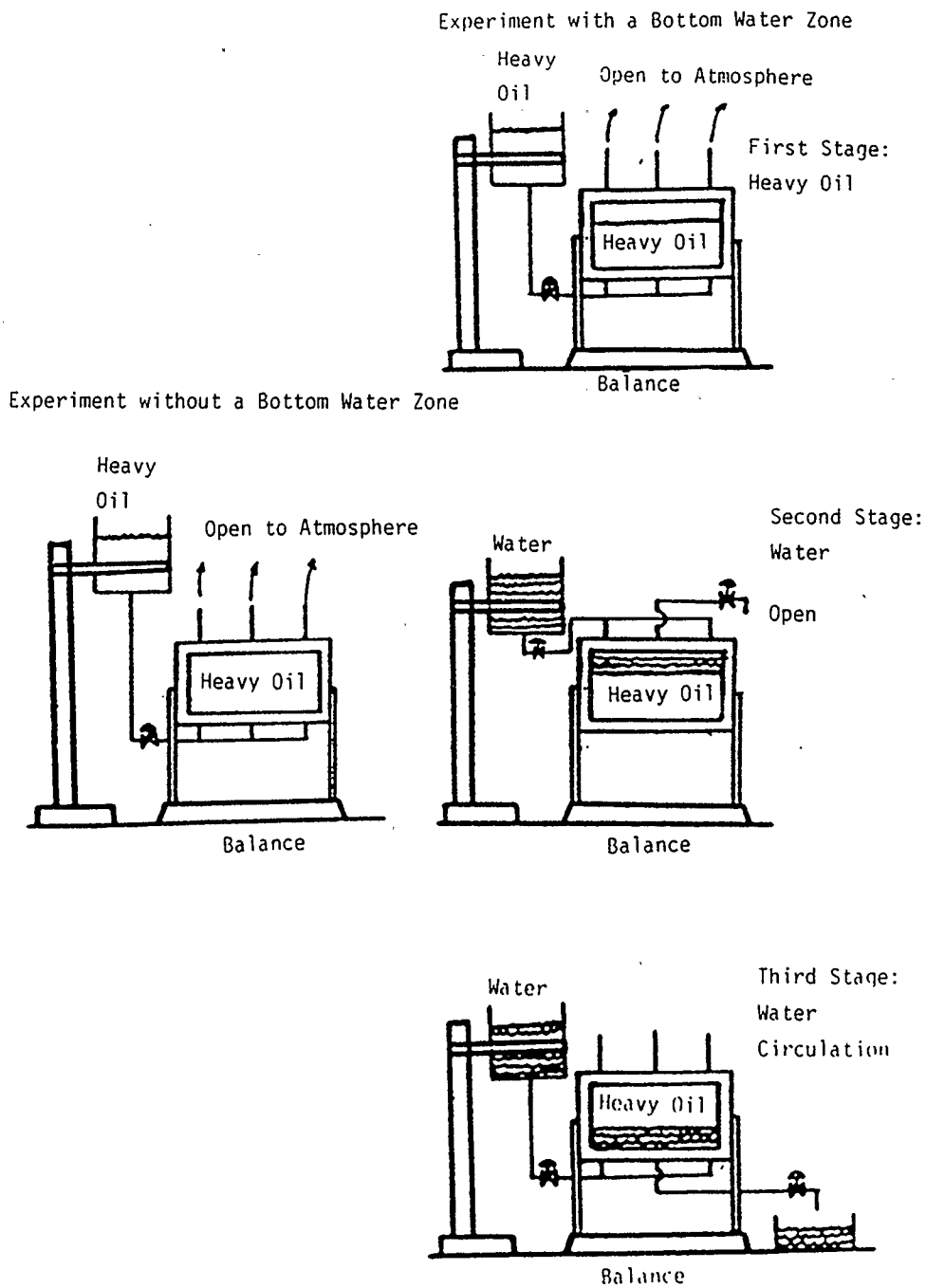


Figure 10: Experiment Preparations for Saturating the Reservoir Model with Heavy Oil and Water

the steam chamber and the movement of the oil and the bottom water. The temperature distribution in the reservoir model was monitored continuously by 42 thermocouples using a Taurus data acquisition system connected to a Radio Shack Model 4 computer. The temperature readings obtained during the experiment were recorded on a magnetic floppy disk and also printed using an Epson FX80 printer.

The changing weight of the reservoir model during the experiment was continuously monitored using a Toledo Model 2300/8139 electronic scale. A Sartorius Model 1507 electronic scale was used to monitor the changing weight of the water tank for experimental runs with a bottom water zone. The results were recorded on a Roland Model PR-1012 printer through the use of a Radio Shack Model 100 portable computer at the rate of one reading per minute. The inventory balance of the weight of steam, water and oil in the reservoir model could be calculated throughout the experiment using the data obtained from the measurements of the changing weight of the reservoir model, the water tank and the weight of oil and water produced during the experiment.

3.4 Sample Analysis

The oil and water produced from the reservoir model during the experimental run was collected in preweighed, 150 g. (5 oz.) capacity glass bottles at 5 minute intervals.

A practical technique for determining the amount of water and oil in the samples collected in the glass bottles during the experiments was adapted from Chung's (1986) work. The samples were cooled in a refrigerator at 5°C for 24 hours. The oil became much more viscous and immobile than the free water after the cooling, and the free water was easily removed from the samples by simply pouring it out of the glass bottles.

For the remaining water/oil emulsion, samples were mixed with 20 ml. of toluene containing 2.5% "Breaxite 8204" demulsifier and the samples were allowed to soak for 24 hours at room temperature (25°C). The main purpose of adding the solvent mixture of toluene and "Breaxite 8204" was to increase the density difference between the two phases (diluted heavy oil and water). The samples were transferred into 100 ml. centrifugal tubes. The bottles were rinsed by adding about 10 ml. toluene and then, the toluene which was used for rinsing the bottles was added to the centrifuge tubes. The centrifuge method, ASTM D4007-81 was applied to analyze the content of the water in the water/oil emulsion samples.

The centrifuge tubes were placed in an IEC Model K for 20 minutes at 3600 rpm. The apparatus is shown in Figure 11.

The clear separation between the oil and water phase could be analyzed easily after the samples were centrifuged. The results were read into an IBM Model PC-XT personal computer and the data was later transferred to the University of Calgary

mainframe computer. They could also be analyzed quickly using a Lotus 1-2-3 electronic spreadsheet.

3.5 Scaled Reservoir Model Characterization

Physical properties of the porous materials used for the experiments are summarized in Table 1. The porous materials used in the experiments are 2 mm and 3 mm glass beads. The selection criteria for using these materials was based on the chemically inert nature of heavy oil, water and steam, the narrow range of size distribution and the spherically shaped particles which provided a uniformly random packing. The density and porosity of the porous materials were determined by the volumetric displacement method. The size distribution of the porous materials was determined by the Tyler Sieves method ASTM.

The permeability of the porous media was determined by the method described in ASTM Designation 2434-68. Water was injected at a constant flow rate through a test apparatus filled randomly with porous materials. A photograph of the test apparatus is shown in Figure 12. The pressure across the test apparatus was measured with manometers when the systems reached steady state.

The permeability for the porous materials was calculated from Darcy's Law. Figure 13 illustrates the schematic diagram of the permeameter.

The relative permeability for the flow of oil in the model was assumed to be 0.4. This assumption was also used in previous



Figure 11: Photograph of Centrifuging Test Apparatus (IEC Model K)

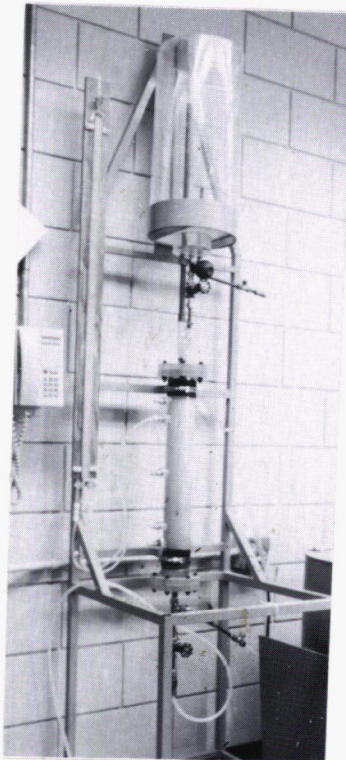


Figure 12: Photograph of the Permeability Test Apparatus

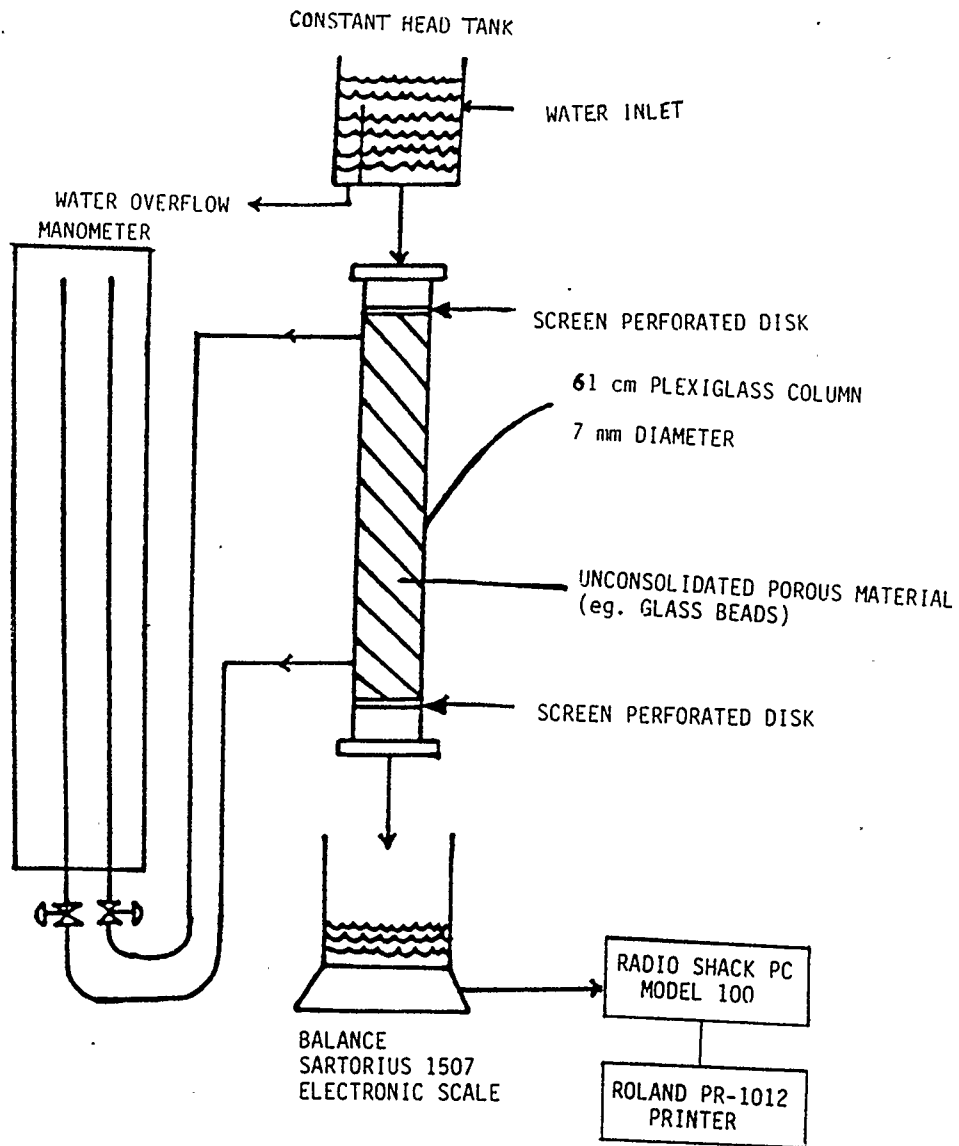


Figure 13: Schematic Diagram of Permeameter

work by Butler et al (1979, 1981) and Chung (1987). Therefore, the absolute permeability shown in Table 1 was multiplied by 0.4 to obtain the effective permeability for the flow of oil in the model.

3.6 Operating Conditions

Several experimental runs were conducted to study the potential application of the steam-assisted gravity drainage process for heavy oil reservoirs with the presence of bottom water. The summary table of the operating conditions applied for the experiments are shown in Table 2 and Figures 14-16. Descriptions explaining the purpose of the experiments are summarized below.

3.6.1 Repeatability of Experimental Results

Two identical experiments (Runs No. 1 and 2) were performed to reassure the repeatability of experimental results. The reservoir model was completely saturated with simulated Winter Cummings heavy oil (3000 cp at 27.8°C). The steam was injected near the top of the reservoir model and the production well placed at the bottom of the reservoir model.

3.6.2 Effect of Reservoir Permeability

The effect of reservoir permeability was studied using two different sizes of glass beads packing: 2 mm and 3 mm diameter. The steam injection pressure was the same at 153 kPa pressure. Two experimental runs were conducted (Runs No. 2 and 4).

The Production of Saskatchewan Heavy Oils Using Steam-Assisted Gravity Drainage

Table 1: PHYSICAL PROPERTIES OF 2 AND 3 MM GLASS BEADS

	2 mm glass beads *	3 mm glass beads
Density, kg/m ³	2490 +/- 50	2200 +/- 50
Porosity, % PV	39.0 +/- 0.2	39.0 +/- 0.2
Permeability, m ²	(2.36 +/- 0.10)*10 ⁻⁹	(4.40 +/- 0.65)*10 ⁻⁹
Size Distribution		
Tyler Screen Scale	Sieve Opening mm	Percent Weight
+8 - 9-	2.00 - 2.36	0.34
+9 - 10-	1.70 - 2.00	53.42
+10 - 12-	1.40 - 1.70	45.65
+12 - 14-	1.18 - 1.40	0.55
+14 -	1.18 and smaller	0.04
+6 - 4-	4.76 - 3.35	0.56
+8 - 6-	3.35 - 2.38	99.44
+9 - 8-	2.38 - 2.00	0.00
+10 - 9-	2.00 - 2.38	0.00

Note : Data for physical properties of 2 mm glass beads are obtained from Chung(1987).

The Production of Saskatchewan Heavy Oils Using Steam-Assisted Gravity Drainage

Table 3: SUMMARY OF THE RESULTS FOR ALL EXPERIMENTAL RUNS

Run No.	Lab Time (Hours)	Effective Permeability Oil Flow (Darcy)	Percentage Bottom Water Layer *	Steam Pressure (kPa)	Bottom Water Pressure (kPa)	Distance between The Injector To The Producer (cm)	Interwell Spacing (cm)	Cumulative Percent Oil Recovery
1	2.5	940	0	153	0	21	35	85
2	2.67	940	0	153	0	21	35	86
3	3.0	940	0	119	0	21	35	85
4	1.33	1760	0	153	0	21	35	87
5	1.5	1760	16	153	143	13	35	79
6	1.5	1760	16	170-153	143	13	35	75
7	1.17	1760	41	170-153	143	13	35	48
8	1.25	1760	41	170-148	143	13	35	56
9	1.5	1760	41	170-153	143	21	35	70
10	3.42	1760	0	153	0	21	68	85
11	2.25	1760	16	153	143	13	68	73
12	2.0	1760	28	153	143	13	68	59

Note: * - The percentage of bottom water layer = (bottom water thickness/(bottom water+oil thickness))*100 %
 The porosity of the porous packing for all experimental runs = 0.39
 The reservoir model is 35 cm wide, 22 cm high and 3 cm thick.

OPERATING PRESSURE PROFILES

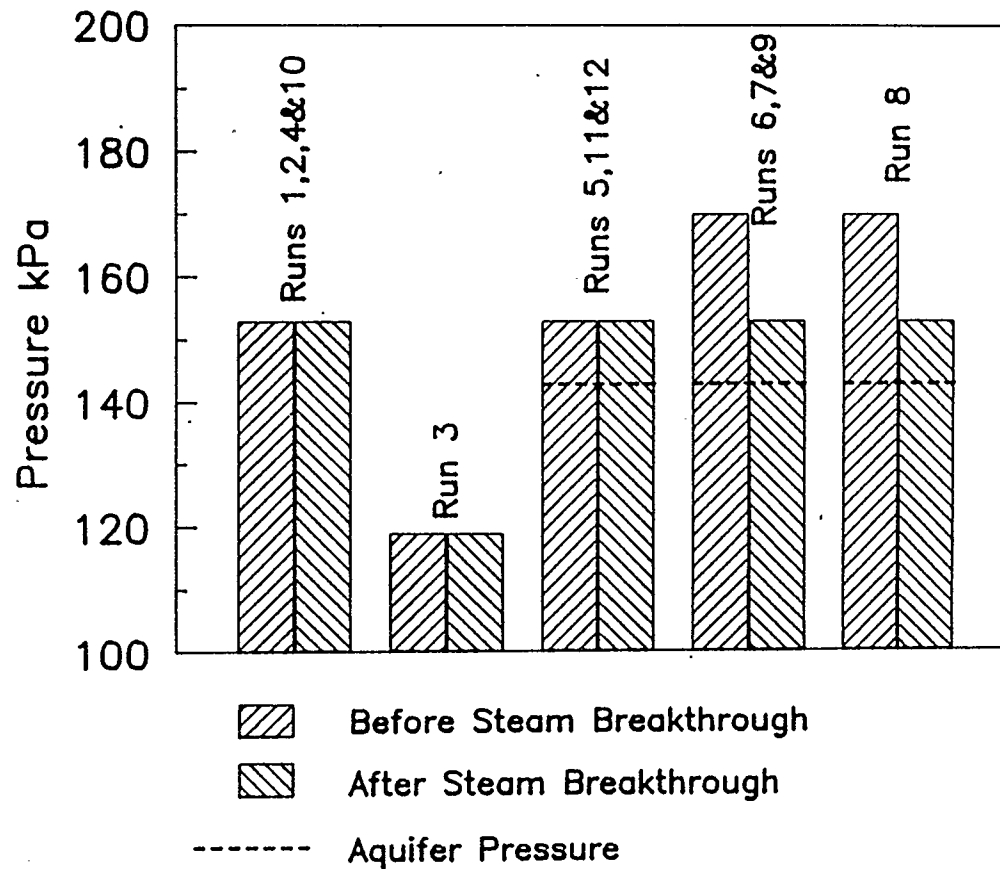
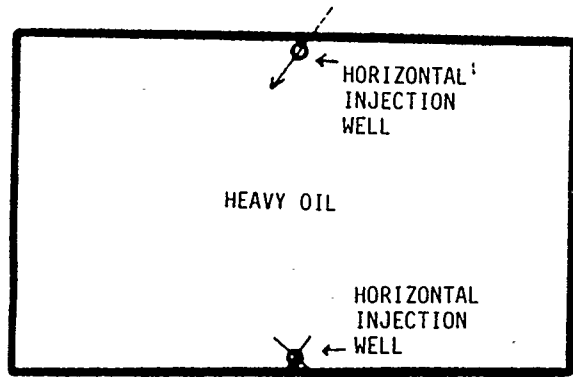
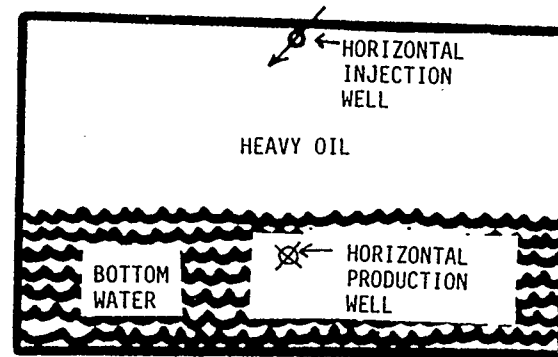


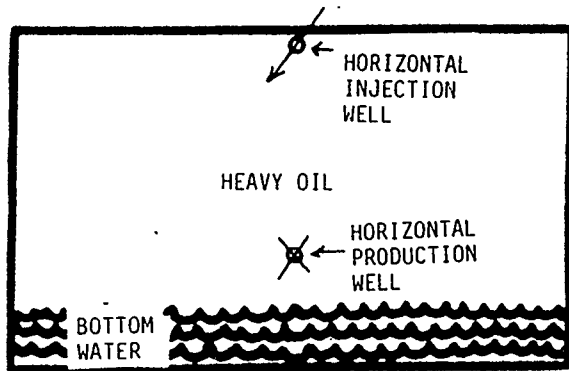
Figure 14: Operating Pressure Profiles for Laboratory Experimental Programs



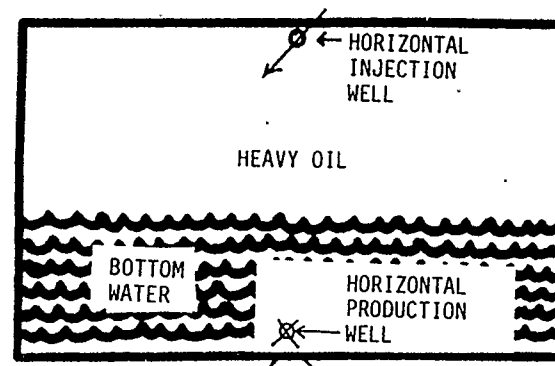
Runs No: 1-4



Runs No: 7 and 8

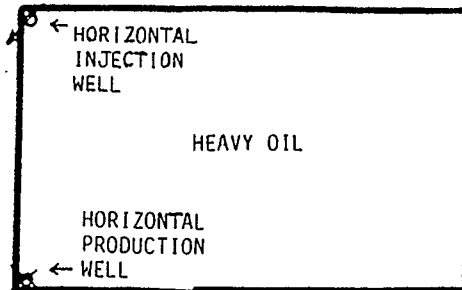


Runs No: 5 and 6

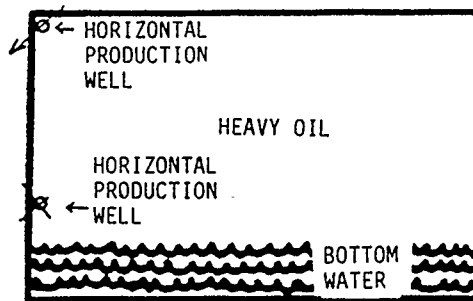


Run No: 9

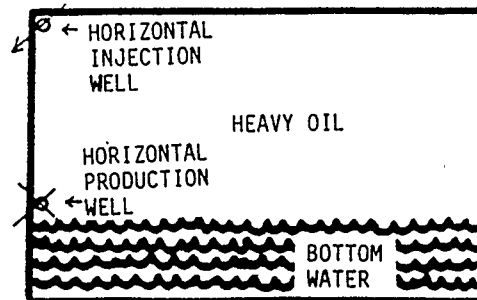
Figure 15: Well Configurations for Experimental Runs No: 1-9



Run No: 10



Run No: 11



Run No: 12

Figure 16: Well Configurations for Experimental Runs No: 10-12

3.6.3 Effect of Steam Injection Pressure

3.6.3.1 Case Without a Bottom Water Zone

Two experimental runs (Runs No. 2 and 3) were conducted using two different steam injection pressures (119 kPa or 2 psig and 153 kPa or 7.5 psig respectively). The steam injection pressure was maintained at a constant level throughout both experiments.

3.6.3.2 Case With a Bottom Water Zone

Four experimental runs were conducted to study the effect of varying the steam injection pressure.

1) Effect of Steam Injection Pressure Before Steam Breakthrough

The initial communication path between the injection and the production wells was created just prior to the steam breakthrough. At this period, the steam chamber was expanding and pushing the cold oil into the production well. The pressure drop between the injection and the production wells was the main driving force for producing the oil. Two experimental runs (Runs No. 5 and 6) were conducted using two different steam injection pressure levels, 153 kPa or 7.5 psig and 170 kPa or 10 psig respectively. The bottom water thickness was 3.5 cm or 16% of the total thickness of the bottom water zone and oil zone for both experimental runs.

ii) Effect of Steam Injection Pressure After Steam Breakthrough

After the steam breakthrough at the production well, the steam injection pressure was maintained. Basically there was almost no pressure drop between the injection and the production well. This condition could be achieved by creating a closed system for the steam chamber inside the reservoir model, thereby maintaining the liquid level above the production well and avoiding any steam bypass. Two experimental runs (Runs No. 7 and 8) were performed using two different steam injection pressures (153 kPa and 148 kPa). The bottom water thickness was 9 cm or 41% of the total thickness of the bottom water plus the oil zone for both experiments.

3.6.4 Effect of Interwell Spacing

3.6.4.1 Case Without a Bottom Water Zone

To study the effect of interwell spacing, two experimental runs (Runs No. 4 and 10) were carried out using two different interwell spacings (0.35 m and 0.68 m). Note: The interwell spacing used here is twice the halfwell spacings in the model (0.175 m and 0.34 m).

3.6.4.2 Case With a Bottom Water Zone

Two experimental runs (Runs No. 5 and 11) were conducted using two different interwell spacings (0.35 m and 0.68 m). The bottom water zone thickness was 3.5 cm or 16% of the total thickness of the bottom water zone and the oil zone.

3.6.5 Effect of Thickness of the Bottom Water Zone

Three experimental runs (Runs No. 10, 11 and 12) were conducted using various thicknesses of the bottom water zone, (0 cm, 3.5 cm and 6 cm or 0%, 16% and 28% respectively of the total thickness.)

3.6.6 Effect of the Location of the Production Well

To study the effect of the location of the production well in the reservoir model, three experiments (Runs No. 5, 7, and 9) were carried out. During experimental Run No. 5, the production well was located 3.5 cm above the water oil contact (WOC). For experimental Run No. 7, the production well was placed 2 cm below the WOC and for experimental Run No. 9, the production well was located 8 cm. below the WOC. The distances from the WOC used in the calculations were measured from the midpoint of the opening of the production well.

It should be noted that the original oil in place (OOIP) volumes are computed based on the volume of the oil above the production well.

CHAPTER 4

THEORY

Steam-assisted gravity drainage is a unique form of steamflood for recovering heavy oil by the continuous injection of steam into a growing steam chamber formed above a horizontal production well. In this process, the steam pressure within the chamber is maintained approximately constant by controlling the steam injection rate. Steam flows to the perimeter of the chamber and condenses. The heat liberated by the steam raises the temperature of the oil which drains parallel to the interface and moves into the production well driven by gravity forces. Butler et al (1979, 1981, 1985 a & b, 1987) developed theoretical predictions for oil production using two parallel horizontal wells.

4.1 Drainage Rate Prediction

The drainage rate prediction for the oil was described by Butler et al (1981). The method described in this paper was called "TANDRAIN" and it involves the following expressions.

4.1.1 Dimensionless Time

$$\tau_d = \frac{t}{W} \sqrt{\frac{K_g \alpha}{\phi \Delta S_o m \nu_S H}} \quad (4.1)$$

where:

τ_d - dimensionless time

W - half of the horizontal interwell spacing, m

- t - time, sec.
 K - effective permeability of the oil flow, m^2
 g - acceleration due to gravity, $m/sec.^2$
 α - thermal diffusivity of the reservoir material, $m^2/sec.$
 H - drainage height of the reservoir, m
 i.e. the vertical distance between the top of the reservoir and the horizontal well
 ϕ - porosity of the reservoir, fraction
 ΔS_o - difference between the initial and residual oil saturation, fraction
 ν_s - kinematic viscosity of oil at steam temperature $m^2/sec.$
 m - a dimensionless constant which is dependent upon the condition used and upon the nature of the heavy oil

4.1.2 Extended Definition of "m"

The exponent "m" is calculated from the viscosity temperature relation for the oil. It is a function of the viscosity of the oil, the steam temperature and the reservoir temperature. The expression "m" is calculated by Butler (1985b) as:

$$m = \left[\nu_s \int_{T_r}^{T_s} \left(\frac{1}{\nu} - \frac{1}{\nu_r} \right) \frac{dT}{T - T_r} \right]^{-1} \quad (4.2)$$

where

- ν - kinematic viscosity at any temperature T , $m^2/sec.$
 ν_s - kinematic viscosity at the steam temperature
 ν_r - kinematic viscosity at initial reservoir temperature, $m^2/sec.$

T_S = steam temperature

T_R = initial reservoir temperature

4.1.3 Viscosity-Temperature Relation

The viscosity-temperature relation used for the calculations in this study was Walther's equation with appropriate constants. The following steps were used during the calculation. First, the viscosities at two temperatures (20°C and 80°C) were obtained from the laboratory data, and then a viscosity temperature equation to pass through these two points was constructed using Walther's equations. This equation is the relationship used to construct the special graph paper known as the "ASTM Viscosity-Temperature Chart for Liquid Petroleum Products" (ASTM D341-39). It is used for viscosity prediction at various temperatures.

Walther's Equation.

$$\ln (\ln (\nu + 0.8)) = A \ln (T + 460) + B \quad (4.3)$$

ν = kinematic viscosity at T, centistokes.

T = temperature, °F

A, B = constants

Values for the simulated Winter crude used in this study:

$$A = - 3.75 \quad B = 25.69$$

4.1.4 Dimensionless Drainage Rate

The dimensionless drainage rate equation is empirically derived by Butler et al (1981), using the "TANDRAIN" assumption. A simple approximation for the dimensionless drainage rate can be

expressed as the following.

$$Q_d = \sqrt{\frac{3}{2}} - \tau_d \sqrt{\frac{2}{3}} \quad (4.4)$$

(one side)

where:

Q_d - dimensionless drainage rate

τ_d - dimensionless time

4.1.5 Total Drainage Rate

The oil production rate was computed for two sides to represent an actual steam chamber during the reservoir depletion. The equation can be illustrated as

$$Q = 2Q_d \sqrt{\frac{Kg\alpha H\phi\Delta S_o}{m\nu_s}} \quad (4.5)$$

(two sides)

where

Q - total drainage rate, $m^3/d m$

The other variables are defined earlier.

4.2 Percent Oil Recovery During the Reservoir Depletion

The oil recovery during the depletion of the reservoir can be computed by integrating the dimensionless drainage rate with respect to changes in the dimensionless time. This can be expressed by the following equation.

$$\text{Percent Oil Recovery} = \left\{ \int Q_d dt_d \right\} * 100\% \quad (4.6)$$

A computer program was developed to calculate the drainage rate prediction and percent oil recovery during the

reservoir depletion using the Lotus 1-2-3 software package (1986). A sample of the input and output for the computer program is shown in Appendix B.

4.3 Scaling Criteria for the Field Condition

The reservoir model is scaled to Winter field conditions by using the method described by Butler (1985a). The reservoir dimensions and the permeability of the porous pack were selected so as to make the model dimensionally similar to the field. For dimensional similarity, it is necessary that the dimensionless number B_3 is the same for the reservoir model as it is for the field.

$$B_3 = \sqrt{\frac{KgH}{\alpha\phi\Delta S_o m' S}} \quad (4.7)$$

Examination of the dimensionless number B_3 indicates that it would be possible to compensate high H and low K in the reservoir with low H and high K in the model.

The dimensionless equation 4.1 is used to relate time for the reservoir model with the time for the field operation.

This scaling would correspond to the same ratio for W/H in the model as in the field. However, as will be seen later, predictions can be made, using equations 4.1, 4.4 and 4.5, for other ratios of W/H.

CHAPTER 5

RESULTS

A total of twelve experiments completed in the scaled physical reservoir model are described. These were divided into two groups: one without bottom water in the reservoir model (Runs 1,2,3,4 and 10), and another group with the presence of bottom water (Runs 5,6,7,8,9,11 and 12). The summary of the results of the experimental runs are shown in Table 3.

5.1 Mechanism

In a typical experimental run, the mechanism of the reservoir depletion was classified into two mechanisms. The first was oil displacement by steam during the initial communication period, and the second was the steam-assisted gravity drainage process after the initial communication period.

Since many phenomena were common to all experimental runs, only two typical experiments (Run 10 without the bottom water zone and Run 11 with the bottom water zone) are described.

5.1.1 Oil Displacement by Steam During the Initial Communication Period

During this initial communication period, a heated flow path between the injection and the production well was created. Steam was injected near the top of the reservoir. The steam chamber grew sideways and downwards and the steam pushed cold oil into the production well located at the bottom of the reservoir

The Production of Saskatchewan Heavy Oils Using Steam-Assisted Gravity Drainage

Table 2: SUMMARY OF OPERATING CONDITIONS FOR ALL EXPERIMENTAL RUNS

Run No.	Lab Time (Hours)	Packing Material (mm)	Effective Permea. Oil Flow (Darcy)	Bottom Water Layer (cm)	Percentage Bottom Water Layer *	Position Of The Producer (cm from bottom)	Interwell Spacing (cm)	Steam Pressure (kPa)	Bottom Water Pressure (kPa)
1	2.5	2	940	0.0	0	0.5	35	153	0
2	2.67	2	940	0.0	0	0.5	35	153	0
3	3.0	2	940	0.0	0	0.5	35	119	0
4	1.33	3	1760	0.0	0	0.5	35	153	0
5	1.5	3	1760	3.5	16	7.5	35	153	0
6	1.5	3	1760	3.5	16	7.5	35	170-153	143
7	1.17	3	1760	9.0	41	7.5	35	170-153	143
8	1.25	3	1760	9.0	41	7.5	35	170-148	143
9	1.5	3	1760	9.0	41	0.5	35	170-153	143
10	3.42	3	1760	0.0	0	0.5	68	153	0
11	2.25	3	1760	3.5	16	7.5	68	153	143
12	2.0	3	1760	6.0	28	7.5	68	153	143

Note: * - The percentage of bottom water layer = (bottom water thickness/(bottom water+oil thickness))*100 %

The position of the injector for all experimental runs is 0.5 cm from the top of the reservoir model

The reservoir model is 35 cm wide, 22 cm high and 3 cm thick.

model. In experiments involving bottom water, some water was displaced from the model into the aquifer reservoir tank during this period. Condensate from the steam fingered through the oil zone and soon started to flow from the production well. During this period, the fluids produced were cold oil and cold condensate from steam.

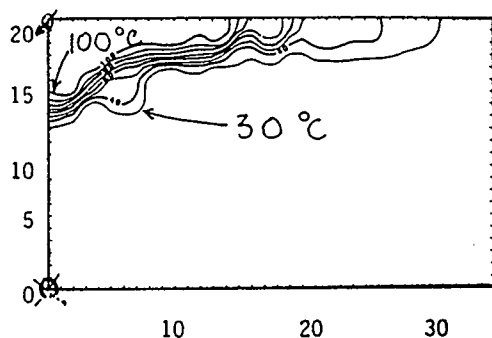
Figure 17 shows the mechanism of the oil displacement by steam as evidenced by isotherms in the reservoir model. As the steam front moved closer towards the production well, it accelerated. Figure 18 shows the temperature of the produced fluids as a function of time. The temperature was constant at the original reservoir temperature until just before steam breakthrough at the production well. After the steam breakthrough, the temperature of the produced fluids rose rapidly to the temperature of the steam injected into the reservoir model.

5.1.2 Steam-Assisted Gravity Drainage after the Initial Communication Period

After the "steam breakthrough", the production well was throttled to avoid steam by-pass and to maintain the liquid level above the production well. This resulted in virtually no pressure differential between the injection and the production wells. The steam chamber grew sideways and condensed at the interface. The liberated heat was conducted to the oil sand and the heated oil and the condensate from the steam drained by gravity into the production well. Figure 19 shows the mechanism

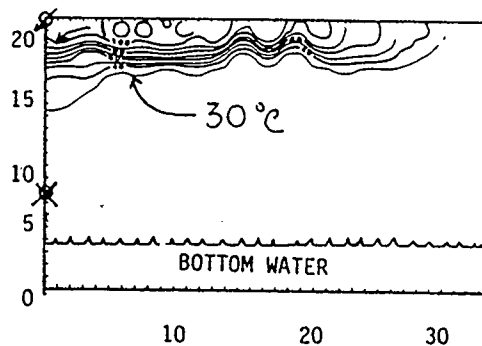
BEFORE STEAM BREAKTHROUGH

RUN NO: 10 WITHOUT BOTTOM WATER(0%)



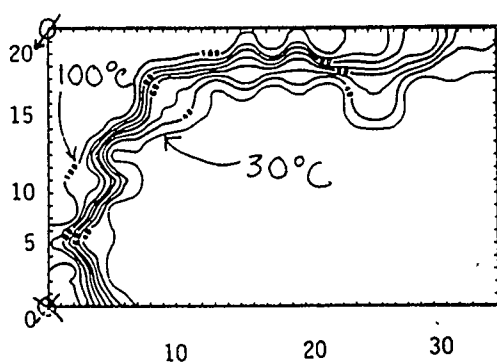
LAB TIME: 8 MINUTES

RUN NO: 11 WITH BOTTOM WATER(16%)



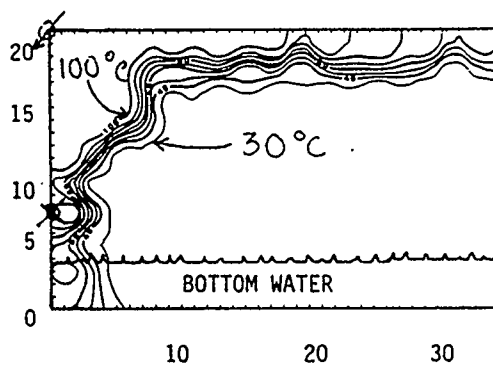
LAB TIME: 6 MINUTES

STEAM BREAKTHROUGH AT 16 MINUTES



LAB TIME: 16 MINUTES

STEAM BREAKTHROUGH AT 10 MINUTES



LAB TIME: 10 MINUTES

⊕ = STEAM INJECTION WELL

⊗ = PRODUCTION WELL

Figure 17: Temperature Distribution in the Reservoir Model at Various Time for Experimental Runs with and without a Bottom Water Zone. The Isotherms are in Degrees Celcius, and the Dimensions of the Reservoir Model are in Centimeters.

TEMPERATURE OF PRODUCED FLUIDS AS A FUNCTION OF TIME

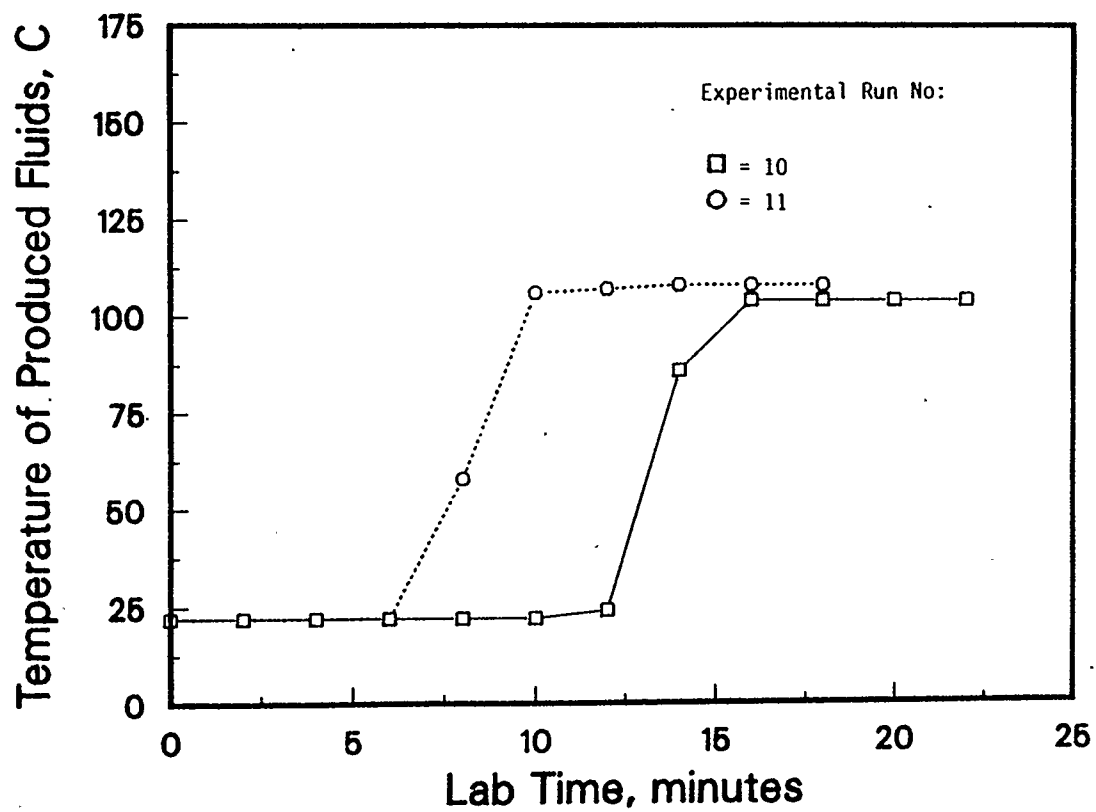


Figure 18: Temperature of Produced Fluids as a Function of Time

AFTER STEAM BREAKTHROUGH

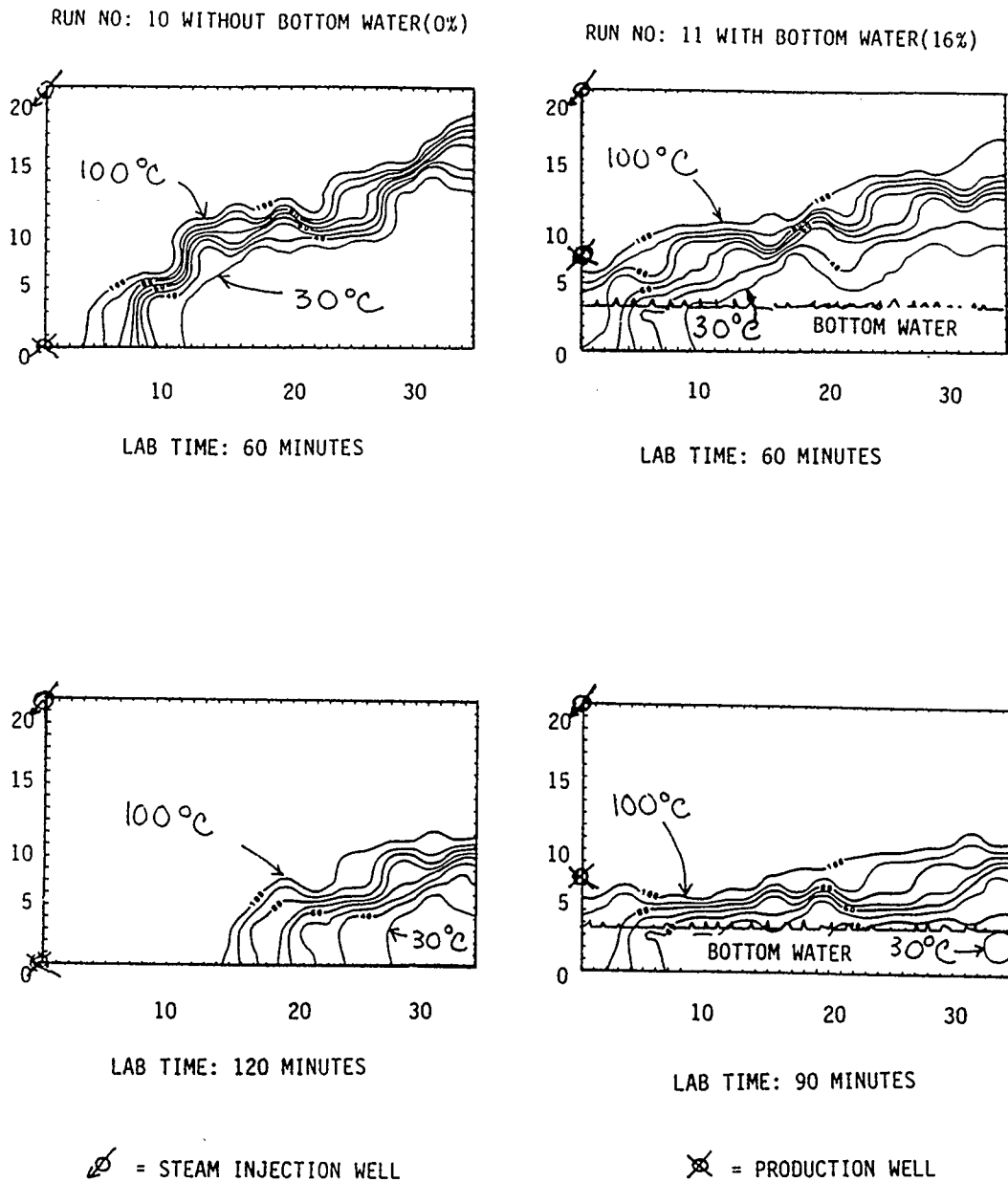


Figure 19: Temperature Distribution in the Reservoir Model at Various Time for Experimental Runs with and without a Bottom Water Zone. The Isotherms are in Degrees Celcius, and the Dimensions of the Reservoir Model are in Centimeters.

of oil displacement by steam as evidenced by isotherms in the reservoir model.

5.2 Temperature Distribution in the Reservoir Model

The temperature readings were stored on a magnetic floppy disk and later downloaded into the University of Calgary's mainframe computer system (Honeywell Multics). "Surface II", a software system for graphical plotting was used to draw the isotherms for the reservoir model. The Piece-Bessel interpolation technique was used in this graphical software to smooth the isotherms within the user specified grid cell (Sampson (1978)).

Since most of the experiments showed similar trends for the temperature distribution in the reservoir model, only two typical experimental runs (Run 10 for the no bottom water group and Run 11 for the bottom water group) have been described. The temperature distribution in the reservoir model at various elapsed times for Runs 10 and 11 are shown in Figures 17 and 19. In these figures, the 100°C isotherms can be used as an approximation of the steam front locations during the experiments (the actual recorded steam temperature for the two runs shown was 109°C).

5.2.1 *Experimental Runs Without A Bottom Water Zone (Run 10)*

The isotherms after eight minutes are shown in Figure 17 for Run 10. The steam front continued to move

downwards and sideways and finally reached the production well after 16 minutes. At the steam breakthrough time, the produced oil analyses showed that about 17% of the OOIP had been produced. The area above the 100°C isotherm was integrated, and multiplied by the thickness of the reservoir model and the porosity to provide another estimate of the oil produced by the steam drive from the top of the reservoir model. The calculation gave a result of 16% of the OOIP. This shows the utility of the thermocouple readings for detecting the locations of the steam front movement in the reservoir model.

From 16 minutes to 205 minutes of experimental time, the steam chamber continued to grow and heated oil and the condensate drained by gravity to the production well. Figure 19 shows the isotherms for Run 10 for 60 and 120 minutes of elapsed time.

5.2.2 *Experimental Runs with A Bottom Water Zone (Run 11)*

In Run 11, the steam chamber grew sideways and downwards for 6 minutes of elapsed time as shown in Figure 17. The steam front reached the production well after 10 minutes. According to the oil analyses, 10% of the OOIP was produced at the steam breakthrough. Using the data from thermocouple readings, the volume of oil displaced by the steam chamber was estimated to be 11% of the OOIP. Again, this indicates the accuracy of the thermocouple readings taken during the

experimental runs.

After the steam breakthrough the production well was throttled so that steam would not bypass to the production well or migrate to the bottom water zone. This is confirmed by the temperature distribution in the bottom water zone. (Refer to Figure 19 for the isotherms in the reservoir model for 60 and 90 minutes of elapsed time). Figure 19 shows that the isotherm for 100°C was always above the original location of the water/oil contact shown in Figure 18. This indicates that the steam did not penetrate into the bottom water. By preventing steam intrusion into the bottom water zone, the steam consumption for steam-assisted gravity drainage will be lower than for a conventional steam flood.

In conventional steam flooding, the steam penetrates into the bottom water zone. Following this steam intrusion into the bottom water zone, the steam cannot be plugged off. This finding was reported by Ehrlich, R. (1977).

5.3 Initial Communication Period

It is essential to establish a fluid flow path between the injection and the production wells. With conventional heavy oils, such displacement can, as shown above, be achieved at the initial reservoir temperature. The method could be described as in the initial operation; injected steam will displace oil into the production well.

The experimental results are compared to the predictions obtained by an analytical method for predicting the breakthrough time developed by Butler and Petela (1987). Table 4 shows a comparison of the experimental results and the theoretical predictions. (Butler and Petela, 1987).

Table 4: Summary of the Theoretical Predictions and the Experimental Results for the Initial Communication Period or the Steam Breakthrough Time.

Experimental No.	<u>Initial Communication Period</u>		Theoretical Predictions (minutes)
	Experimental Results Visual Observ. (min.)	Thermocouple Readings (minutes)	
1	18	26	16.6
2	19	26	16.6
3	64	66	48.8
4	12	16	8.85
6	3	4	2.4
10	8	16	8.85
11	6.5	10	3.2
12	5	8	3.2

Figure 20 shows the comparison of the experimental results and the theoretical prediction for the length of the steam breakthrough period compared to the experimental observations. For the experimental results, there were two methods of measuring the time for the initial communication period. The first method was by visual observation when the steam breakthrough occurred at the

Initial Communication Period

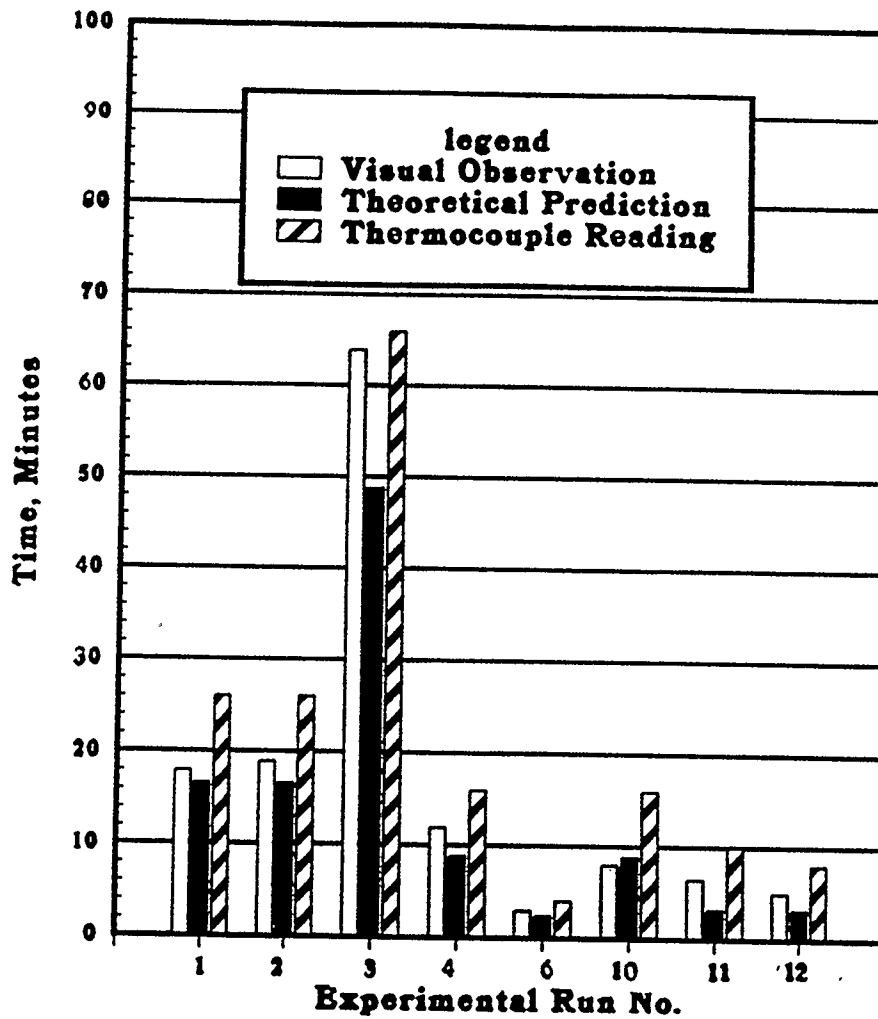


Figure 20: Comparison of Initial Communication Period Between Experimental Results and Theoretical Predictions

production well. The second method was by taking the thermocouple readings located near the production well. The first method was more accurate and more realistic, but the second method was used to prove that the steam had actually reached the production well as evidenced by the temperature reaching the steam saturation temperature. The reasons for the longer initial communication periods for the second method were:

- a) Some of the thermocouples used to detect the steam finger were not located exactly above the production well so it took several minutes for the steam to reach them.
- b) The data acquisition system for the reservoir model was set up to take thermocouple readings at two minute intervals. Therefore, a lag time occurred between the time the actual temperature was reached and the time the thermocouple readings were taken.

Using the theoretical prediction method, Dr. Petela has calculated the initial communication periods for typical heavy oil and bitumen situations found in Alberta and Saskatchewan; the results are shown in Table 5. The results indicate that the steam drive method for creating the initial communication path between the injector and the producer can be applied realistically in fields containing less viscous heavy oil such as Lloydminster type crudes. The reason is that Lloydminster heavy oil is mobile even at the reservoir temperature (3000 cp at

The Production of Saskatchewan Heavy Oils Using Steam-Assisted Gravity Drainage

Table 5: Comparison of Initial Communication Period Predicted by Analytical Method for Various Heavy Oils and Bitumens Found in Alberta and Saskatchewan

Crude Type	Oil Visc. @ Res. Temp.(cp)	Reservoir Temp. (C)	Absolute Permeability Oil Flow (Darcy)	Pressure Diff. Between Injector and Producer (psig)	Pressure Diff. (kPa)	Distance Between Injector and Producer (m)	Initial Communication Period (years)
Llyodminster	3000	20	4.5	700	4826	14.0	0.3
Cold Lake	100000	13	1.5	700	4826	12.5	23.5
Athabasca	1000000	13	2.5	200	1379	2.0	7.4

27.8°C), so the communication path can be created in relatively short period of time. For more viscous oil such as Cold Lake (100,000 cp at 13°C), it is possible to create a communication path in a relatively short period by placing the production well relatively close to the injection well. Another potential method is to preheat the area between the injection well and the production well through circulating the steam in the annulus of the injection well (Chung et al, 1987). The heat liberated by the steam will reduce the viscosity of the oil. The heated oil is then displaced by the steam to create a communication path between the injector and the producer. For a very viscous bitumen such as Athabasca bitumen with a viscosity of 1,000,000 cp at 12°C, the potential methods described for Cold Lake may be applied with more restricted criteria by selecting a closer distance between the injector and the producer, or applying a longer time for preheating the area between the injector and the producer.

The theoretical prediction developed by Butler and Petela (1987) can be used to screen the reservoirs that are suitable for implementing the steam drive method to create an initial communication path between the production and injection wells. The basis for selecting a suitable reservoir is from the length of the initial communication period. If the initial communication period is very long, the project life of a commercial steamflood becomes uneconomic.

5.4 Repeatability of Results

Repeatability of results of the experimental runs was examined in Runs 1 and 2 using the same conditions. Although slight differences in the initial conditions did occur, the results showed a good overall repeatability. (see Table 3).

Figure 21 compares the production rates for experimental Runs 1 and 2. The production rates for both experiments increased rapidly and reached a peak after 20 minutes of production time. The steam breakthrough at the production well was recorded after 18 minutes for Run 1 and 19 minutes for Run 2. The production of oil before the steam breakthrough was due to steam flooding from the top of the reservoir. The produced oil and water were essentially at the original reservoir temperature until the steam breakthrough, and then the temperature of the produced fluids increased to almost that of the steam temperature. The peak production rate occurred around the time shortly after steam breakthrough for both experiments after which the production rate declined rapidly as the reservoir depleted. The mechanism of oil production after the steam breakthrough was through steam-assisted gravity drainage.

For example, comparison of the two experimental runs (Figures 21 and 22) at virtually identical times near the end of each run (2.5 lab hours) yielded nearly the same cumulative oil recoveries (85% for Run 1 and 86% for Run 2), the steam breakthrough at the production well (18 min. production time with 19%

DUPLICATE BASE RUNS

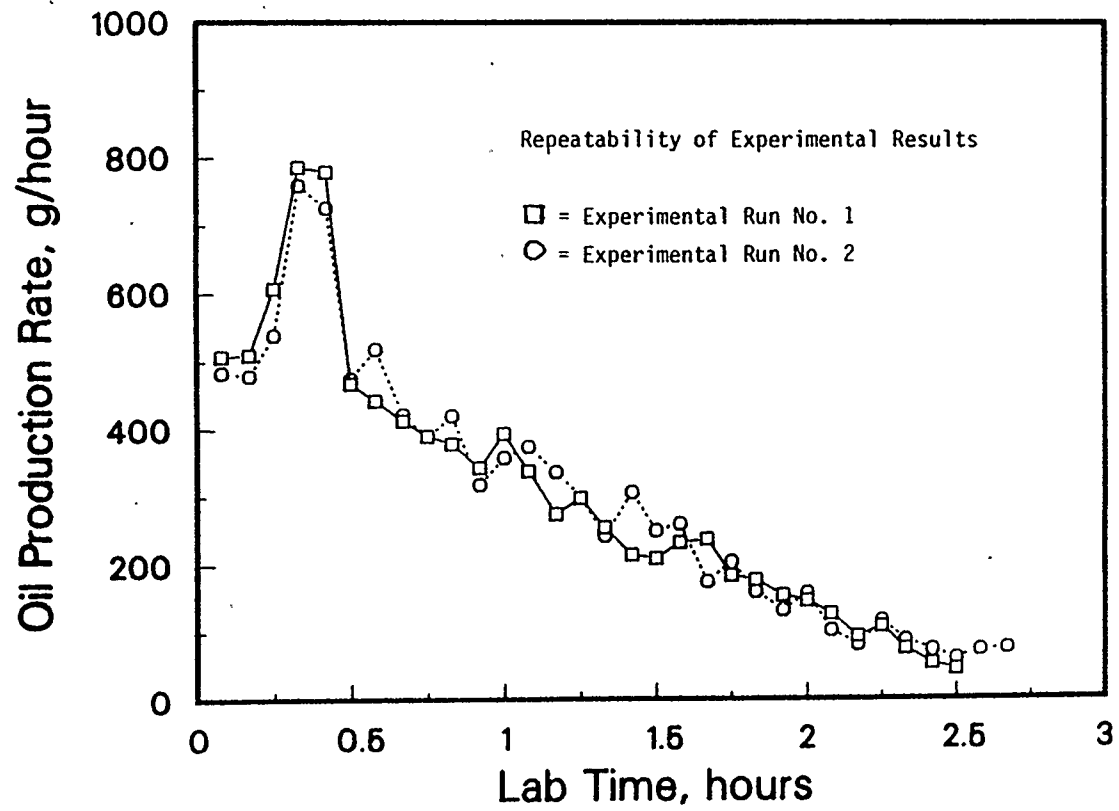


Figure 21: Oil Production Rate as a Function of Time

DUPLICATE BASE RUNS

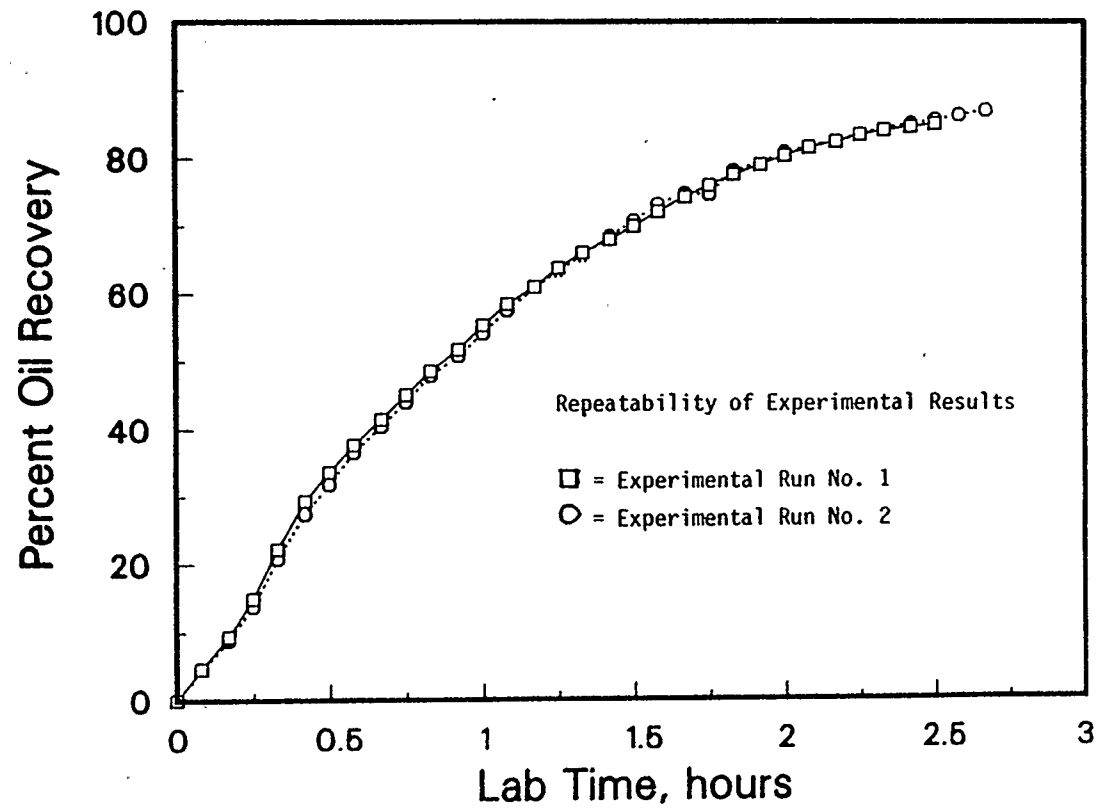


Figure 22: Percent Oil Recovery as a Function of Time

of OOIP produced for Run 1 and 19 min. production time with 19% of OOIP produced for Run 2), and the same production rate trend. It was concluded that the reservoir model yielded consistent, repeatable data.

5.5 Effect of Steam Injection Pressure

5.5.1 Experimental Runs Without A Bottom Water Zone

The effect of steam injection pressure was investigated using two similar experiments operating at different pressure levels. Run 2 used 153 kPa steam pressure and Run 3 used 119 kPa steam pressure. The experiment at the higher pressure showed a higher production rate and shorter production time (Figure 23). Both experimental runs showed similar trends in the production curve. The maximum rate for both experiments was reached just after the steam breakthrough times which were 19 minutes for Run 2 and 64 minutes for Run 3. The amount of oil recovered at the steam breakthrough was 19% for Run 2 and 44% for Run 3. The results indicate that the amount of oil produced and the steam breakthrough times decreased as the steam injection pressure increased.

Figure 24 shows the effect of steam pressure on the cumulative oil recovery. Faster oil recovery was achieved faster using the higher steam pressure but the cumulative oil recovery near the end of both experiments was approximately the same (87% of OOIP for Run 2 at 160 minutes and 85% of OOIP at 180 minutes for Run 3).

EFFECT OF STEAM PRESSURE

EXPERIMENTS WITHOUT A BOTTOM WATER ZONE

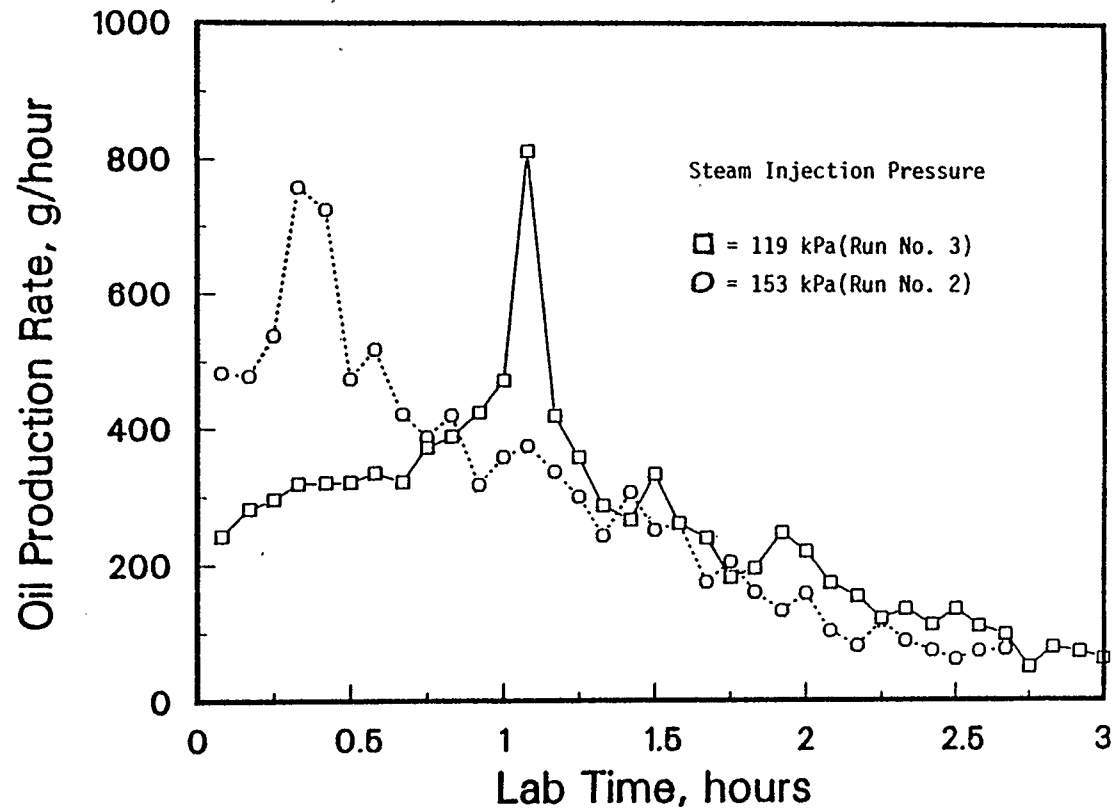


Figure 23: Oil Production Rate as a Function of Time

EFFECT OF STEAM PRESSURE

EXPERIMENTS WITHOUT A BOTTOM WATER ZONE

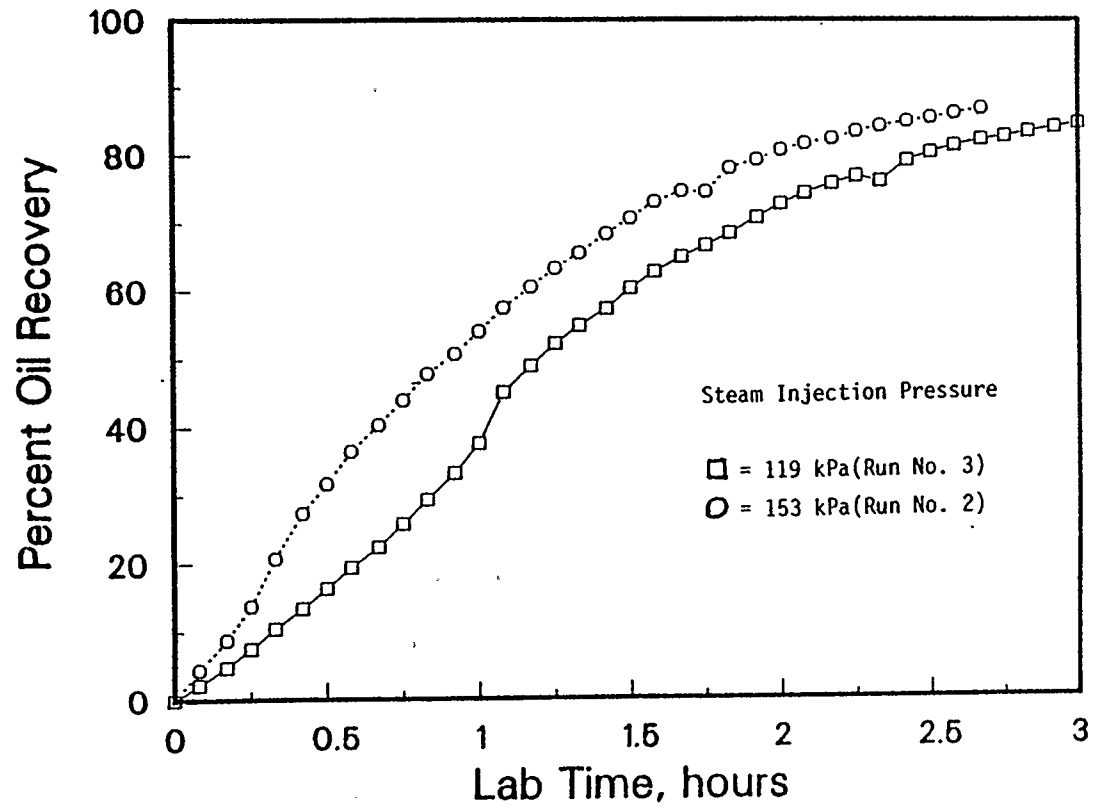


Figure 24: Percent Oil Recovery as a Function of Time

5.5.2 Experimental Runs with a Bottom Water Zone

i) Before Breakthrough

Two runs were conducted to study the effect of steam injection pressure on the formation of the initial communication path between the injector and the producer. In Run 6 where the steam injection pressure was set at 170 kPa, the initial communication path was created after 3 minutes of production time. In Run 5, the initial communication path was created after 10 minutes of production time with an injection pressure of 153 kPa. The higher steam injection pressure pushed oil towards the production well more rapidly however, this advantage was offset by more oil being lost into the bottom water zone which was a "pressure sink".

Figure 25 shows the cumulative oil recoveries. The oil recovery at the end of 90 minutes production time was 79% of the OOIP for Run 5 and 75% of the OOIP for Run 6. The cumulative oil recovery was better for the experimental runs using a lower steam injection pressure.

Figure 26 compares the oil production rate at various times; both peaked after the steam breakthrough. The production history curves for both experiments showed rapid increases and reached a maximum peak at 15 minutes in Run 5 and 10 minutes in Run 6. After that, the oil production rates decreased steadily as the reservoir became depleted.

EFFECT OF STEAM PRESSURE BEFORE STEAM BREAKTHROUGH
EXPERIMENTS WITH A BOTTOM WATER ZONE

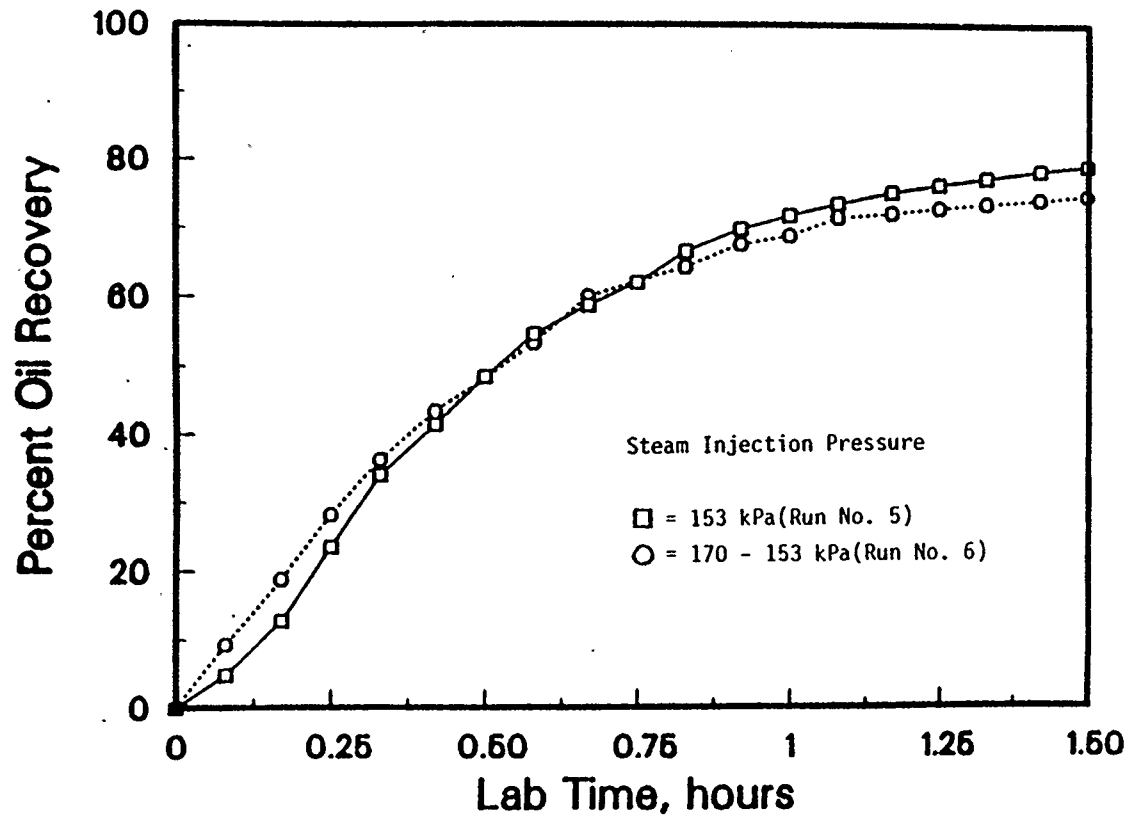


Figure 25: Percent Oil Recovery as a Function of Time

EFFECT OF STEAM PRESSURE BEFORE STEAM BREAKTHROUGH
EXPERIMENTS WITH A BOTTOM WATER ZONE

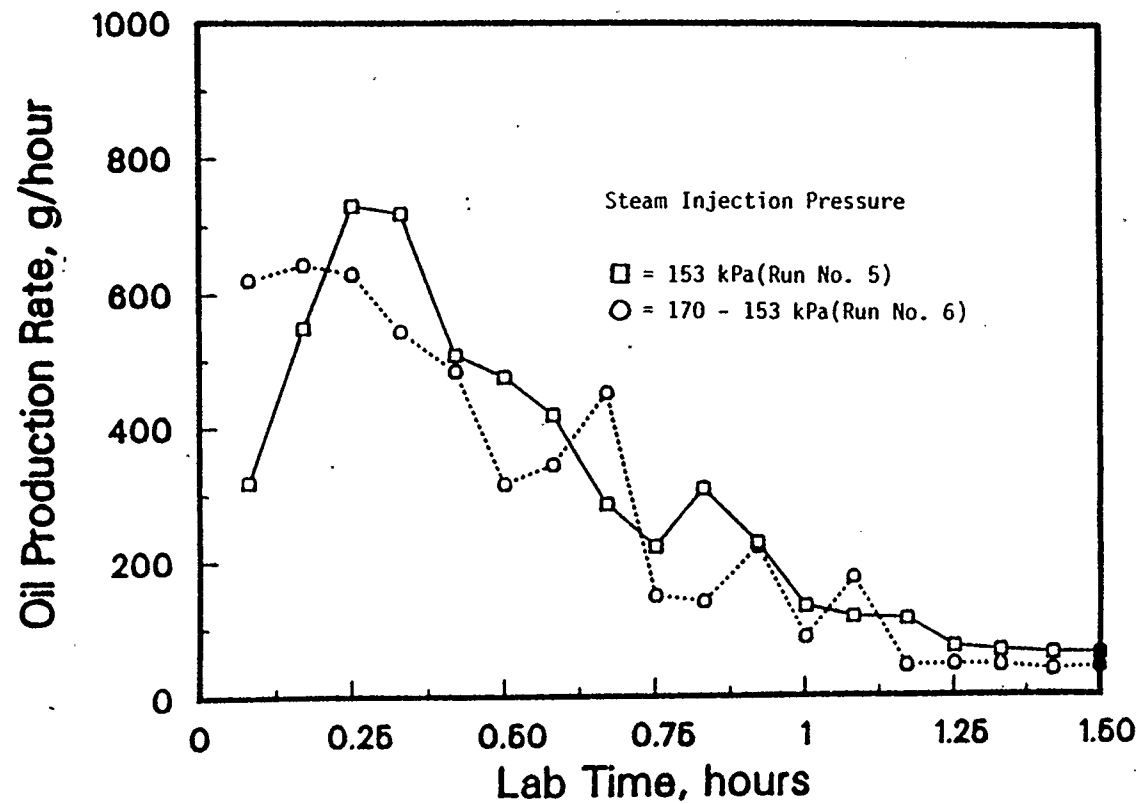


Figure 26: Oil Production Rate as a Function of Time

ii) After Breakthrough

The previous experiments studied the effect of steam injection pressure before the steam breakthrough and the result was lower cumulative recovery for a typical reservoir with a bottom water zone. The study was extended to include the effect of reducing pressure after the steam breakthrough in Runs 7 and 8. The steam injection pressures were reduced from 170 kPa to 153 kPa for Run 7 and from 170 kPa to 148 kPa for Run 8. Figure 27 compares the cumulative oil recoveries. In Run No. 8, with the lower steam pressure, a better cumulative oil recovery (56% of OOIP compared to a recovery of 48% OOIP) was obtained after 70 minutes of production time. Figure 28 compares the oil production rates.

5.6 Effect of Bottom Water Zone Thickness

It is known that the bottom water thickness affects the production performance either in conventional light oil or in heavy oil reservoirs. Numerous attempts have been conducted to address the bottom water problems but the results have not been encouraging for heavy oil reservoirs. In this study, three experiments with different water thicknesses were performed to study the effect of bottom water.

Figure 29 shows the cumulative recovery for experiments with ratios of bottom water zone thickness to total thickness of 0, 0.16 and 0.28. In Run 10 where there was no bottom water present, the total cumulative oil recovery reached 85% of the OOIP. In

EFFECT OF STEAM PRESSURE AFTER STEAM BREAKTHROUGH
EXPERIMENTS WITH A BOTTOM WATER ZONE

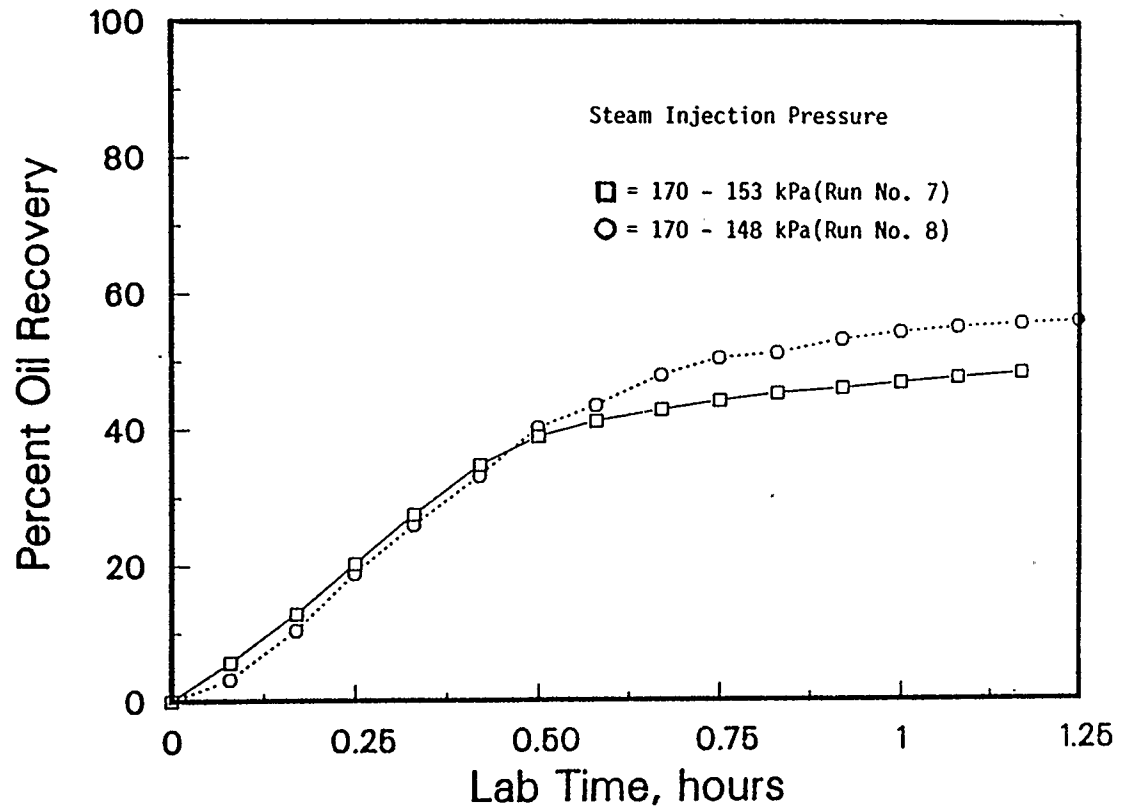


Figure 27: Percent Oil Recovery as a Function of Time

EFFECT OF STEAM PRESSURE AFTER STEAM BREAKTHROUGH
EXPERIMENTS WITH A BOTTOM WATER ZONE

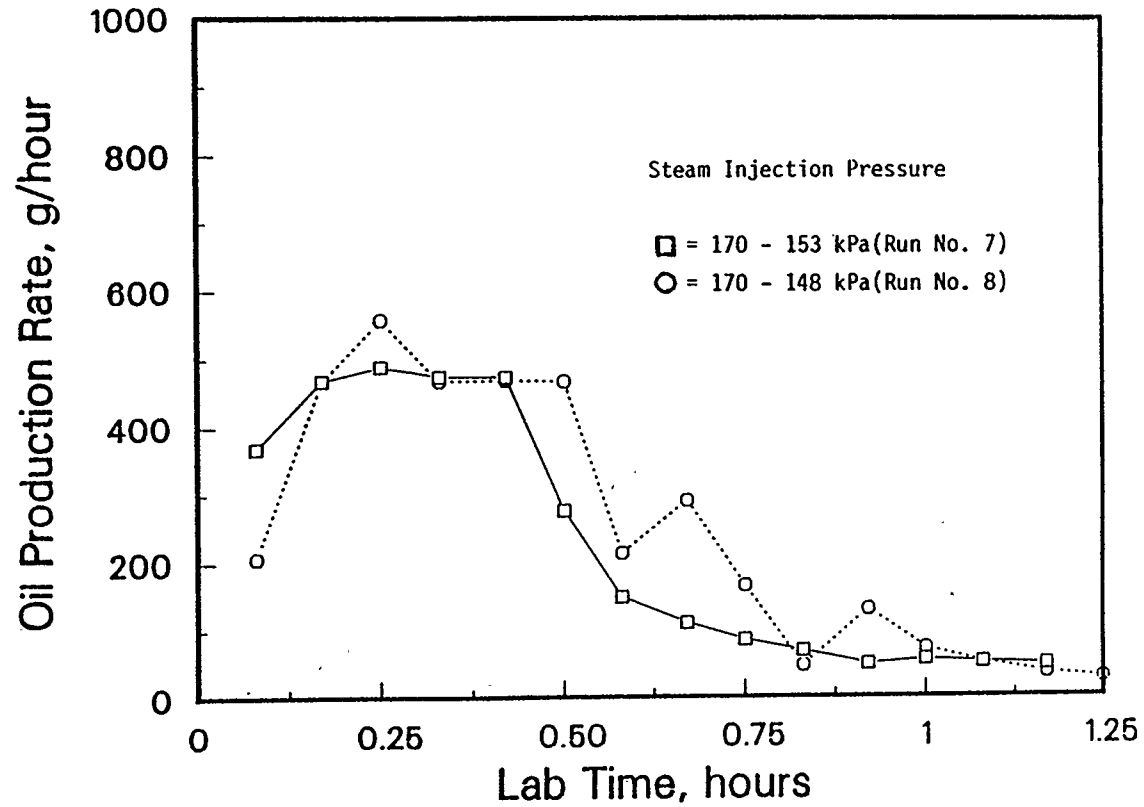


Figure 28: Oil Production Rate as a Function of Time

Run 11, where there was a ratio of 0.16; the total cumulative oil recovery decreased to only 73% of the OOIP. The poorest total cumulative recovery was 59% of the OOIP from Run 12 where the ratio was 0.28. In the bottom water zone, the water could be easily displaced. If the bottom water zone increased, more oil was pushed by the steam chamber into the bottom water zone. Cumulative oil recovery decreased as the thickness of the bottom water zone increased.

Figure 30 shows the comparison of the production rates. In each run, the oil production rate was relatively constant and then declined steadily as the reservoir depleted.

5.7 Effect of Location of Production Well

The production well location is an important factor in determining performance. If the production well is completed too high above the water oil contact (WOC), the amount of recoverable oil is reduced. The reason is that there is no driving force to produce the oil from below the production well. Three experimental runs with different well configurations were conducted to study the effect of the location of the production well.

As discussed in the Introduction, it was possible to produce oil with a production well located below the WOC by applying a specific strategy into the operation.

Figure 31 shows the cumulative oil recovery and the oil production rate for Runs 5, 7 and 9.

EFFECT OF BOTTOM WATER ZONE THICKNESS

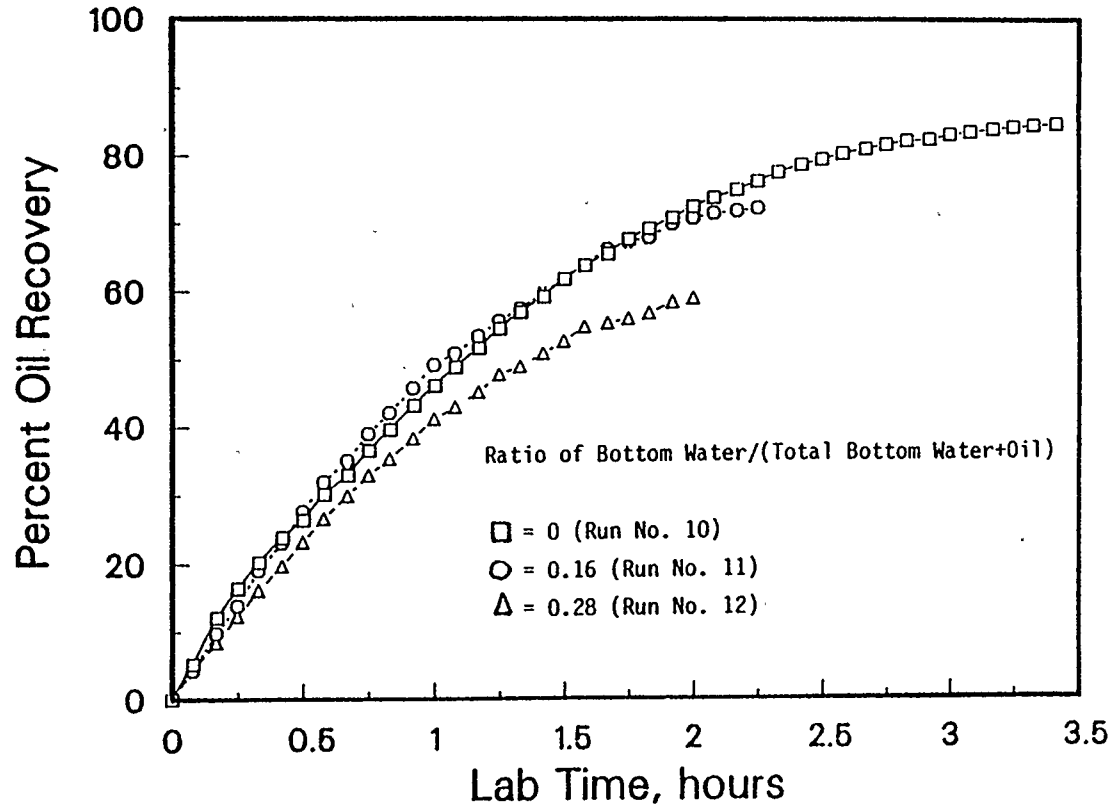


Figure 29: Percent Oil Recovery as a Function of Time

EFFECT OF BOTTOM WATER ZONE THICKNESS

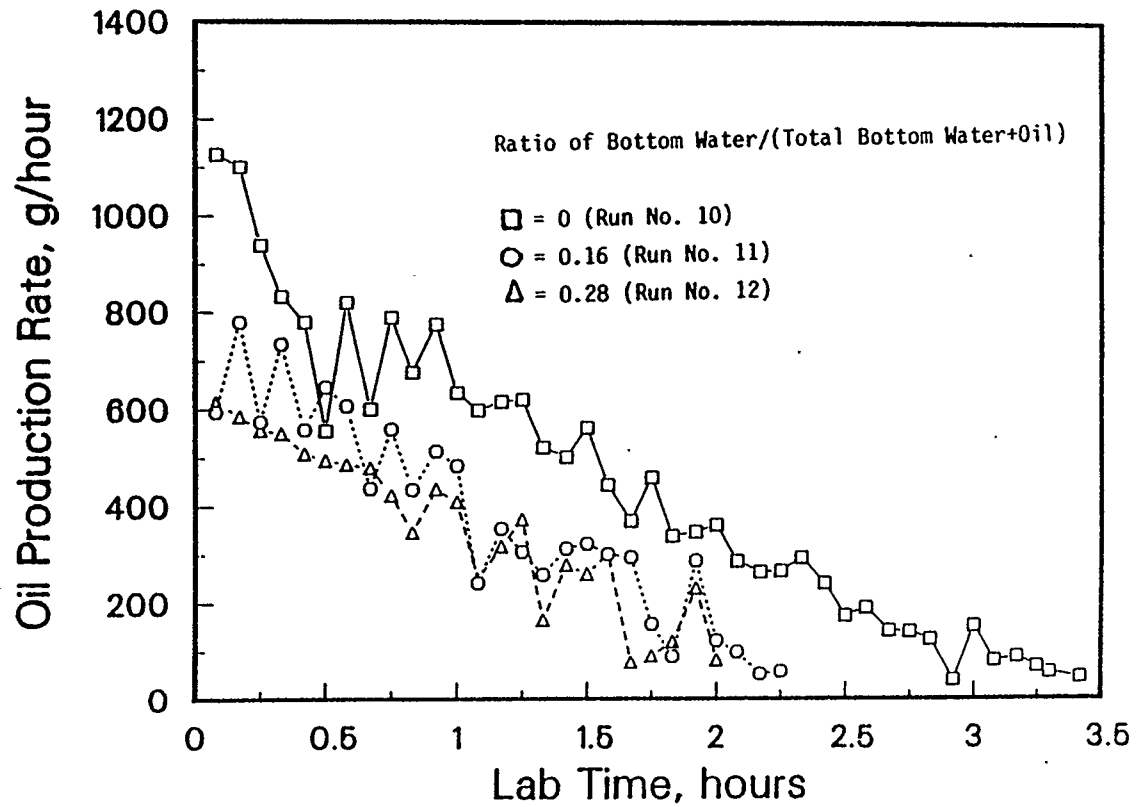


Figure 30: Oil Production Rate as a Function of Time

In Run 5, the production well was located 3.5 cm. above the WOC. The cumulative oil recovery was the highest (79% of the OOIP above the well), but the total amount of the oil was the smallest.

As the location of the production well above the WOC increased, the amount of recoverable oil above the production well decreased.

In Run 7, the production well was located 2 cm. below the WOC. The steam was injected for about two minutes at the beginning without any production being allowed. During this period, the oil was pushed downwards by the growing steam chamber near the top of the reservoir model. After the oil layer position was lower than the production well, the production was allowed.

The cumulative oil recovery near the end of Run No. 7 was only 48%. Large amounts of oil were pushed away into the bottom water zone during the steam injection without any production.

In Run 9, an idea to capture the "oil lost" into the bottom water zone was introduced. The production well was located close to the bottom of the reservoir model. The results were very encouraging. The strategy used to make the operation successful was to withhold production until the WOC being pushed by the growing steam chamber was below the production well. Oil pushed into the bottom water zone was captured and produced.

EFFECT OF LOCATION OF PRODUCTION WELL

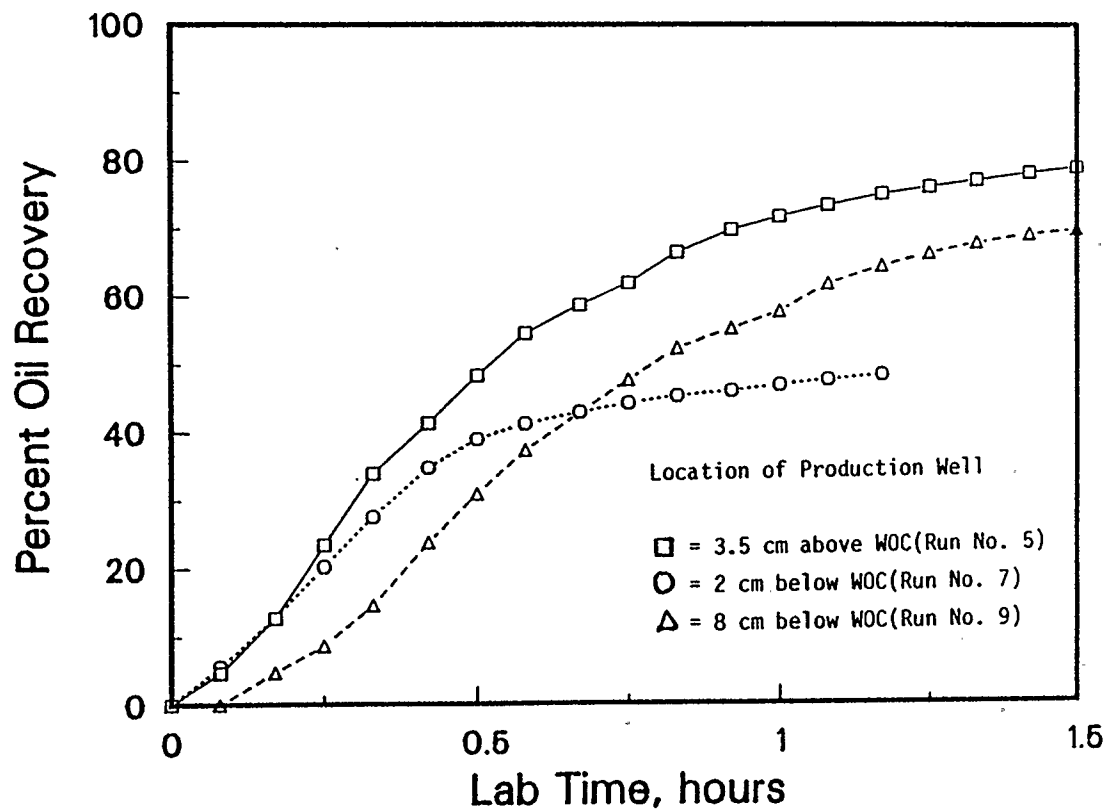


Figure 31: Percent Oil Recovery as a Function of Time

EFFECT OF LOCATION OF PRODUCTION WELL

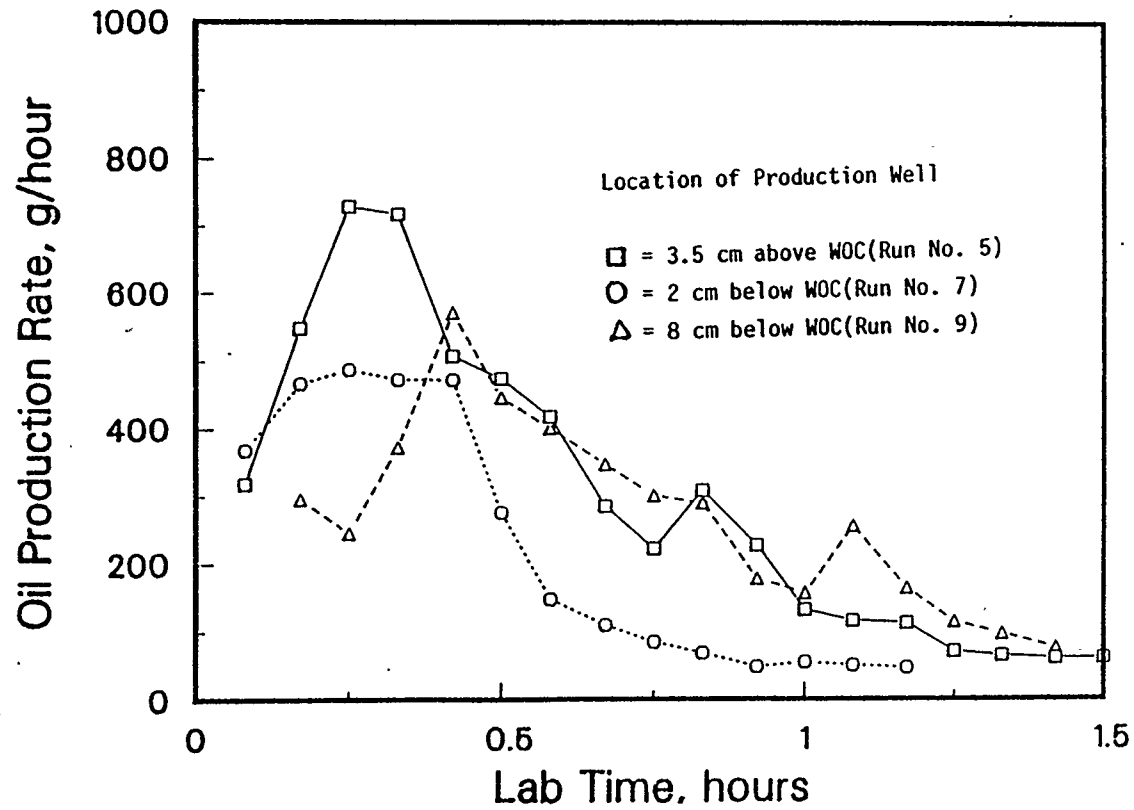


Figure 32: Oil Production Rate as a Function of Time

The cumulative oil recovery in Run 9 was moderately high (70% of the OOIP). The field application of this idea needs to be studied cautiously because the reservoir model quality was homogeneous and without barriers. In a real reservoir condition the bottom water zone needs an active aquifer system so that the bottom water layer can be displaced by the oil pushed by the steam chamber.

Figure 32 shows the oil production rates; they were relatively constant in early production time and then declined steadily when the reservoir was depleted. The oil production rates could not be compared directly because of different OOIP for each experimental runs. However, the cumulative oil recovery comparison could be used for designing the optimum recovery scheme to deplete a heavy oil reservoir with a bottom water zone.

5.8 Effect of Interwell Spacing

Objectives of most in-situ thermal recovery processes include achieving high ultimate recovery and fast production. These goals can be approached by reducing the interwell spacing. Closer interwell spacing gives rates which increase more rapidly than those with wider interwell spacing. Although, in these experimental programs, a single pair of injection and the production wells was used, it can be imagined that the vertical flow boundaries on both sides of the wells are equivalent to planes of symmetry between adjacent well patterns.

5.8.1 *Experimental Run Without a Bottom Water Zone*

Figure 33 shows the comparison of the production rates for two different well spacings. In Run 4, with the closer well spacing, the production rate increased and attained a maximum rate at 15 minutes. After that, the production rate decreased rapidly. In Run 10, the production rate was relatively constant for a short time then decreased steadily as the reservoir depleted.

Figure 34 shows the comparison of the cumulative oil recoveries. In Run 4, where the well spacings were smaller, the total oil recovery increased more rapidly to reach 87% OOIP at 80 minutes production time whereas, in Run 10, it took 205 minutes to yield 85% OOIP. High cumulative recovery was achieved faster using smaller interwell spacing. The ratio of times for approximately the same recovery was $80/205 = 0.4$. From theory it would be expected that this time ratio would be equal to the ratio of the well spacing, i.e. to $1.6/3.1 = 0.5$.

5.8.2 *Experimental Run With a Bottom Water Zone*

In experimental runs with a bottom water zone, the trends for the cumulative oil recovery and the production rates were similar to experimental runs without a bottom water zone. Figure 35 shows the comparison of the oil production rate for two well spacings.

EFFECT OF INTERWELL SPACING

EXPERIMENTS WITHOUT A BOTTOM WATER ZONE

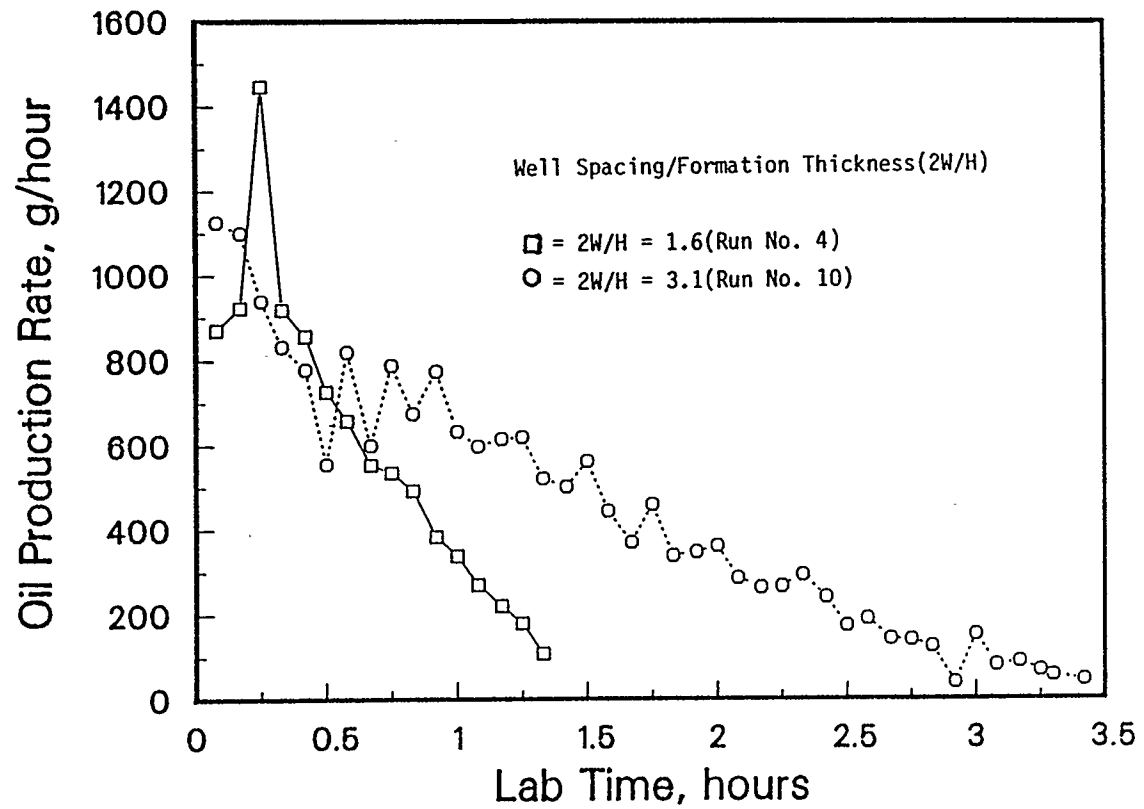


Figure 33: Oil Production Rate as a Function of Time

EFFECT OF INTERWELL SPACING
EXPERIMENTS WITHOUT A BOTTOM WATER ZONE

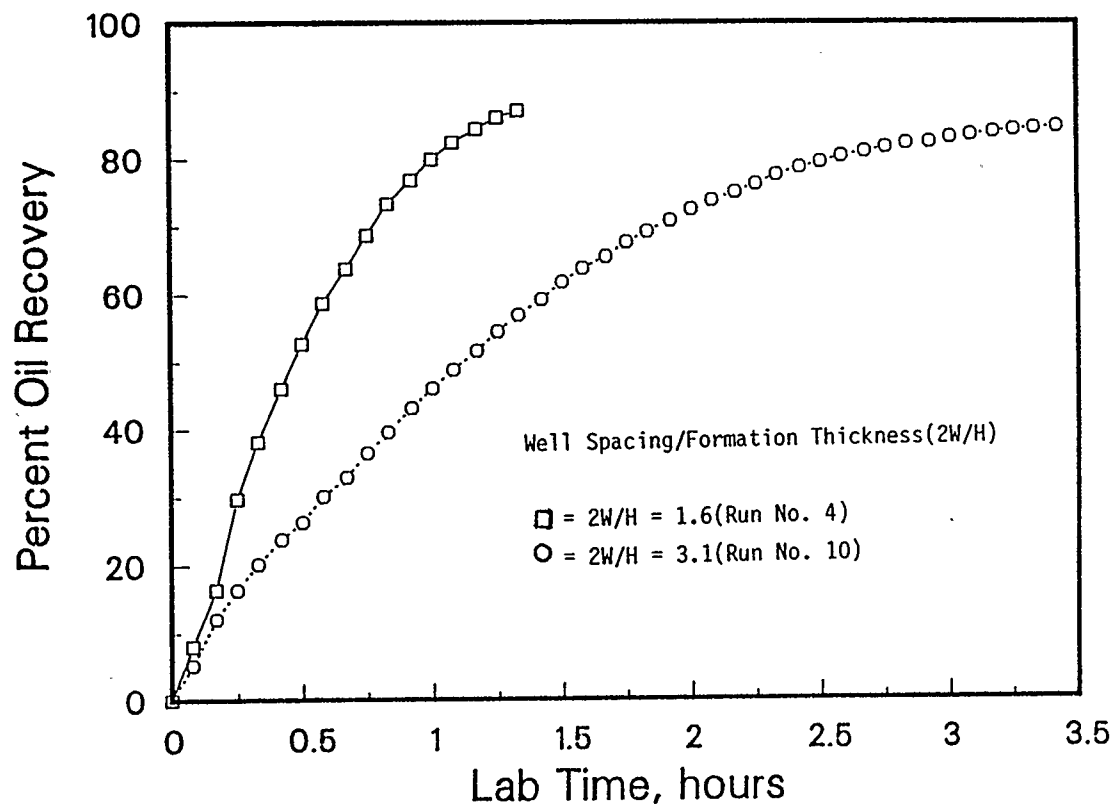


Figure 34: Percent Oil Recovery as a Function of Time

EFFECT OF INTERWELL SPACING
EXPERIMENTS WITH A BOTTOM WATER ZONE

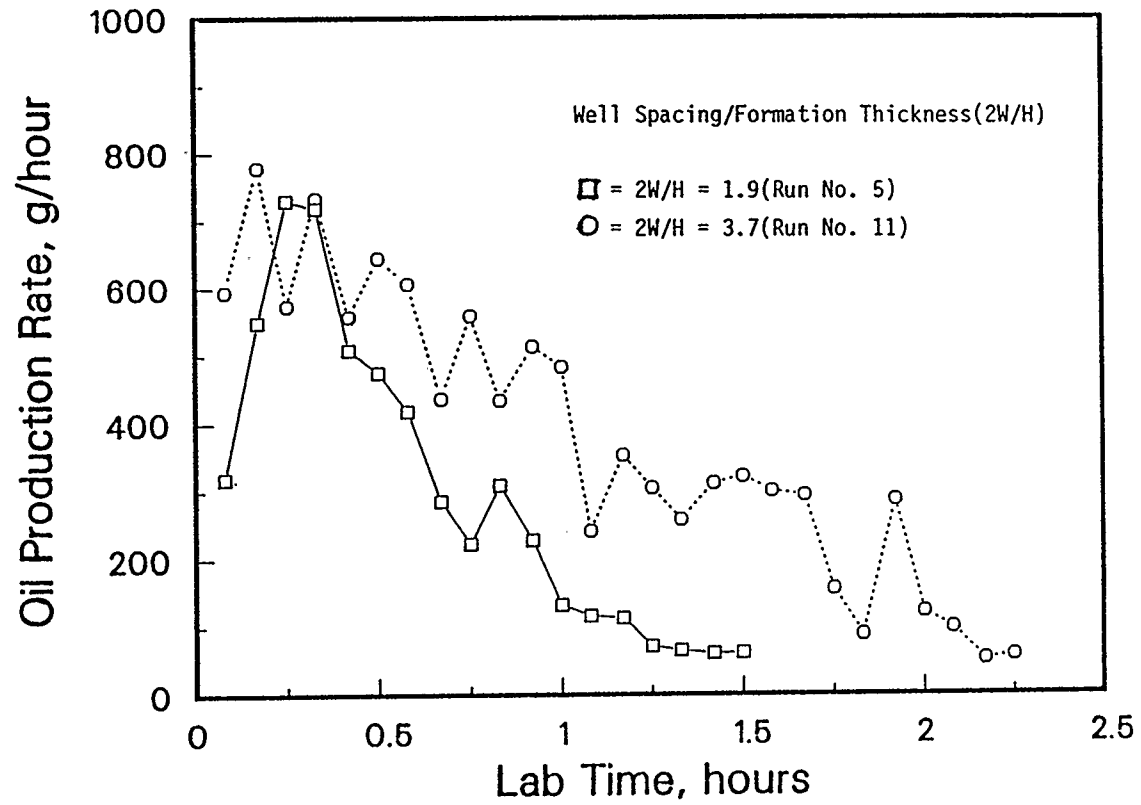


Figure 35: Oil Production Rate as a Function of Time

EFFECT OF INTERWELL SPACING
EXPERIMENTS WITH A BOTTOM WATER ZONE

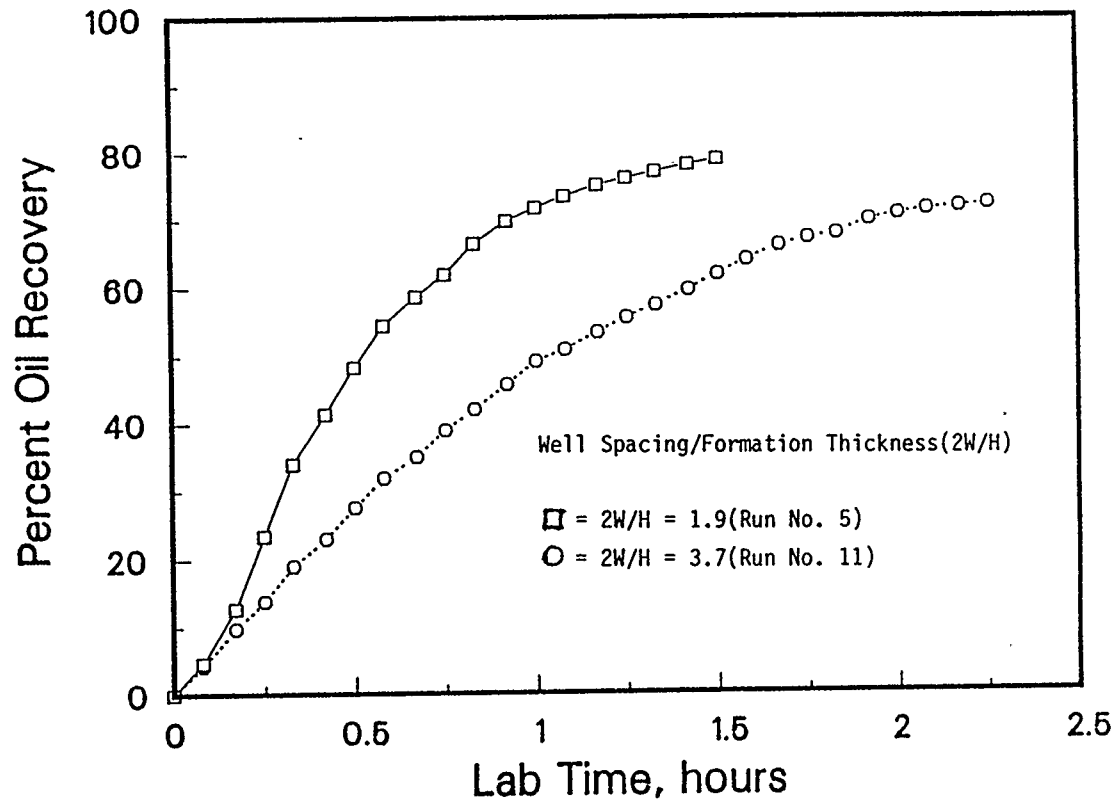


Figure 36: Percent Oil Recovery as a Function of Time

Figure 36 illustrates the cumulative oil recoveries; they were 79 and 73% of the OOIP. As interwell spacing was increased, the cumulative oil recovery decreased. The reason for this was that more oil was lost into the bottom water zone. For the wider spacings, the rate of production increased slowly, so a longer steam injection time was needed to deplete the reservoir. The pressure differential between the steam injection pressure and the bottom water caused more oil to be pushed into the bottom water zone. The experimental results indicate that the wider interwell spacings were less desirable because of a slower rate of recovery and lower cumulative oil recovery.

5.9 Effect of Effective Permeability to the Flow of the Oil

It was found that higher reservoir permeability increases the production rate but it does not increase the ultimate oil recovery. Figure 37 shows the comparison of the oil production rate for two permeabilities. The production rate for the run with an effective permeability of 940 Darcies was lower than that for the run with an effective permeability of 1760 Darcies.

Figure 38 shows the comparison of the cumulative oil recoveries. In the run with the higher permeability, the cumulative oil recovery was 87% of the OOIP at 80 minutes production time and in the other, the cumulative oil recovery was 85% of the OOIP at 205 minutes of production time.

EFFECT OF RESERVOIR PERMEABILITY

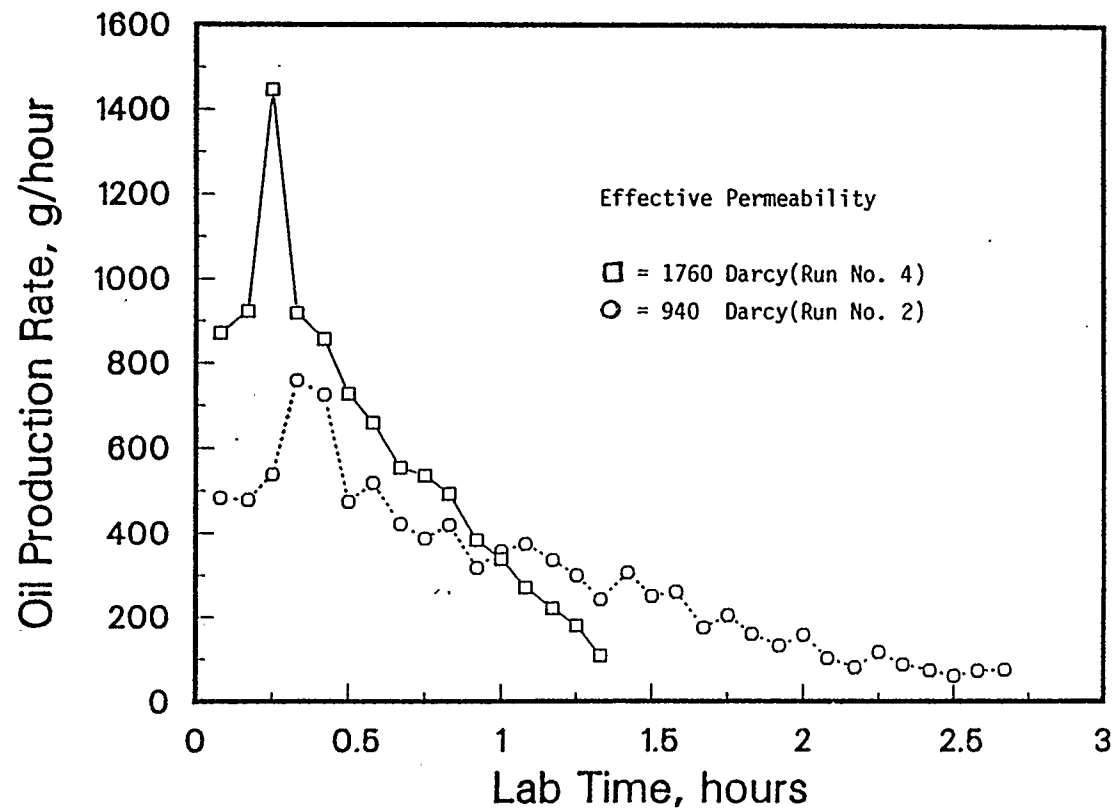


Figure 37: Oil Production Rate as a Function of Time

EFFECT OF RESERVOIR PERMEABILITY

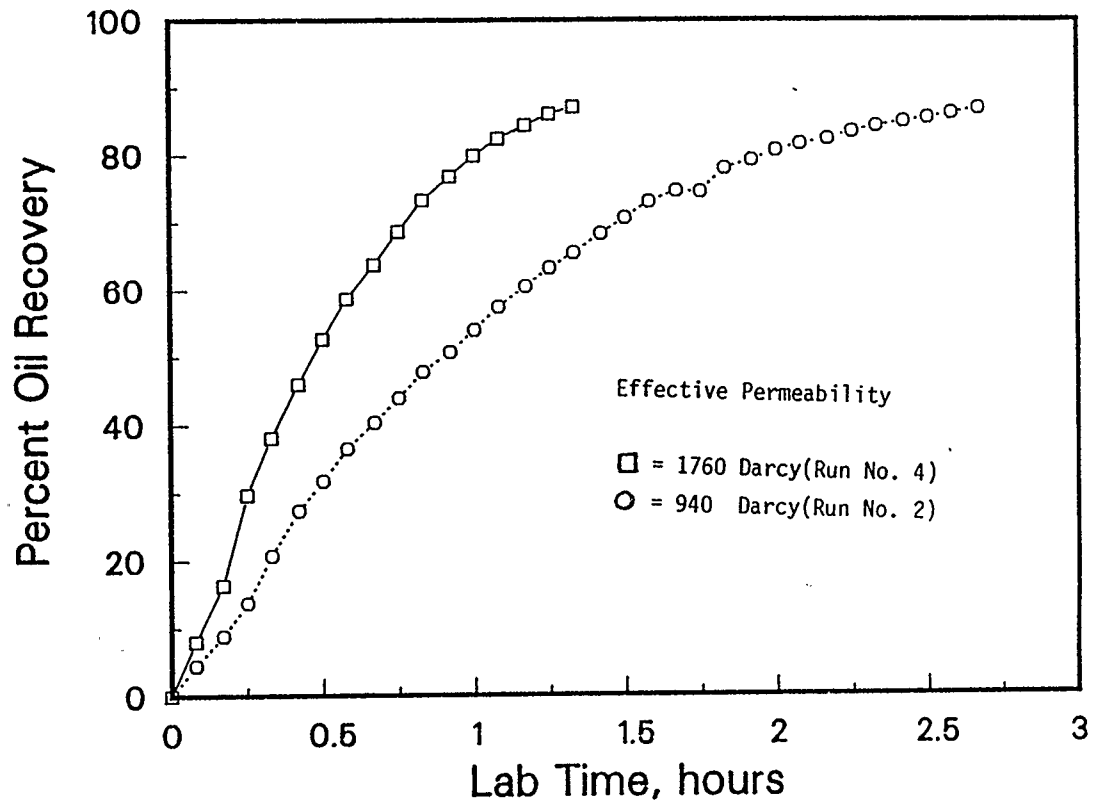


Figure 38: Percent Oil Recovery as a Function of Time

CHAPTER 6

DISCUSSION

6.1 Effect of Steam Injection Pressure on the Steam Breakthrough

A higher steam injection pressure increases the pressure differential between the injection and the production wells. Higher pressure differential provides a larger driving force to push the oil ahead of the steam front down into the production well. The steam front moves more rapidly as it approaches the production well because the oil ahead of the steam front has a progressively shorter distance to move to the production well.

In 1934, Muskat developed a mathematical model to predict the production performance of the direct drive between two wells with the assumption of homogenous fluid displacement. He indicated that the velocity of the front moved faster as the front approached the production well.

In 1987, Butler and Petela developed a mathematical model to predict the breakthrough time in steamflooding from the top of the reservoir using parallel horizontal wells. Their theoretical prediction was based on the Buckley-Leverett theory and on the energy balance. The experimental results obtained in this study were in good agreement with these theoretical predictions.

In experimental runs with lower steam pressure, the volume of oil produced at the steam breakthrough was higher than that produced with high steam pressure. Using a lower steam pressure

allows a longer time for the steam chamber to grow and sweep a larger area of the reservoir model. The experimental results indicated that the steam breakthrough time decreased, and the oil recovered at breakthrough time decreased as the steam injection pressure increased. The most important findings were that the idea of steamflooding from the top of the reservoir showed a very interesting method to create an initial communication fluid path between the injector and the producer for less viscous heavy oil such as Lloydminster type crude with a viscosity of 3000 cp at reservoir conditions.

6.2 Effect of Steam Injection Pressure on the Production Performance

For a case without a bottom water zone, the oil production rate increases as the steam injection pressure increases. The effect of operating at higher steam pressure is to raise the temperature of the steam chamber. This allows the oil to drain more rapidly.

In 1985, Butler presented similar results of the effect of steam pressure on the predicted production rate from horizontal wells using steam-assisted gravity drainage. He used reservoir parameters similar to those for Cold Lake with a viscosity of 100 cs at 99°C. He indicated that the average oil production rate was higher using higher steam pressure. Also, he showed that because of the shorter production time involved in the operation at higher steam pressure, the thermal efficiency is also higher,

i.e. a smaller fraction of the injected heat is lost to the overburden and the reservoir beyond the steam chamber.

In the present study, another reason for a higher production rate was due to a higher pressure drop creating an enhanced "pushing effect" to move oil more rapidly to the production well. This pushing effect occurred primarily before the steam breakthrough time when the pressure drop was the major driving force for producing oil.

With a bottom water zone, a counteracting effect is created by higher steam injection pressure. This results from more oil being pushed into the bottom water zone by higher steam injection pressure. This oil is lost and left in the bottom water zone. It cannot be recovered when the production well is located above the bottom water zone. This effect offsets the advantage of the higher oil production rate using higher steam pressure. More oil was lost into the bottom water as the production time increased. Also, the drainage height decreases as the oil migrating into the bottom water increases. These findings were evidenced in four experimental runs (Runs 5,6,7 and 8).

In summary:

1. For cases without a bottom water zone, it was desirable to operate at the highest steam injection pressure.
2. For cases with a bottom water zone, it was undesirable

to operate at the highest steam injection pressure (i.e. at high pressure differentials).

6.3 Effect of Bottom Water Zone Thickness on the Production Performance

The thickness of the bottom water zone affects the success of any enhanced recovery scheme. In steamflooding, the bottom water zone usually causes more problems than advantages because the steam tends to migrate into the bottom water zone and also there can be excessive water production due to water coning. There were three important findings that may allow improved recovery in the presence of bottom water.

1. The tendency of the bottom water to move into the production well was reduced by maintaining a balancing pressure in the production well. This idea was demonstrated in the models. The steam was injected at a slightly higher pressure than the bottom water pressure level and the production well was throttled so as to prevent coning of water (and steam).
2. The tendency of the steam to migrate into the bottom water zone can be eliminated by controlling the injection pressure. Steam bypass into the production well can also be eliminated by throttling the production well. The steam consumption will be lower than that of conventional steam-floods since little or no steam is wasted to heat the bottom

water zone and little or no steam passes uncondensed to the production well.

3. If the steam migrates into the bottom water zone, the oil above the bottom water zone will be heated. This heated oil becomes mobile and migrates into the bottom water zone. This oil is left behind in the bottom water zone and is not recovered. This problem can also be prevented by controlling the production well in such a way that no steam migrates into the bottom water zone.

The findings described above were supported by results from the three experimental runs performed (Runs 10,11 and 12).

6.4 Effect of Location of Production Well on the Production Performance

The production performance using steam-assisted gravity drainage was sensitive to the location of the production well. Locating the production well as far as possible above the water oil contact is undesirable because only the oil above the production well can be drained.

For the case without a bottom water zone, it is desirable to use the longest distance between the injector and the producer. The production well should be located slightly above the underburden and the injection well should be located near to the top of the reservoir. This provides the highest drainage height, the highest oil production rate and also the highest oil recovery.

In this experimental study, it was found that the production well could be placed below the water oil contact. The ultimate oil recoveries from this well configuration were good and the oil recoveries were still in the order of 50% of the OOIP. These results were evidenced in two experimental runs (No. 7 and 8). Further, the ultimate oil recovery was improved to 70% of the OOIP if the production well was located right at the bottom of the water zone. This was evidenced in experimental run No. 9. The idea behind the improved ultimate oil recovery was that the "lost oil" into the bottom water was captured and produced through the production well.

The recoveries found in these experiments (Runs 7,8 and 9) were obtained by controlling the pressures in the production well and the injection well. The steam was injected into the reservoir without any production for a short time (2 to 5 minutes). The steam pushed the oil, causing it to migrate into the bottom water zone and the bottom water was displaced by the migrating oil. In these experiments, the bottom water migrated into the water tank. Once the cold oil migrated into the bottom water zone, the oil created an effect like a "cold oil blanket" surrounding the production well. This cold oil blanket gave a favourable mobility ratio surrounding the production well such that the bottom water migration tendency into the production well was reduced.

6.5 Effect of Interwell Spacing on the Production Performance

The objective of most in-situ thermal recovery processes is to achieve high ultimate recovery and the shortest project life. This goal can be approached by reducing the interwell spacing. From experimental results it was found that closer interwell spacings gave rates which increased more rapidly than those found with wider spacings. The ultimate oil recovery indicated an insignificant difference for either case, i.e. with closer or wider interwell spacings.

These results were evidenced in four experimental runs (No. 4,5,10 and 11) with and without a bottom water zone.

6.6 Comparison of the Production Performance of Experimental Runs and the Theoretical Predictions

Figures 39-44 show comparisons of the production performance for Runs No.10 and 11 with those predicted from the Tandrain theory using the physical parameters from Tables 6 and 7. The results show a fairly good agreement, even though the Tandrain theory assumes that the steam chamber extends over the whole depth of the reservoir from the very start.

In both experimental runs, it was found that the production rates have the same trend. However, at initial production time, the experimental oil production rates are higher compared to the rate predicted by the theory. The reason is that the theory was developed with the assumption that the existence of the initial

communication path between the injection and the production wells started from the beginning of the steam injection. However, in experimental runs, there is no initial communication path established between the injector and the producer. The steam chamber grows and displaces the cold oil into the production well. During this period of oil displacement by steam chamber growth, the main driving force for producing the oil is the pressure difference between the injector and the producer. After the communication path is created, the production well is throttled so that no steam is bypassed through the production well. There is little pressure difference between the injector and the producer. The oil heated by the steam becomes mobile. Then the oil and the condensate drain downwards by the gravity forces into the production well. By maintaining the steam pressure close to the aquifer pressure, there is little tendency for steam to heat the bottom water.

During the initial communication period, the rate of recovery calculated from experimental results is slightly higher than the theoretical predictions for initial production by gravity drainage. This occurs because the pressure difference is the main driving force rather than the gravity force. However, after the communication path is established, the rate of recovery computed from the experimental results is of the same order as that predicted theoretically, but slightly lower. The agreement is encouraging. The deviation of the experimental results is

thought to be due to factors not recognized in the derivation of the Tandrain theory. One of the factors is that the effective height became lower than the actual height used in the theoretical prediction due to the depletion of the reservoir model.

Table 6: Scaling parameters for the Experimental Run No. 10 and the field

Physical Parameters

	<u>Model</u>	<u>Field</u>
K, m^2	1.760×10^{-9}	2.00×10^{-12}
$g, m/d^2$	7.323×10^{10}	7.323×10^{10}
$\alpha, m^2/d$	0.0507	0.056
$\phi\Delta S_o$	0.37	0.18
m	2.61	2.54
H, m	0.21	14.0
W, m	0.34	22.7
$T_S, ^\circ C$	110	200
$\nu_S, m^2/d(cs)$	2.16 (25)	0.31 (3.56)
$\rho_o, kg/m^3$	974	974

Dimensionless Constant (equation 4.7)

$$B_3 = \sqrt{\frac{KgH}{\alpha\phi\Delta S_o m\nu_S}} \quad 15.89 \quad 15.89$$

Dimensionless Time (equation 4.1)

$$\tau_d = \frac{\tau}{W} \sqrt{\frac{Kg\alpha}{\phi\Delta S_o m\nu_S H}} \quad 11.3 \tau \quad 2.80 \times 10^{-3} \tau$$

$$\frac{\tau_{Field}}{\tau_{model}} = \frac{11.3}{2.80 \times 10^{-3}} = 4036 \quad \text{i.e. } 1 \text{ hr}_{model} = 0.46 \text{ yrs}_{field}$$

Table 7: Scaling parameters for Experimental Run No. 11 and the field

Physical Parameters

	<u>Model</u>	<u>Field</u>
K, m^2	1.76×10^{-9}	1.20×10^{-12}
$g, m/d^2$	7.323×10^{10}	7.323×10^{10}
$\alpha, m^2/d$	0.0507	0.056
$\phi\Delta S_o$	0.37	0.18
m	2.61	2.54
H, m	0.13	14.0
W, m	0.34	36.6
$T_S, ^\circ C$	110	200
$\nu_S, m^2/d(cs)$	2.16 (25)	0.31 (3.56)
$\rho_o, kg/m^3$	974	974

Dimensionless Constant (equation 4.7)

$$B_3 = \sqrt{\frac{KgH}{\alpha\phi\Delta S_o m\nu_S}} \quad 12.51 \quad 12.51$$

Dimensionless Time (equation 4.1)

$$t_d = \frac{t}{W} \sqrt{\frac{Kg\alpha}{\phi\Delta S_o m\nu_S H}} \quad 14.3 t \quad 1.37 \times 10^{-3} t$$

$$\frac{t_{\text{Field}}}{t_{\text{model}}} = \frac{14.3}{1.37 \times 10^{-3}} = 10500 \quad \text{i.e. } 1 \text{ hr}_{\text{model}} = 1.2 \text{ yrs}_{\text{field}}$$

COMPARISON OF EXPERIMENTAL RESULTS AND THEORETICAL PREDICTIONS FOR EXPERIMENTS WITHOUT A BOTTOM WATER ZONE

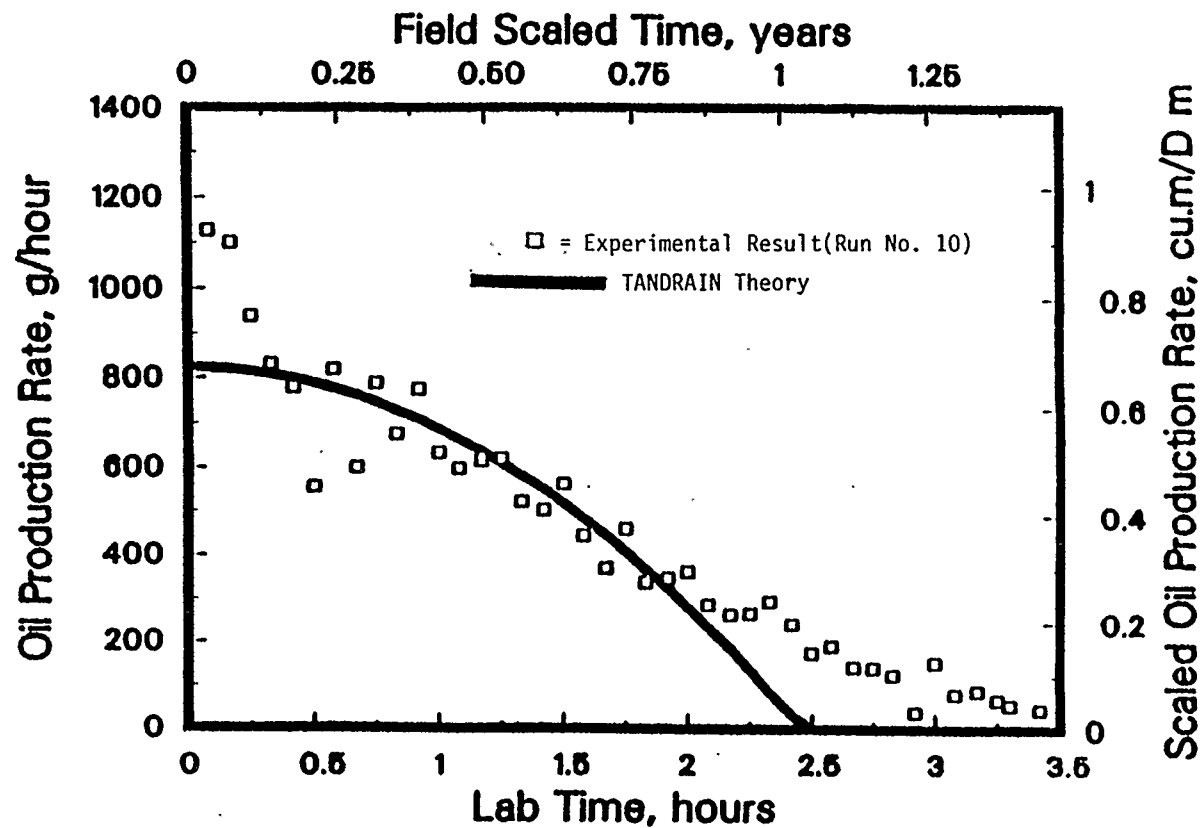


Figure 39: Oil Production Rate as a Function of Time

COMPARISON OF EXPERIMENTAL RESULTS AND THEORETICAL PREDICTIONS FOR EXPERIMENTS WITHOUT A BOTTOM WATER ZONE

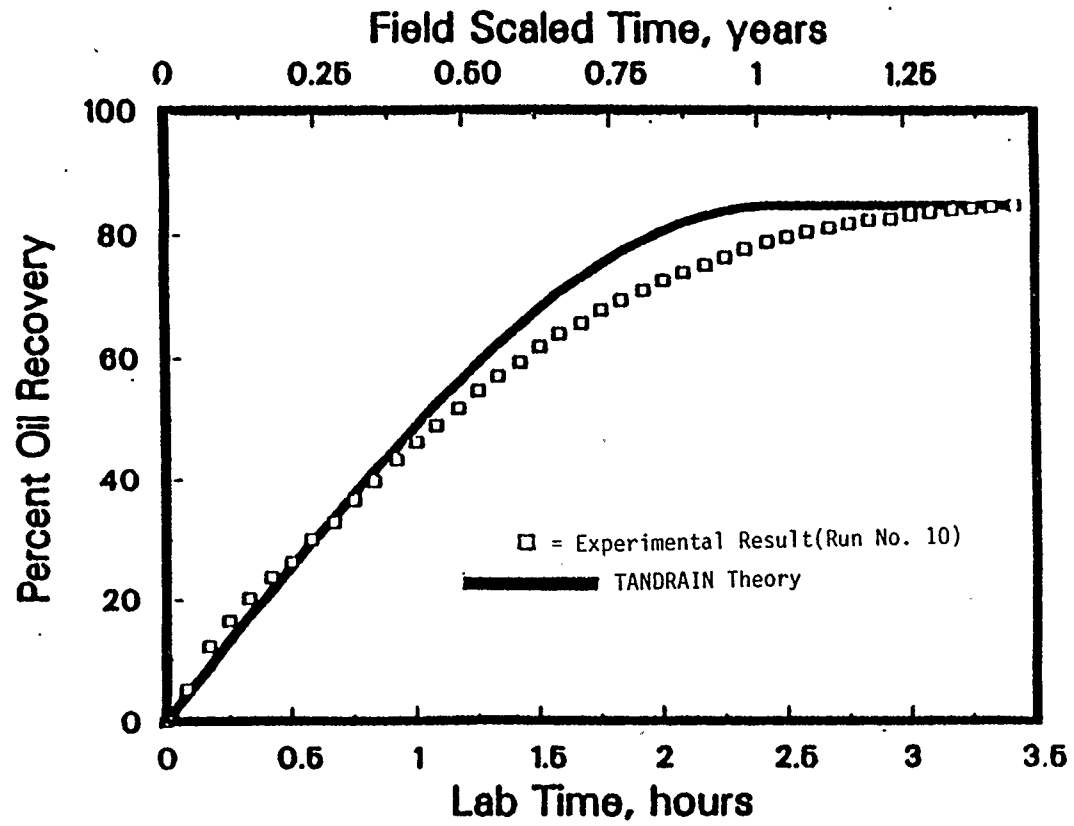


Figure 40: Percent Oil Recovery as a Function of Time

COMPARISON OF EXPERIMENTAL RESULTS AND THEORETICAL PREDICTIONS FOR EXPERIMENTS WITHOUT A BOTTOM WATER ZONE

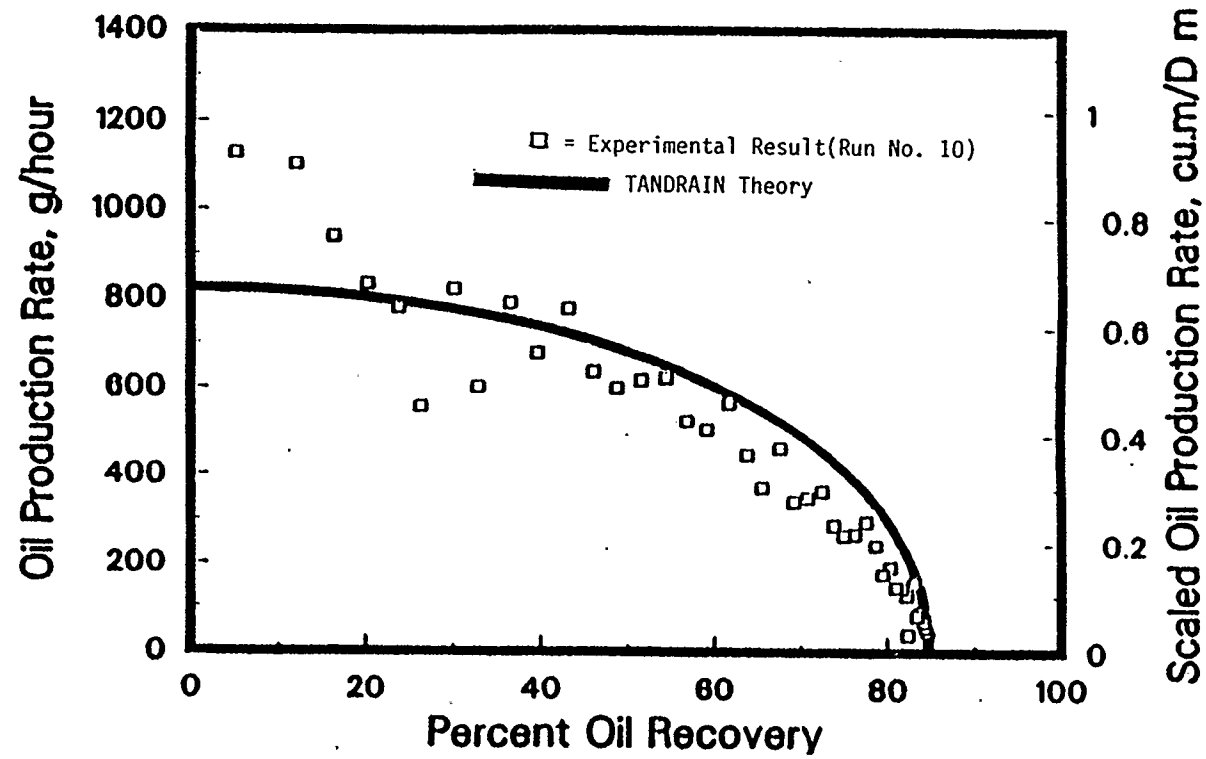


Figure 41: Oil Production Rate as a Function of Percent Oil Recovery

COMPARISON OF EXPERIMENTAL RESULTS AND THEORETICAL PREDICTIONS FOR EXPERIMENTS WITH A BOTTOM WATER ZONE

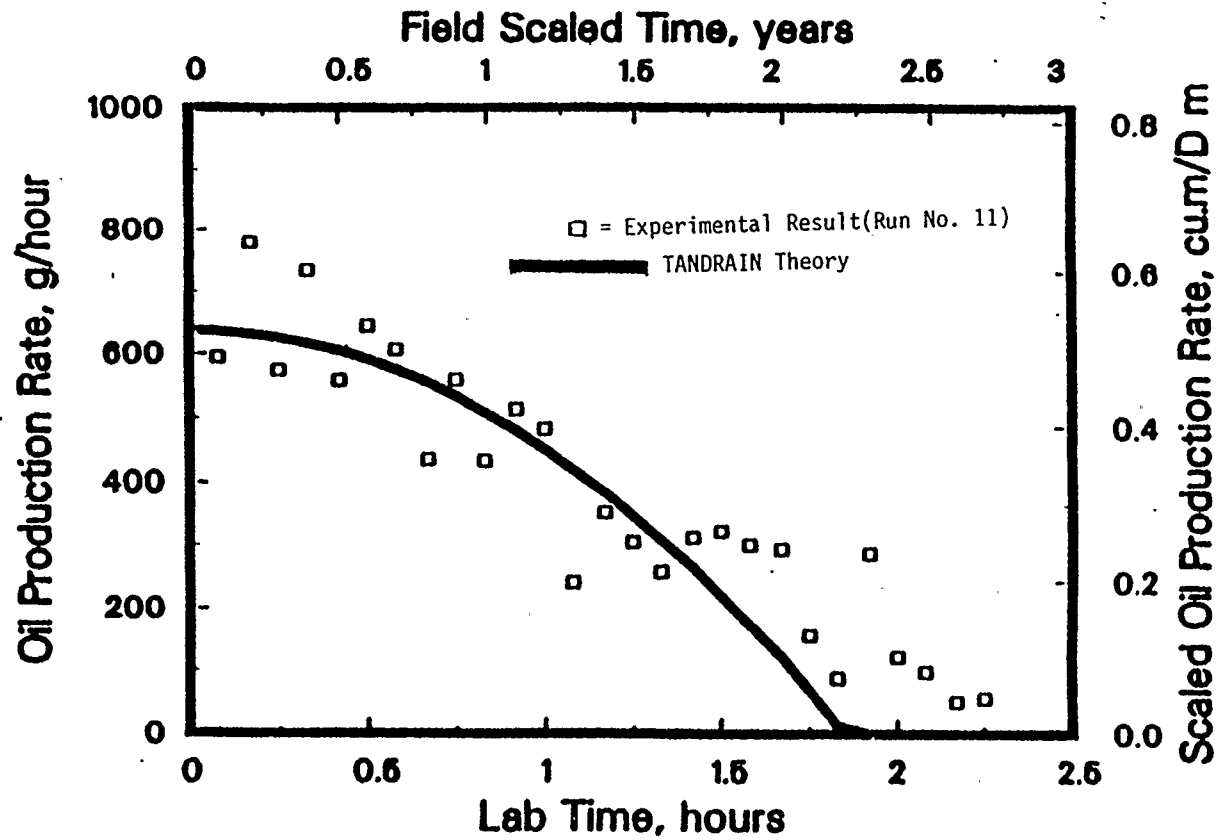


Figure 42: Oil Production Rate as a Function of Time

COMPARISON OF EXPERIMENTAL RESULTS AND THEORETICAL PREDICTIONS FOR EXPERIMENTS WITH A BOTTOM WATER ZONE

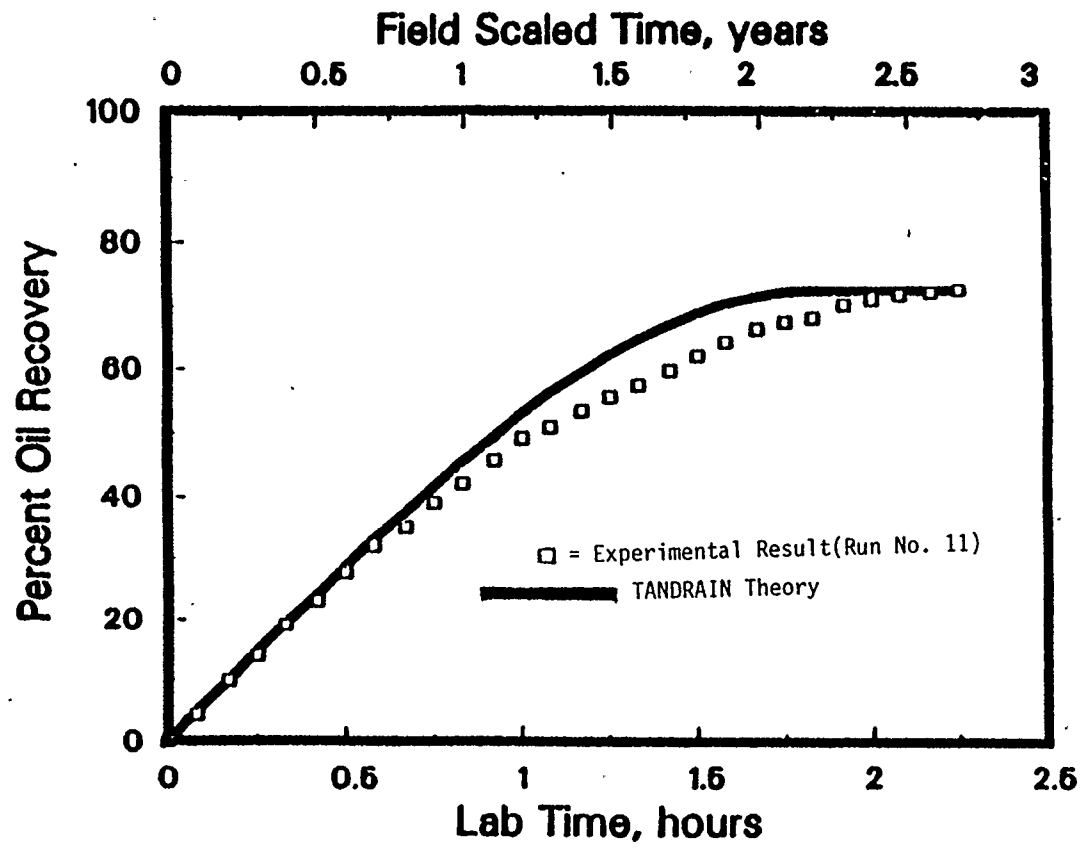


Figure 43: Percent Oil Recovery as a Function of Time

COMPARISON OF EXPERIMENTAL RESULTS AND THEORETICAL PREDICTIONS FOR EXPERIMENTS WITH A BOTTOM WATER ZONE

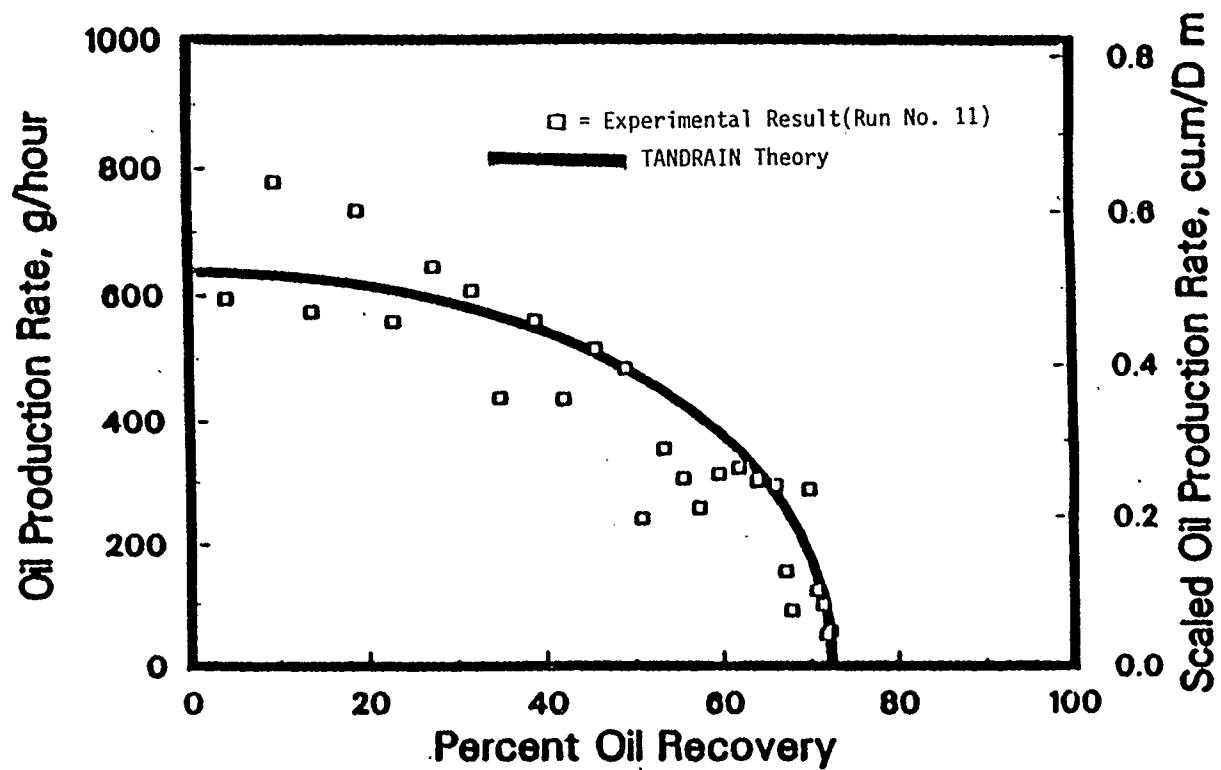


Figure 44: Oil Production Rate as a Function of Percent Oil Recovery

6.7 Applications in Canada's Oilfields

In Canada, there is a vast amount of heavy oil reserves (3.5 billion m³ or 20 billion barrels) underlying the Lloydminster area of Alberta and Saskatchewan (Farouq Ali, 1986). These heavy oils are usually mobile even at reservoir conditions, and most of these heavy oils can be produced, but at low recovery, by primary production. However, these heavy oils have some unique problems of their own.

In a typical Lloydminster heavy oil reservoir, the formation is too thin for the application of thermal recovery processes. The heat loss to the overburden and underburden can be so severe that the application of thermal recovery processes becomes uneconomic.

Some of the thicker reservoirs have a water table underlying the heavy oil deposits. This bottom water zone causes more problems for producing the heavy oil above it. The relatively high oil density and viscosity make the mobility ratio unfavourable. In conventional production, the bottom water penetrates, like "a cone", into the production well. The water production is excessive and the well has to be abandoned because it becomes uneconomic to operate.

Secondary processes like waterflooding are not effective because the mobility ratio of heavy oil to water is not favourable. Therefore, the chance of recovering this type of petroleum reserves is further limited.

Significant new ideas were derived from this present work. The applications of steam-assisted gravity drainage will improve the economics of a typically marginal heavy oil commercial project through several improvements:

- a) higher ultimate oil recovery
- b) higher oil production rates.

In most cases, the experimental results showed a cumulative recovery of higher than 50% of the OOIP. The typical oil recovery in heavy oil reservoirs using primary production processes is usually in the range of 3 to 8% of the OOIP. The recovery is even worse if the heavy oil deposits have a water table below. The oil recovery may be less than 1% of the OOIP before wells are abandoned due to excessive water production.

The applications of steam-assisted gravity drainage in heavy oil fields can boost recovery to more conventional levels. The scaled production rate from the experiments described here indicates daily production from a 500 m length of a horizontal production well to be more than 1000 barrels, compared to a typical primary production of 15 to 20 barrels per day.

The results from the experiments show significant benefits for the application of the steam-assisted gravity drainage process to a typical "Lloydminster" heavy oil reservoir. All experiments show a similar mechanism, therefore, only two experimental results (Experimental Runs No. 10 and 11) will be

discussed. Experiment No. 10 can be imagined as a depletion process from a typical heavy oil reservoir without a bottom water zone, and Experiment No. 11 can be envisaged as a depletion process from a typical heavy oil reservoir with a bottom water zone.

Figures 45 and 46 illustrate the extrapolation of Experiments No. 10 and 11 to the field conditions respectively. The reservoir parameters used in the experiments and their extrapolated field conditions were shown in Tables 6 and 7.

Figures 40 and 43 (in Section 6.6) show an ultimate recovery of 87% and 73% of the OOIP respectively. These recoveries for a typical heavy oil are very high and are much like a conventional oil. Figures 39 and 42 illustrate the oil production rate as a function of time. For a typical 500 m length of horizontal well, it needs a value of over $0.32 \text{ m}^3/\text{D m}$ to produce over 1000 barrels per day from a single well. By observing Figures 39 and 42, it seems that daily production of 1000 barrels per day from a single, 500 m horizontal well is not an unreasonable expectation for heavy oil reservoirs with 14 m thickness of oil zone.

However, for real reservoir conditions, the ultimate recovery may be less than that obtained from experimental laboratory conditions. This may be due to several factors not recognized in the laboratory conditions. The ultimate recovery is sensitive to the reservoir quality such as the variations of

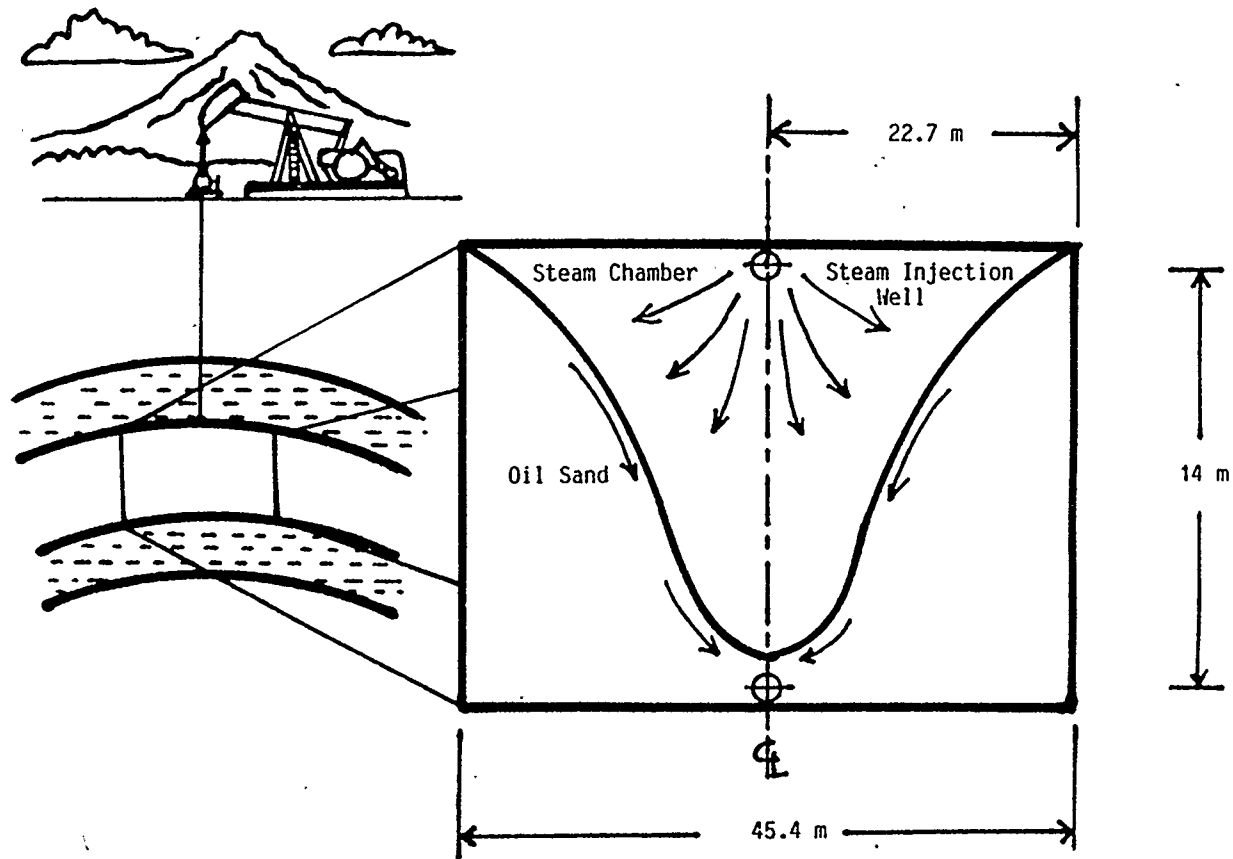


Figure 45: Illustration for Experimental Run No: 10 Extrapolated to Field Conditions

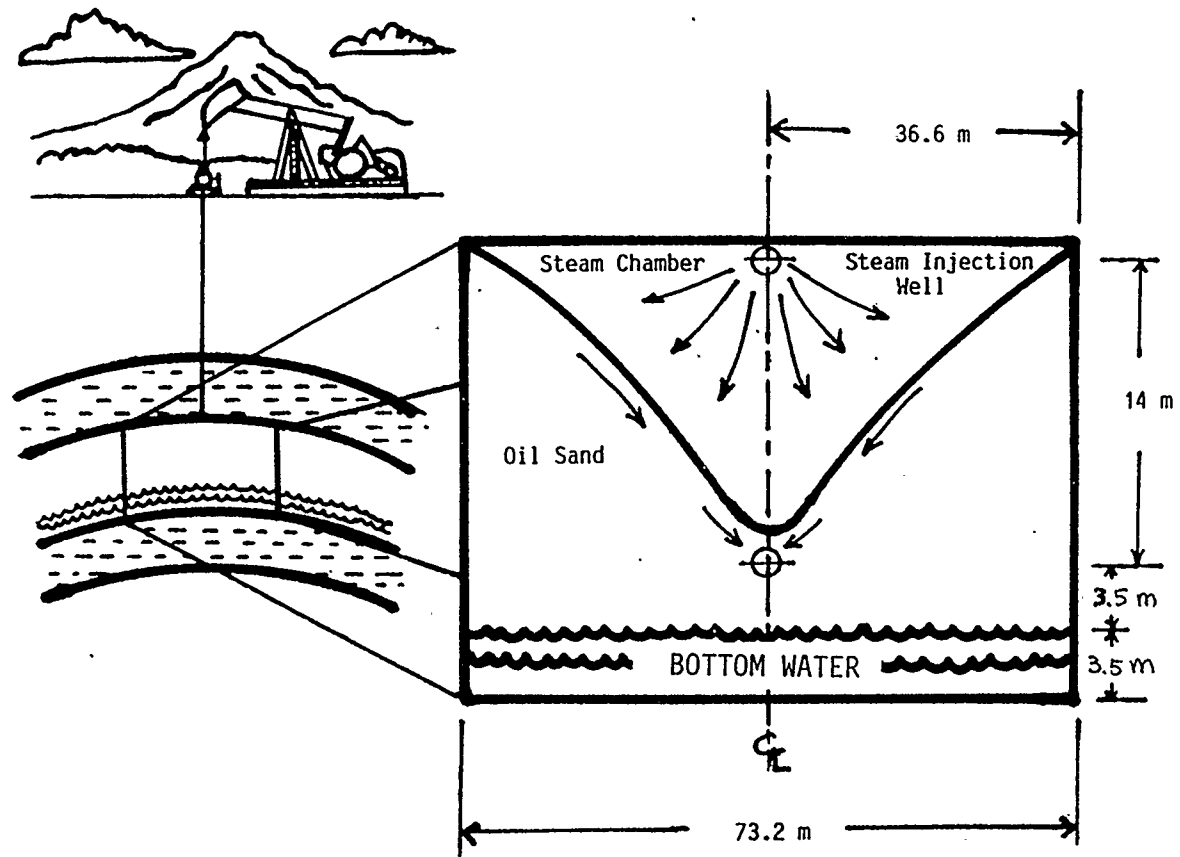


Figure 46: Illustration for Experimental Run No: 11 Extrapolated to Field Conditions

oil saturation and heterogeneity of the formation throughout the reservoir.

The economics of a commercial in-situ oil recovery project are sensitive to the well spacing. Closer well spacings can give a better sweep and a faster depletion time, but the disadvantage of using closer well spacings is a high capital investment for drilling more wells. However, larger well spacings also have their own problems. Although larger well spacings allow lower capital investment because fewer wells need to be drilled, they also result in a poorer oil/steam ratio. This means that a higher operation cost for injecting more steam is required. Therefore, there will be an optimum distance for selecting well spacings.

For case studies, the Winter reservoir was chosen as an example of the application of the steam-assisted gravity drainage process. The reservoir is characterized by high porosity (0.30) and high permeability (5.0 Darcies). The thickness of the oil zone is 14 metres and the oil viscosity is 3000 cP at 27.8°C. The horizontal steam injection well is located near the top of the oil zone and is completed 14 metres above the horizontal production well. Both horizontal wells are 500 metres in length. Table 8 shows the parameters used for calculating the effect of well spacing variations to Winter reservoir production performances and economics. The relative permeability for the flow of oil in the model was assumed to be 0.4. This assumption was also

used in previous work by Butler et al (1979, 1981, 1985) and Chung et al (1987). Therefore, the absolute permeability shown in Table 8 was multiplied by 0.4 to obtain the effective permeability for the flow of oil in the model.

The results were calculated using an existing program (HWELLTX) developed by Butler using the theory that he published in 1981 and 1985. The assumption made is that the reservoir is depleted using the steam-assisted gravity drainage process. It should be noted that this program uses different methods for creating an initial communication fluid path between the injector and the producer during early production time. The software was developed using the rising steam chamber method. This method assumed that the initial communication path was created by injecting steam near the production well and then the steam chamber grew sideways and rose to the top of the reservoir. In the present study, the steam was injected near the top of the reservoir and then the steam chamber grew sideways and moved downwards into the production well. The difference in overall production performance for both methods should be insignificant for a reservoir with a thin formation such as the Winter reservoir. The reason for this is that the production during the communication stage and time for this stage are only a small fraction of the totals.

Figure 47 shows the effect of varying the horizontal well spacing on the oil/steam ratio. There is a rapid decrease in the

Table 8: Reservoir and Economics Parameters for Calculating
The Effect of Well Spacing Variations to Winter
Reservoir Production Performances and Economics

Chamber Pressure, Mpa	6
Steam Temperature, C	276
Steam Quality	0.7
Reservoir Height, m	14
Reservoir Temperature, C	28
Porosity	0.3
Initial Oil Saturation	0.75
Residual Oil Saturation	0.15
Oil Viscosity @28C, mm ² /s	2
Effective Horizontal Perm., D	1
Ratio Vertical/Horizontal Perm.	0.042
Reservoir Thermal Diff., m ² /d	0.054
Overburden Thermal Diff., m ² /d	3073
Start-up year	1988
Capital Cost, \$/m	4000
Annual Maint., frac. of Capital	0.06
Steam Cost, \$/bbl in 1988	2
% Return (Constant \$)	15
Netback, \$/bbl in 1988	14

oil/steam ratio as the well spacings increase.

Figure 48 shows the predicted average production rate from a single horizontal production well as a function of the horizontal well spacings. From 30.5 to about 61.0 metres (100 to 200 feet), the production rate increases rapidly. Above 61.0 metres (200 feet), the production rate increases slowly. However, the results showed that a production of 1000 barrels per day is not unreasonable for any well spacing pattern ranging from 30.5 to 305 metres (100 to 1000 feet). This result is supported by the previous extrapolated results discussed in Chapter 5.11, although the extrapolated results from the laboratory scaled model used lower steam injection temperature and is assumed to have 100 percent steam saturation.

Figure 49 shows the project life as a function of well spacing variations. The project life period increases linearly as the well spacing increases.

Figure 50 shows the supply cost of producing heavy oil from the Winter reservoir as a function of well spacing variation. The results indicated that there is an optimum well spacings to achieve the lowest supply cost. The optimum well spacing for the Winter reservoir is found to be about 122 m (400 feet).

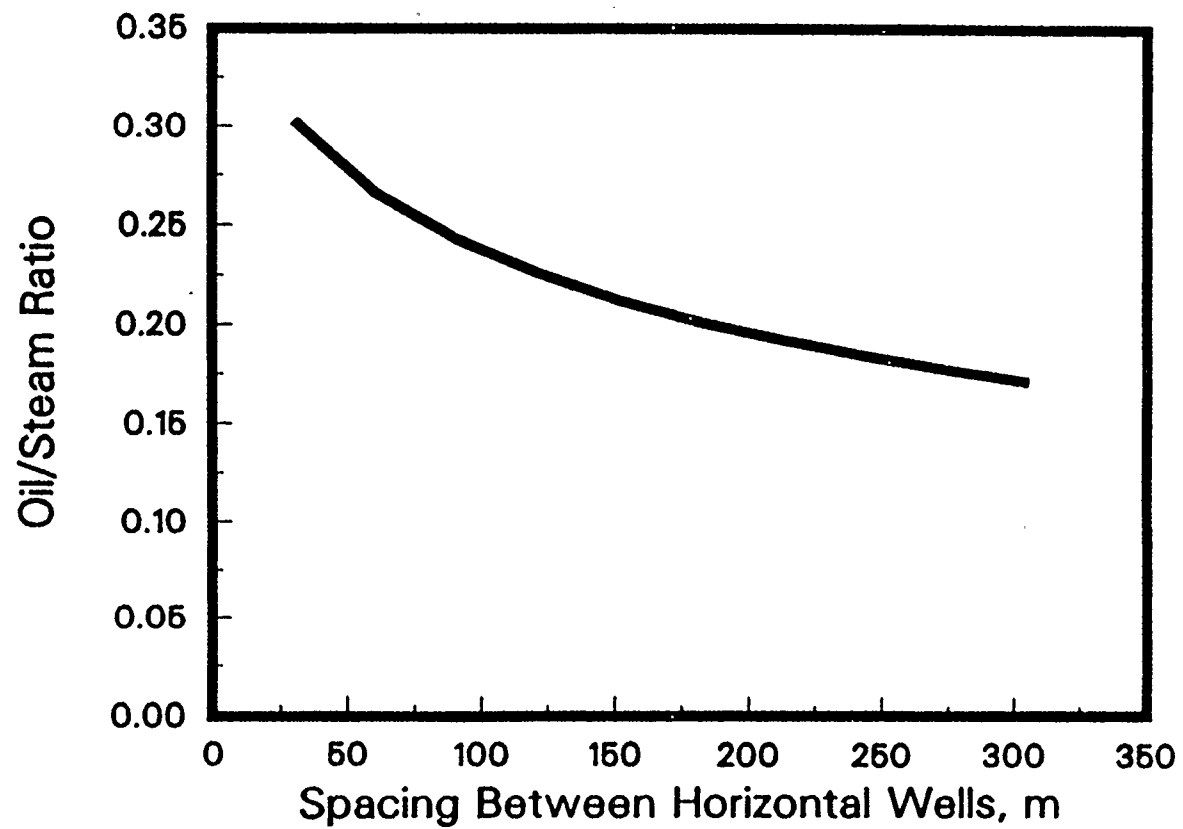


Figure 47: Oil Steam Ratio as a Function of Spacing Between Horizontal Wells

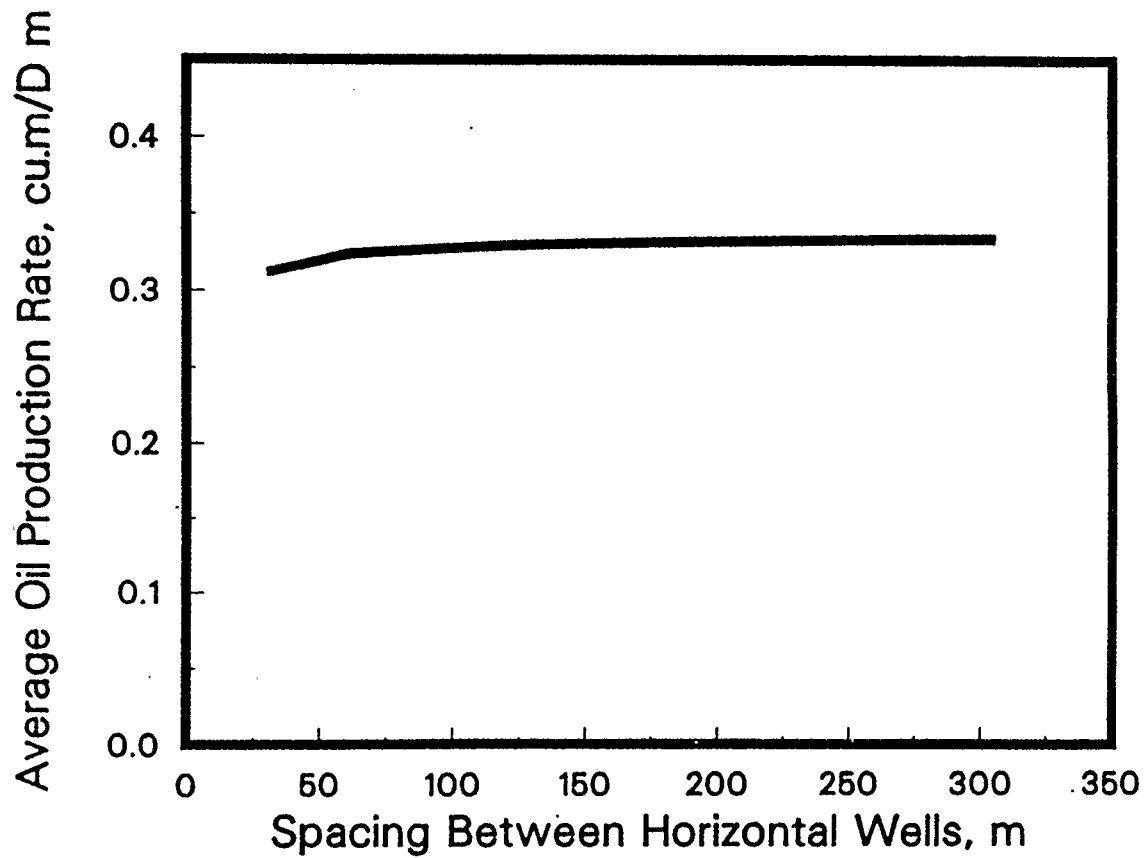


Figure 48: Average Oil Production Rate as a Function of Spacing Between Horizontal Wells

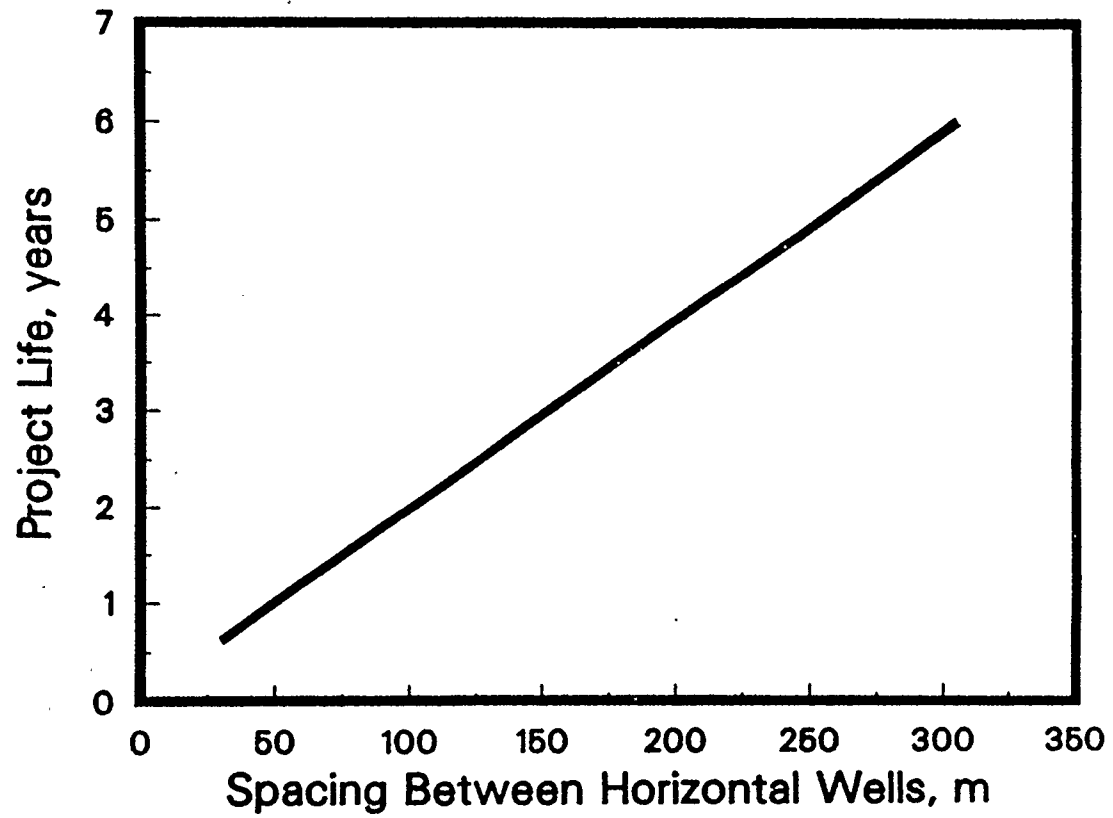


Figure 49: Project life as Function of Spacing between Horizontal Wells

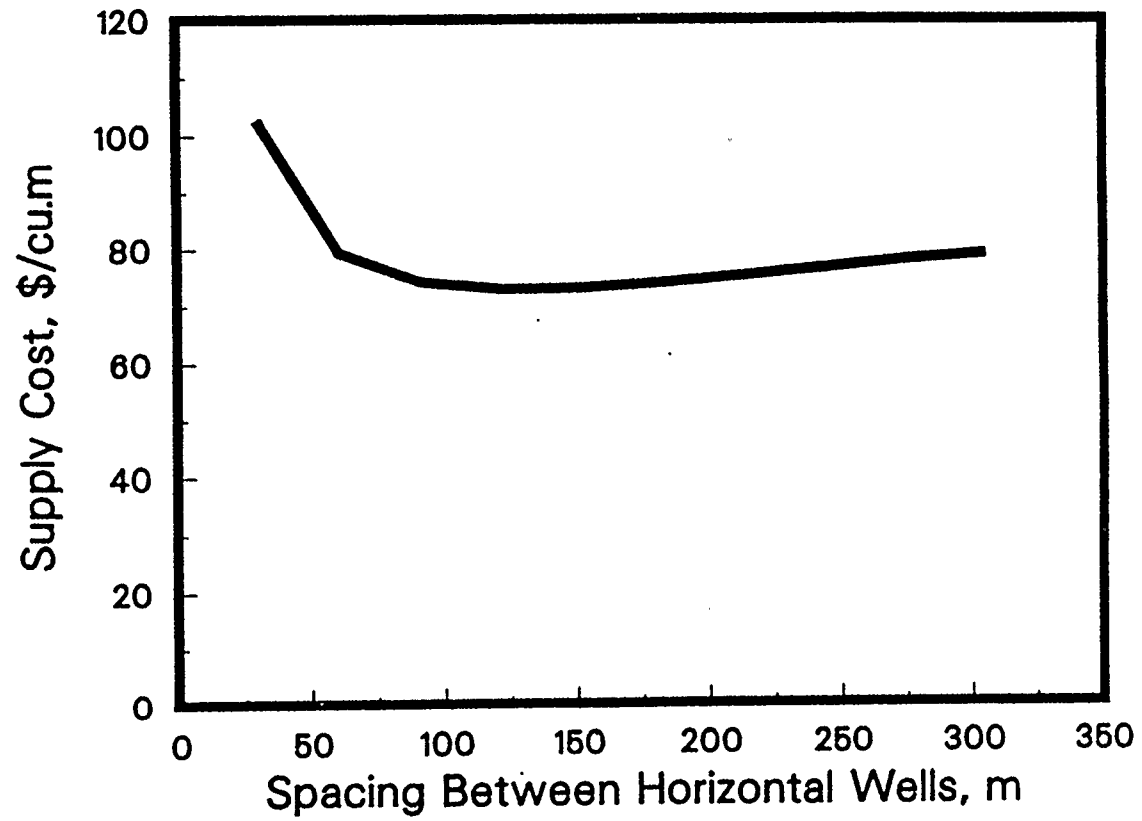


Figure 50: Supply Cost as a Function of Spacing between Horizontal Wells

CHAPTER 7

SUMMARY AND CONCLUSIONS

1. Twelve experiments using a two-dimensional physical reservoir model with an aquifer system have been conducted successfully to investigate the applications of the steam-assisted gravity drainage process in a typical heavy oil reservoir with a bottom water zone.
2. The steam-assisted gravity drainage process combined with the steam drive used to create an initial communication path between the injector and the producer from the top of the reservoir model showed very promising results in recovering heavy oil from reservoirs where recovery is limited by water coning.
3. The best recovery is 87% of the OOIP for the experimental run without a bottom water zone, and the poorest recovery is 48% of the OOIP for the experimental run with a ratio of bottom water zone/total bottom water and oil zone of 0.41.
4. The extrapolated field results showed that a typical 14 m thick Lloydminster formation could produce over 1000 barrels per day from a single well over 500 m length using the steam-assisted gravity drainage process and steamflooding which is used to create the initial communication fluid path from the injector and the producer.
5. The theoretical prediction developed by Butler and Petela (1987) for estimating the steam breakthrough times or initial

communication periods agreed well with the experimental results. This theoretical prediction can be used as a tool to screen the reservoirs which are suitable for implementing the steam drive method to create the initial communication fluid path between the injector and the producer.

6. The theoretical predictions developed by Butler et al (1981) were used to calculate the oil production rate and the cumulative percentage of oil recovery. Experimental results are in good agreement with the theoretical predictions.

7. The presence of a bottom water zone in a heavy oil reservoir can act as a "pressure sink" and provide the steam injectivity missing in immobile, very viscous bitumen reservoirs such as Cold Lake or Athabasca.

8. The water coning tendencies during production can be reduced by applying steam injection pressure slightly above the pressure of the bottom water zone.

9. For a typical experimental run, the mechanism of the reservoir depletion can be classified into two mechanisms.

i) First, the oil was displaced by steam into the production well before the steam breakthrough at the production well or during the initial communication period.

ii) The second was the steam-assisted gravity drainage after the initial communication period. Initially, the steam

chamber spreads sideways and downwards and cold oil was displaced into the production well. . Also, the condensate from the steam fingers through the oil and is produced with cold oil at the production well.

10. When the steam interface, or steam front, reaches the production well, a complete steam-saturated path between the injection and the production well is created and the steam-assisted gravity drainage process begins. The steam continues to condense and heat the oil. The heated oil and the condensate from the steam flow by gravity along the steam interface into the production well.

11. Higher steam injection pressure is desirable for experiments without a bottom water zone. The rate of recovery is higher due to the higher steam temperature associated with the higher steam injection pressure.

12. In experiments with a bottom water zone, the ultimate cumulative oil recovery is lower when the steam injection pressure is higher because the oil is being pushed and migrates downwards into the bottom water zone. This oil cannot be produced because no driving force is available to move the oil upwards into the production well which is located above the water oil contact (WOC).

13. The cumulative oil recovery is lower as the thickness of the bottom water increases.

14. As the interwell spacing decreases, the rate of recovery increases, but the ultimate oil recovery is almost the same.

15. The ultimate cumulative oil recovery is sensitive to the location of the production well. It is desirable to locate the production well above the water/oil contact to avoid excessive water production and to improve the cumulative oil recovery.

CHAPTER 8

RECOMMENDATIONS

In the time available, certain tests could not be performed. However, I believe it to be my responsibility to recommend further laboratory tests. These are necessary for a complete evaluation of the potential application of the steam-assisted gravity drainage process in heavy oil reservoirs with the presence of a bottom water zone.

1) High Pressure Reservoir Model

All experiments in this study were performed in a low pressure model. Unlike the low pressure model, the high pressure model could employ pressures as high as 600 psig. This condition is closer to the reservoir conditions. Therefore it is important to perform laboratory experiments with a high pressure model in order to obtain data for comparison with those of the present study.

2) Gas Cap

In many cases, the reservoir has a gas cap overlying the oil deposits. The effect of this on the steam-assisted gravity drainage should be investigated using model experiments. The results of this type of experiment together with the data reported in this study will facilitate the evaluation of the effectiveness of

the steam-assisted gravity drainage process for heavy oil reservoirs in Saskatchewan.

3. Shale Barrier in the Reservoir

The presence of shale barriers in typical Lloydminster heavy oil formations is common. It is essential to study the susceptibility of the steam-assisted gravity drainage process. The results of this type of experiments could be utilized to evaluate the suitability of a heavy oil reservoir for the steam-assisted gravity drainage process.

APPENDIX A

COMPUTER PROGRAM FOR CALCULATING THE MATERIAL BALANCE

A.1 THEORY

Oil recovered from each time interval.

Total weight of oil recovered = total wt. of sample
and bottle

- total wt. of free water
- total wt. of emul. water
- total wt. of bottle.

A program was developed using Lotus 1-2-3 (1986).

A.2 PROGRAM INPUT

Recommended steps in using the computer program.

- a) Input time interval of five minutes (column 1).
- b) Input the total weight of the sample (water and oil) and the bottle from each time interval of five minutes (column 3).
- c) Input the total weight of free water removed from each sample (column 5).
- d) Input the total weight of emulsified water extracted from each sample (column 6).
- e) Input the weight of empty bottle from each sample (column 8).

A.3 PROGRAM OUTPUT

- a) The program will compute the amount of oil and water produced instantaneously and also cumulatively.
- b) The program will also compute automatically the oil production rate and the cumulative oil recovery from the input data in Section A.1. The results are presented in tabular form. Data from Experimental Run No. 14 is used for an example of the calculation.

THE PRODUCTION OF SASKATCHEWAN HEAVY OILS PROJECT

EXPERIMENT NO:14

GLASS BEADS : 3.00 MM PRESSURE : 7.50 PSIG

INJECTION POSITION : TOP

PRODUCTION POSITION : BOTTOM

OIL AT TIME=0 = 2.00 LBS = 907.20 g

MASS BALANCE

TIME (MINUTES)	TIME (HOURS)	TOTAL WT		EMULSIF. TOTAL H2O		WT. EMPTY		OIL (g)
		TOTAL WT (g)	-FREE H2O (g)	FREE H2O (g)	H2O (g)	EMUL+FREE (g)	BOTTLE (g)	
0.00	0.00	0.00	0.00	0.00	0.00	0.00	0.00	0.00
5.00	0.08	203.19	184.04	0.76	0.05	0.81	155.46	46.92
10.00	0.17	229.15	196.03	11.66	0.03	11.68	154.96	62.51
15.00	0.25	203.06	171.73	15.07	0.08	15.14	148.81	39.11
20.00	0.33	212.14	176.85	21.71	0.35	22.06	155.42	34.66
25.00	0.42	210.87	175.38	22.21	0.35	22.56	155.86	32.45
30.00	0.50	195.98	169.33	13.64	2.95	16.59	156.23	23.16
35.00	0.58	210.31	193.98	16.33	2.55	18.88	157.27	34.16
40.00	0.67	195.33	181.41	13.92	1.50	15.42	154.89	25.02
45.00	0.75	206.70	189.36	17.34	1.50	18.84	155.00	32.86
50.00	0.83	199.33	185.85	13.48	1.60	15.08	156.09	28.16
55.00	0.92	207.39	189.95	17.44	1.30	18.74	156.36	32.29
60.00	1.00	200.61	184.24	16.37	1.45	17.82	156.38	26.41
65.00	1.08	191.07	174.64	16.43	0.35	16.78	149.36	24.93
70.00	1.17	194.19	177.79	16.40	0.30	16.70	151.83	25.66
75.00	1.25	196.58	177.38	19.20	0.20	19.40	151.33	25.85
80.00	1.33	185.39	170.51	14.88	0.25	15.13	148.52	21.74
85.00	1.42	188.88	173.31	15.57	0.40	15.97	151.98	20.93
90.00	1.50	191.12	173.71	17.41	0.30	17.71	149.96	23.45
95.00	1.58	181.52	166.96	14.56	0.30	14.86	148.13	18.53
100.00	1.67	179.85	163.64	16.21	0.75	16.96	147.47	15.42
105.00	1.75	189.64	168.38	21.26	1.10	22.36	148.11	19.17
110.00	1.83	177.65	163.45	14.20	1.25	15.45	148.09	14.11
115.00	1.92	180.14	163.52	16.62	0.95	17.57	148.08	14.49
120.00	2.00	180.60	164.20	16.40	0.95	17.35	148.16	15.09
125.00	2.08	176.52	161.13	15.39	0.50	15.89	148.68	11.95

130.00	2.17	177.31	160.33	16.98	0.35	17.33	148.96	11.02
135.00	2.25	175.32	160.31	15.01	0.60	15.61	148.59	11.12
140.00	2.33	179.69	161.84	17.85	0.35	18.20	149.24	12.25
145.00	2.42	174.22	159.36	14.86	0.35	15.21	148.94	10.07
150.00	2.50	170.88	155.97	14.91	0.10	15.01	148.59	7.28
155.00	2.58	175.46	157.63	17.83	0.35	18.18	149.31	7.97
160.00	2.67	168.37	154.15	14.22	0.50	14.72	147.67	5.98
165.00	2.75	171.03	155.07	15.96	1.10	17.06	148.08	5.89
170.00	2.83	173.14	154.71	18.43	1.25	19.68	148.23	5.23
175.00	2.92	159.74	150.28	9.46	0.95	10.41	147.67	1.66
180.00	3.00	178.36	156.31	22.05	0.95	23.00	148.97	6.39
185.00	3.08	167.60	152.58	15.02	0.50	15.52	148.70	3.38
190.00	3.17	171.58	152.09	19.49	0.35	19.84	148.03	3.71
195.00	3.25	168.58	152.39	16.19	0.60	16.79	148.94	2.85
200.00	3.33	165.48	150.14	15.34	0.35	15.69	147.45	2.34
205.00	3.42	163.17	150.38	12.79	0.35	13.14	148.13	1.90

TIME (MINUTES)	TIME (HOURS)	EMULSIF. TOTAL H2O				TOTAL CUMULATIVE PRODUCTION				
		FREE H2O (g)	H2O (g)	EMUL+FREE (g)	OIL (g)	FREE H2O (g)	H2O (g)	EMUL+FREE (g)	OIL (g)	TOTAL H2O + OIL (g)
0.00	0.00	0.00	0.00	0.00	0.00	0.00	0.00	0.00	0.00	0.00
5.00	0.08	0.76	0.05	0.81	46.92	0.76	0.05	0.81	46.92	47.73
10.00	0.17	11.66	0.03	11.68	62.51	12.41	0.08	12.49	109.43	121.92
15.00	0.25	15.07	0.08	15.14	39.11	27.48	0.15	27.63	148.54	176.17
20.00	0.33	21.71	0.35	22.06	34.66	49.19	0.50	49.69	183.20	232.89
25.00	0.42	22.21	0.35	22.56	32.45	71.40	0.85	72.25	215.65	287.90
30.00	0.50	13.64	2.95	16.59	23.16	85.04	3.80	88.84	238.81	327.65
35.00	0.58	16.33	2.55	18.88	34.16	101.37	6.35	107.72	272.97	380.69
40.00	0.67	13.92	1.50	15.42	25.02	115.29	7.85	123.14	297.99	421.13
45.00	0.75	17.34	1.50	18.84	32.86	132.63	9.35	141.98	330.85	472.83
50.00	0.83	13.48	1.60	15.08	28.16	146.11	10.95	157.06	359.01	516.07
55.00	0.92	17.44	1.30	18.74	32.29	163.55	12.25	175.80	391.30	567.10
60.00	1.00	16.37	1.45	17.82	26.41	179.92	13.70	193.62	417.71	611.33
65.00	1.08	16.43	0.35	16.78	24.93	196.35	14.05	210.40	442.64	653.04
70.00	1.17	16.40	0.30	16.70	25.66	212.75	14.35	227.10	468.30	695.40
75.00	1.25	19.20	0.20	19.40	25.85	231.95	14.55	246.50	494.15	740.65
80.00	1.33	14.88	0.25	15.13	21.74	246.83	14.80	261.63	515.89	777.52
85.00	1.42	15.57	0.40	15.97	20.93	262.40	15.20	277.60	536.82	814.42
90.00	1.50	17.41	0.30	17.71	23.45	279.81	15.50	295.31	560.27	855.58
95.00	1.58	14.56	0.30	14.86	18.53	294.37	15.80	310.17	578.80	888.97
100.00	1.67	16.21	0.75	16.96	15.42	310.58	16.55	327.13	594.22	921.35
105.00	1.75	21.26	1.10	22.36	19.17	331.84	17.65	349.49	613.39	962.88
110.00	1.83	14.20	1.25	15.45	14.11	346.04	18.90	364.94	627.50	992.44
115.00	1.92	16.62	0.95	17.57	14.49	362.66	19.85	382.51	641.99	1024.50
120.00	2.00	16.40	0.95	17.35	15.09	379.06	20.80	399.86	657.08	1056.94
125.00	2.08	15.39	0.50	15.89	11.95	394.45	21.30	415.75	669.03	1084.78
130.00	2.17	16.98	0.35	17.33	11.02	411.43	21.65	433.08	680.05	1113.13
135.00	2.25	15.01	0.60	15.61	11.12	426.44	22.25	448.69	691.17	1139.86
140.00	2.33	17.85	0.35	18.20	12.25	444.29	22.60	466.89	703.42	1170.31
145.00	2.42	14.86	0.35	15.21	10.07	459.15	22.95	482.10	713.49	1195.59
150.00	2.50	14.91	0.10	15.01	7.28	474.06	23.05	497.11	720.77	1217.88
155.00	2.58	17.83	0.35	18.18	7.97	491.89	23.40	515.29	728.74	1244.03
160.00	2.67	14.22	0.50	14.72	5.98	506.11	23.90	530.01	734.72	1264.73
165.00	2.75	15.96	1.10	17.06	5.89	522.07	25.00	547.07	740.61	1287.68
170.00	2.83	18.43	1.25	19.68	5.23	540.50	26.25	566.75	745.84	1312.59
175.00	2.92	9.46	0.95	10.41	1.66	549.96	27.20	577.16	747.50	1324.66
180.00	3.00	22.05	0.95	23.00	6.39	572.01	28.15	600.16	753.89	1354.05
185.00	3.08	15.02	0.50	15.52	3.38	587.03	28.65	615.68	757.27	1372.95
190.00	3.17	19.49	0.35	19.84	3.71	606.52	29.00	635.52	760.98	1396.50
195.00	3.25	16.19	0.60	16.79	2.85	622.71	29.60	652.31	763.83	1416.14
200.00	3.33	15.34	0.35	15.69	2.34	638.05	29.95	668.00	766.17	1434.17
205.00	3.42	12.79	0.35	13.14	1.90	650.84	30.30	681.14	768.07	1449.21

TIME (MINUTES)	TIME (HOURS)	OIL PROD % RECOV.	
		RATE (g/hr)	OIL
0.00	0.00	0.00	0.00
5.00	0.08	563.04	5.17
10.00	0.17	750.12	12.06
15.00	0.25	469.32	16.37
20.00	0.33	415.92	20.19
25.00	0.42	389.40	23.77
30.00	0.50	277.92	26.32
35.00	0.58	409.92	30.09
40.00	0.67	300.24	32.85
45.00	0.75	394.32	36.47
50.00	0.83	337.92	39.57
55.00	0.92	387.48	43.13
60.00	1.00	316.92	46.04
65.00	1.08	299.16	48.79
70.00	1.17	307.92	51.62
75.00	1.25	310.20	54.47
80.00	1.33	260.88	56.87
85.00	1.42	251.16	59.17
90.00	1.50	281.40	61.76
95.00	1.58	222.36	63.80
100.00	1.67	185.04	65.50
105.00	1.75	230.04	67.61
110.00	1.83	169.32	69.17
115.00	1.92	173.88	70.77
120.00	2.00	181.08	72.43
125.00	2.08	143.40	73.75
130.00	2.17	132.24	74.96
135.00	2.25	133.44	76.19
140.00	2.33	147.00	77.54
145.00	2.42	120.84	78.65
150.00	2.50	87.36	79.45
155.00	2.58	95.64	80.33
160.00	2.67	71.76	80.99
165.00	2.75	70.68	81.64
170.00	2.83	62.76	82.21
175.00	2.92	19.92	82.40
180.00	3.00	76.68	83.10
185.00	3.08	40.56	83.47
190.00	3.17	44.52	83.88
195.00	3.25	34.20	84.20
200.00	3.33	28.08	84.45
205.00	3.42	22.80	84.66

APPENDIX B

COMPUTER PROGRAMS FOR PREDICTING THE PRODUCTION PERFORMANCES USING THE STEAM-ASSISTED GRAVITY DRAINAGE THEORY DEVELOPED BY BUTLER ET AL (1981)

B.1 THEORY

All equations are described earlier in the theory in Chapter four.

B.2 PROGRAM INPUT

The input data used for these calculations are taken from the same input data used for calculating the material balance (Section A). No input data is needed for this program because the program will access automatically from the previous section program.

B.3 PROGRAM OUTPUT

The program will compute the theoretical predictions for the cumulative oil recovery and oil production rate at each time interval of five minutes.

THE PRODUCTION OF SASKATCHEWAN HEAVY OILS PROJECT

LAB NO: 14

EXPERIMENT NO:14

GLASS BEADS : 3.00 MM PRESSURE : 7.50 PSIG

INJECTION POSITION : TOP

PRODUCTION POSITION : BOTTOM

DATA :

k = 1760.00 DARCY = 1.74E-09 M²g = 7.32E+10 M/D²ALPHA = 0.05 M²/D

POR*dSo= 0.33

n = 2.61

VIS₀TS = 2.16 M²/D

H = 0.20 M

W = 0.35 M

G/HR CONVERSION = 8.21E-04 M³/DMQFACTOR = 3.63 DAYS/M³

T* = 1.19E+01 TDAYS

CALCULATION OF RATES & RECOVERY FOR DEPLETION ASSUMING CHAMBERS
START AS VERTICAL PLANES

LAB TIME (MINUTES)	LAB TIME (HOURS)	LAB TIME (DAYS)	T*	Q*	Q THEORY (M ³ /DM)	Q EXPR. (M ³ /DM)	THEORY PERCENT RECOVERY	EXPR. PERCENT RECOVERY	THEORY PERCENT RECOVERY	2 sides Q EXPR. (M ³ /DM)
0.00	0.00	0.0000	0.0000	1.2247	0.3375	0.0000	0.00	0.00	0.00	0.00
5.00	0.08	0.0035	0.0414	1.2233	0.3371	0.4620	5.07	5.17	4.30	0.92
10.00	0.17	0.0069	0.0829	1.2191	0.3360	0.6155	10.14	12.06	8.59	1.23
15.00	0.25	0.0104	0.1243	1.2121	0.3341	0.3851	15.17	16.37	12.86	0.77
20.00	0.33	0.0139	0.1657	1.2023	0.3314	0.3413	20.17	20.19	17.09	0.68
25.00	0.42	0.0174	0.2071	1.1897	0.3279	0.3195	25.12	23.77	21.29	0.64

30.00	0.50	0.0208	0.2486	1.1743	0.3236	0.2281	30.02	26.32	25.45	0.46
35.00	0.58	0.0243	0.2900	1.1561	0.3186	0.3364	34.85	30.09	29.53	0.67
40.00	0.67	0.0278	0.3314	1.1351	0.3128	0.2464	39.59	32.85	33.55	0.49
45.00	0.75	0.0313	0.3728	1.1113	0.3063	0.3236	44.24	36.47	37.50	0.65
50.00	0.83	0.0347	0.4143	1.0846	0.2989	0.2773	48.80	39.57	41.36	0.55
55.00	0.92	0.0382	0.4557	1.0552	0.2908	0.3180	53.23	43.13	45.11	0.64
60.00	1.00	0.0417	0.4971	1.0230	0.2819	0.2601	57.53	46.04	48.76	0.52
65.00	1.08	0.0451	0.5385	0.9880	0.2723	0.2455	61.69	48.79	52.29	0.49
70.00	1.17	0.0486	0.5800	0.9501	0.2618	0.2527	65.71	51.62	55.70	0.51
75.00	1.25	0.0521	0.6214	0.9095	0.2506	0.2546	69.56	54.47	58.96	0.51
80.00	1.33	0.0556	0.6628	0.8661	0.2387	0.2141	73.24	56.87	62.08	0.43
85.00	1.42	0.0590	0.7042	0.8198	0.2259	0.2061	76.73	59.17	65.03	0.41
90.00	1.50	0.0625	0.7457	0.7708	0.2124	0.2309	80.03	61.76	67.83	0.46
95.00	1.58	0.0660	0.7871	0.7189	0.1981	0.1825	83.11	63.80	70.44	0.36
100.00	1.67	0.0694	0.8285	0.6643	0.1831	0.1518	85.98	65.50	72.87	0.30
105.00	1.75	0.0729	0.8699	0.6068	0.1672	0.1888	88.61	67.61	75.10	0.38
110.00	1.83	0.0764	0.9114	0.5466	0.1506	0.1389	91.00	69.17	77.13	0.28
115.00	1.92	0.0799	0.9528	0.4835	0.1333	0.1427	93.13	70.77	78.94	0.29
120.00	2.00	0.0833	0.9942	0.4177	0.1151	0.1486	95.00	72.43	80.52	0.30
125.00	2.08	0.0868	1.0356	0.3490	0.0962	0.1177	96.59	73.75	81.86	0.24
130.00	2.17	0.0903	1.0771	0.2776	0.0765	0.1085	97.89	74.96	82.97	0.22
135.00	2.25	0.0938	1.1185	0.2033	0.0560	0.1095	98.88	76.19	83.81	0.22
140.00	2.33	0.0972	1.1599	0.1262	0.0348	0.1206	99.56	77.54	84.39	0.24
145.00	2.42	0.1007	1.2013	0.0464	0.0128	0.0992	99.92	78.65	84.69	0.20
150.00	2.50	0.1042	1.2428	-0.0363	-0.0100	0.0717	100.00	79.45	84.76	0.14
155.00	2.58	0.1076	1.2842	-0.1218	-0.0336	0.0785	100.00	80.33	84.76	0.16
160.00	2.67	0.1111	1.3256	-0.2100	-0.0579	0.0589	100.00	80.99	84.76	0.12
165.00	2.75	0.1146	1.3670	-0.3011	-0.0830	0.0580	100.00	81.64	84.76	0.12
170.00	2.83	0.1181	1.4085	-0.3950	-0.1089	0.0515	100.00	82.21	84.76	0.10
175.00	2.92	0.1215	1.4499	-0.4917	-0.1355	0.0163	100.00	82.40	84.76	0.03
180.00	3.00	0.1250	1.4913	-0.5911	-0.1629	0.0629	100.00	83.10	84.76	0.13
185.00	3.08	0.1285	1.5327	-0.6934	-0.1911	0.0333	100.00	83.47	84.76	0.07
190.00	3.17	0.1319	1.5742	-0.7985	-0.2201	0.0365	100.00	83.88	84.76	0.07
195.00	3.25	0.1354	1.6156	-0.9064	-0.2498	0.0281	100.00	84.20	84.76	0.06
200.00	3.33	0.1389	1.6570	-1.0171	-0.2803	0.0230	100.00	84.45	84.76	0.05
205.00	3.42	0.1424	1.6984	-1.1306	-0.3116	0.0187	100.00	84.66	84.76	0.04

BIBLIOGRAPHY

- American Society for Testing and Materials (ASTM), "Standard Test Method for Permeability of Granular Solids (Constant Head)", Designation D 2434-68.
- American Society for Testing and Materials (ASTM), "Standard Test Method for Water and Sediment in Crude Oil by The Centrifuge Method (Laboratory Procedure)", Designation D 4007-81.
- Butler, R.M., McNab, G.S. and Lo, H.Y., "Theoretical Studies on The Gravity Drainage of Heavy Oil During In-Situ Steam Heating", J.Can.Pet.Tech., 59, 4, 455-460 (August 1979).
- Butler, R.M. and Stephens, D.J., "The Gravity Drainage of Steam-Heated Oil to Parallel Horizontal Wells", J.Can.Pet.Tech., 90-96, (April-June 1981).
- Butler, R.M., "A New Approach to the Modelling of Steam-Assisted Gravity Drainage", J.CanPet.Tech., 24,3, 42-52 (May-June 1985a).
- Butler, R.M., "New Interpretation of the Meaning of the Exponent "m" in the Gravity Drainage Theory for Continuously Steamed Wells", AOSTRA J. of Research, Vol.2, Number 1, 1985b.
- Butler, R.M. and Petela, G., "Theoretical Estimation of Breakthrough Time During a Steamflood Between Long Parallel Horizontal Wells", Internal Report for Sask. Energy and Mines, Contract No. 7348-1, University of Calgary, December 1987.
- Chung, K.H. and Butler, R.M., "Geometrical Effect of Steam Injection on the Formation of Emulsions in the Steam-Assisted Gravity Drainage Process", Proc. 38th Ann. Tech. Mtg. of Petroleum Society of CIM, Calgary, Alberta, 373-392, (June 1987).
- Doscher, T.M. and Huang, W., "Steam Drive Performance Judged Quickly from Use of Physical Models", Oil & Gas J. 52-57, (Oct. 22, 1979).
- Erlich, R., "Laboratory Investigation of Steam Displacement in the Wabasca Grand Rapid "A" Sand", Oil Sands of Canada - Venezuela, 364-379, CIM (1977).
- Farouq Ali, S.M., "Effect of Bottom Water and Gas Cap on Thermal Recovery", SPE Paper 11732, presented at the 53rd Annual California Regional Meeting, March 23-25, 1983.

- Farouq Ali, S.M., "Prospects of EOR Techniques in Saskatchewan Oil Reservoirs", J.Can.Pet. Tech., 64-67, (March-April, 1986).
- Ferguson, F.R. Scott and Butler, R.M., "Steam-Assisted Gravity Drainage Model Incorporating Energy Recovery from a Cooling Steam Chamber", Proc. 37th Annual Technical Meeting of the Petroleum Society of CIM, Calgary, Alta. 349-371 (June 1986).
- Griffin, P.J. and Trofimenkoff, P.N., "Laboratory Studies of the Steam-Assisted Gravity Drainage Process", Presented at the 5th Annual "Advances in Petroleum Recovery & Upgrading Technology" Conference, Calgary, Alberta (June 1984).
- Huygen, H.A. and Lowry, W.E., Jr., "Steam Flooding Wabasca Tar Sand Through the Bottom Water Zone - Scaled Lab Experiments", SPE Paper 8398, presented at the 54th Annual Fall Meeting of SPE, Las Vegas, Sept. 23-26, 1979.
- Jain, S. and Khosla, A., "Predicting Steam Recovery of Athabasca Oil Through Horizontal Wells", Proc. of the 36th Ann. Tech. Mtg. of the Petroleum Society of CIM, Calgary, Alta., 705-720, (June 1985).
- Kasrie, M. and Farouq Ali, S.M., "Heavy Oil Recovery in the Presence of Bottom Water", Proc. of the 35th Ann. Tech. Mtg. of the Petroleum Society of CIM, Calgary, Alta., 753-761, (June 1984).
- Lotus 1-2-3, Version 2.01 Manual, Lotus Development Corp., Cambridge, MA., (1986).
- Muskat, M., "The Flow of Homogeneous Fluids Through Porous Media", IHRDC, Boston, 1982.
- Prats, M., "Peace River Steam Drive Scaled Model Experiments", Oil Sands of Canada - Venezuela, 346-363, CIM (1977).
- Sampson, R.J., Surface II Graphical System, rev. 1, Computer Services Section, Kansas Geological Survey, Lawrence, Kansas (1978).